STRUCTURE-FUNCTION RELATIONSHIP OF

EXCHANGEABLE APOLIPOPROTEINS

BY

PALANIAPPAN SEVUGAN CHETTY

Master of Science
Maharaj Sayaji Rao University
Baroda, India
1999

Submitted to the faculty of the
Graduate College of the
Oklahoma State University
in partial fulfillment of
requirements for the Degree of
Doctorate of philosophy
May, 2006

STRUCTURE-FUNCTION RELATIONSHIP OF

EXCHANGEABLE APOLIPOPROTEINS

Thesis Approved:

_____

Chang An Yu (Chairperson)

_____

Jose L. Soulages (Advisor)

_____

Ulrich Melcher (Committee Member)

_____

Robert L. Matts (Committee Member)

_____

Robert Burnap (External Member)

_____

Dean Graduate College

ACKNOWLEDGEMENTS

This work is a result of the exceptional mentoring from Dr. Jose L. Soulages and Estela L. Arrese; unfailing guidance of my committee members Drs. Ulrich Melcher, Chang-An Yu, Robert Matts and Robert Burnap and meticulous training in mass spectrometry from Dr. Steve Hartson.

I would have not accomplished this goal without the blessings of my parents; the constant support from my wife and cumulative efforts of my friends and lab members.

Finally, I would like to extend my regards to the Biochemistry Department and Core Facility for all the support extended during my stay at OSU.

TABLE OF CONTENTS

LIST OF FIGURES

LIST OF TABLES

ABBREVIATIONS

^{14}N apoAI	Wild-type human apoAI
^{15}N apoAI	recombinant ^{15}N labeled human apoAI fusion protein
AKH	Adipokinetic Hormone
Apo	Apolipoproteins
ApoAI	Apolipoprotein AI
ApoAII	Apolipoprotein AII
ApoC	Apolipoprotein C
ApoE	Apolipoprotein E
ApoLp	Apolipophorin
ApoLp I	Apolipophorin I
ApoLp II	Apolipophorin II
ApoLp III	Apolipophorin III
BS^3	(Bis[sulfosuccinimidyl] suberate)
CD	Circular dichorism spectroscopy
CE	Cholesterol esters
CHD	Coronary heart diseases
CNBr	Cyanogen bromide
DG	Diglycerides
DMPC	Dimyrsitoyl phosphatidyl choline
DSP	(Dithiobis[succinimidylpropionate])
ESI	Electrospray ionization

HDL	High density lipoprotein
HDLp	High density lipophorin
ITC	Isothermal titration calorimetry
LCAT	Lecithin cholesterol acyl transferase
LC-ESI MS	Liquid Chromatography-Electrospray ionization mass spectrometry
LDL	Low density lipoprotein
LDLp	Low density lipophorin
Lp	Lipophorin
LTP	Lipd transfer protein
m/z	mass/charge
MALDI-TOF	Matrix assisted laser desorption ionization time of flight
MS	Mass spectrometry
NMR	Nuclear magnetic resonance spectroscopy
PMF	Peptide mass fingerprinting
POPC	Palmitoyl oleyl phosphocholine
TG	Triglycerides
VLDL	Very low density lipoprotein

CHAPTER-I

INTRODUCTION

Lipoproteins (**lipophorins** in insects) have a surface monolayer of phospholipids and cholesterol enclosing a central core of neutral lipids mostly cholesterol esters (CE) and triclycerides (TG) (**Figure-1**), in insects the core lipids are predominantly diglycerides (DG) (*1, 2*). The proteins associated with lipoproteins are of two types, the exchangeable apolipoproteins which readily exchange between various lipoprotein types or exist in the lipid-free or lipid-bound state and integral or non-exchangeable apolipoproteins. There are three major classes of exchangeable apolipoproteins in humans, apolipoproteins class A, C and E designated as apoA, apoC and apoE with subclasses in each. In insects there is one exchangeable apolipoprotein apolipophorinIII (apoLp-III). The non-exchangeable apolipoproteins have a stronger interaction with the surface phospholipids and core lipids and are associated to specific lipoprotein types (*1*). Different combinations of apolipoproteins and lipids in human circulation lead to heterogeneity in the observed properties of lipoproteins like flotation densities (*3*) (**Table-1**) or mobility in an electrophoretic field (*4*).

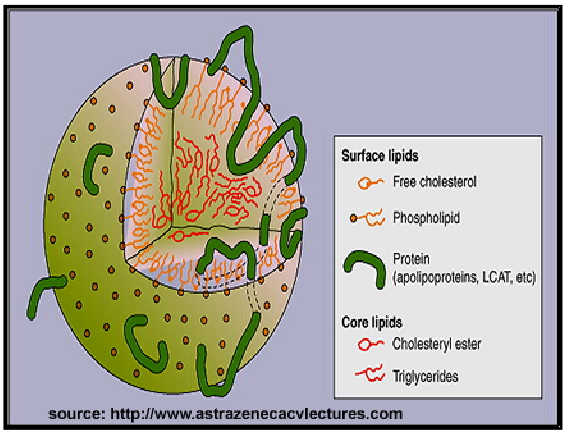

Figure-1: Schematic representation of a lipoprotein molecule.

Organism	**Human**				**Insects**	
Particle	HDL	LDL	VLDL	Chylomicrons	High density Lipophorin (HDLp)	Low Density Lipophorin (LDLp)
Density(g/ml)	1.063-1.21	1.019-1.063	0.93-1.006	0.93-1.006	1.065	1.03
Protein (%)	50	20	10	1	50	40
Major	A-I	B	B	C-III	ApoLp-I, II	ApoLp-I, II, III
Minor	A-II, C-I, C-II, C-III, E	--	C-I, C-II, C-III, E	B,C-I, C-II, E	ApoLp-III	--
Phospholipid (%)	30	24	19	4	14	7
Cholesterol (%)	18	45	19	6	4	<1
Triglycerides (%)	5	10	50	90	2	2
Diglycerides (%)	Not Applicable	Not Applicable	Not Applicable	Not Applicable	26	47

Table-1: Heterogeneity in density, size and composition among various lipoprotein classes in Human and Insect lipoproteins (*1, 2*).

Based on the mobility in an electrophoretic field human lipoproteins are classified as having α mobility or β mobility. The densest lipoprotein high density lipoprotein or HDL moves farthest from origin, has α-mobility while the less dense very low density lipoprotein or VLDL has β mobility. LDL has an intermediate mobility (pre- β mobility) between HDL and VLDL. The least dense chylomicrons remain at origin. This difference in electrophoretic mobility is due to the presence of varying amounts of protein in the various lipoprotein classes. Based on heterogeneity in the lipid/protein composition in a specific class of lipoprotein type listed in **Table-1** they may be further classified into subclasses based on density or electrophoretic mobility (*1*).

Insect ApolipophorinIII (ApoLp-III):

ApoLp-III And Lipid Transport In Insect Hemolymph- ApoLp-III binding to LDLp and transport of DG to flight muscles is a well characterized process (reviewed in (*2, 5*)). Adipokinetic hormone (AKH) is released from the corpus cardiacum of insects in response to a flight stimulus. AKH leads to lipolysis (synthesis of DG from TG) in the fat body. The newly synthesized DG is mobilized from the fat body to High Density Lipophorin (HDLp) by Lipid-Transfer Protein (LTP), eventually converting the HDLp to Low Density Lipophorin (LDLp). Free apoLp-III in the insect hemolymph binds to DG rich LDLp and aids in the transport of LDLp to the flight muscles where the DG molecules are used for energy production during flight. After the DG is delivered to the flight muscles the apoLp-III bound to LDLp goes to the lipid-free state in the hemolymph and LDLp

is converted back to HDLp. Thus the HDLp serves as a reversible shuttle in the transport of neutral lipids in insect hemolymph.

Apolipophorin-III Structure- Apolipophorin-III (apoLp-III), a 17KDa (161 residues) protein is synthesized in insect fat body and secreted into the hemolymph (*2*). In the lipid-free state apoLp-III exists as a five helix bundle. *Locust migratoria* (locust) apoLp-III structure was the first full length apolipoprotein structure to be solved by X-ray crystallography (*6*). The solution-structures of apoLp-III from locust (*7*) and moth*, Manduca sexta (8)* have also been solved by NMR spectroscopy. ApoLp-III from both the insects is made up of 5 amphipathic α-helices (H1-H5) arranged in an up-down (anti-parallel) topology connected by loops (L1-L4) (**Figure-2**).

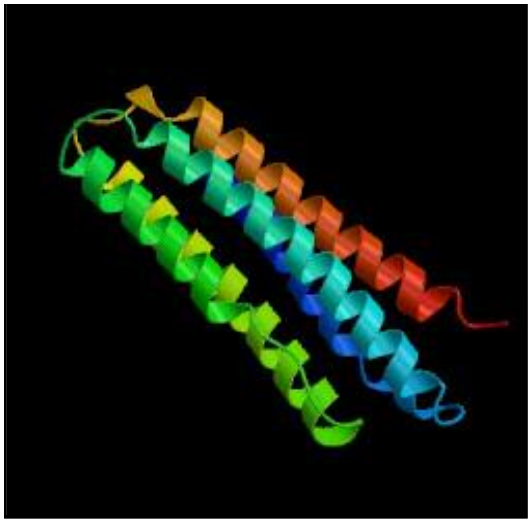

Figure-2: **Structure of *locust* apoLp-III, (Source: PDB, 1aep)**

The NMR and crystal structures of locust apoLp-III are identical. This up-down topology is also found in the N-terminal lipid binding 4-helical domain of human apolipoprotein E (apoE) (*9*). ApoLp-III from moth and locust share this

high level of structural similarity despite having only 25% of primary sequence identity (*10*).

ApoLp-III Lipid-Binding and Conformational flexibility-Surface Plasmon Resonance measurements of binding of apoLp-III to phospholipid bilayers as a function of DG concentration identified two steps in the process of lipid-binding of apoLp-III (*11*). A similar multi-step process has been proposed for the lipid-binding of human apoE and apoAI (*12, 13*). Surface-pressure measurements of apoLp-III at the air-water interface suggests apoLp-III to exist in a highly extended conformation on binding to lipids (*14*). Fluorescence resonance energy transfer between Trp113 in helix4 and introduced cysteine residues in helices 1, 2, 3 and 5 of apoLp-III suggest the five helices to adopt a highly extended conformation in the lipid-bound state (*15*). This observation is consistent with the surface pressure measurement studies. Fluorescence quenching studies using nitroxide-labeled phospholipids and fatty acids suggest that all the five helices of apoLp-III interact massively with acyl chains in phospholipid discoidal lipoprotein complexes (*16*).

Although, it is known that apoLp-III adopts a highly extended conformation on binding to lipids/lipoproteins and apoLp-III binding requires DG loading in the lipophorin molecules it is still not clear what triggers the conformational opening and the steps in reorganization of apoLp-III in going to a fully extended conformation. Conserved leucine (Leu 32, 34 and 95) residues in insect apoLp-III sequences were proposed to act as triggers in recognizing the hydrophobic defects on lipid surfaces eventually leading to the conformational reorganization

of the five helix bundle (*6*). Site directed mutagenesis of the conserved leucine residues 32, 34 suggests the leucines are not involved as hydrophobic triggers as proposed (*17*). There are three models to explain the initial steps in the lipid-binding associated reorganization of the constituent α-helices of apoLp-III. The first model (Breiter, et. al, 1991) based on the crystal structure of apoLp-III identified L2 and L4 as the most flexible regions in apoLp-III based on the high B-values (temperature factor) (*6*). This model proposed L2 and L4 to act as flexible hinges in the opening of the closed helix-bundle. In the process of binding to lipids the apoLp-III molecule opens asymmetrically by the putative hinges at loops 2 and 4 with helices 3 and 4 moving away from the helix bundle (**Figure-3a**), to expose the hydrophobic core. The second model (*18*) was proposed based on the fluorescence anisotropy measurements of introduced Trp residues in each of the five helices of lipid-free apoLp-III. Helices 1 and 5 were identified to be the most flexible helices in lipid-free apoLp-III. According to this model the apoLp-III helix bundle opening was postulated to proceed through the separation of helices 1 and 5 (**Figure-3b**). The third model (*7*) based on the NMR structure

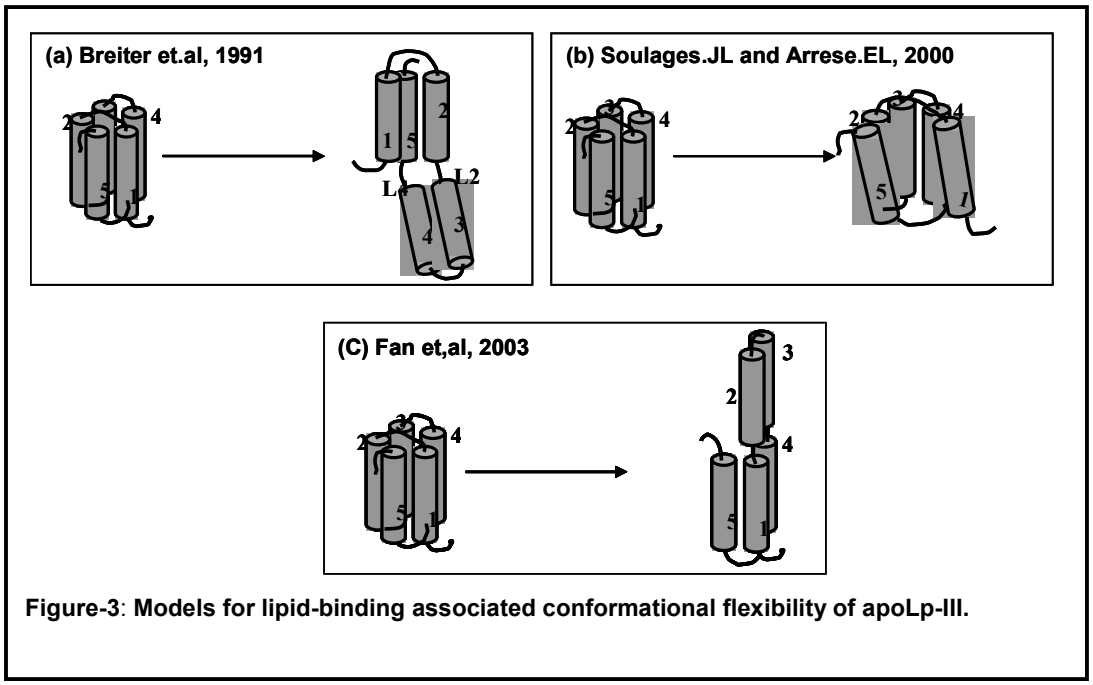

Figure-3: **Models for lipid-binding associated conformational flexibility of apoLp-III.**

of locust apoLp-III proposed L4 to act as a molecular trigger in the recognition of hydrophobic defects on lipid-surfaces. Subsequent to the recognition of hydrophobic defect by L4 the helix-bundle was postulated to open asymmetrically by the flexible loops L1 and L3 leading to the movement of helices 2 and 3 away from the helix bundle (**Figure-3c**).

No direct experimental evidence exists to support any of the three proposed models of apoLp-III helix-bundle reorganization. ApoLp-III goes from a compact globular structure to a fully extended conformation but how apoLp-III reaches the final lipid-bound state is still not clear. Two areas which need to be investigated to understand the lipid-binding associated conformational flexibility of apoLp-III are (a) identify regions of apoLp-III which initiate lipid binding and (b) identify the steps in the lipid-binding associated helix-bundle reorganization of

apoLp-III. The full length atomic resolution structure of insect apoLp-III are known, this simplifies the use of site-directed mutagenesis to generate mutants and characterize the structure-function relationship of the apoLp-III molecule. Attempts have been made to apply the insight gained from the structure of insect apoLp-III to human exchangeable apolipoproteins (*8*). The fact that insect apoLp-III shares the same amphipathic α-helical nature like human exchangeable apolipoproteins and the structural similarity with the N-terminal 4 helix-bundle of human apoE the insight gained by understanding the lipid-binding mechanism of apoLp-III can be applied to the human apolipoproteins.

Human ApolipoproteinAI:

Reverse Cholesterol Transport and Human ApoAI-Human apoAI is the major component of HDL in circulation. HDL mediates the transport of cholesterol from peripheral tissues to liver for catabolism in a process known as reverse cholesterol transport, (RCT) a vital process in the prevention of atherosclerosis and Coronary Heart Diseases (CHDs). Circulating HDL levels are negatively correlated with the incidence of atherosclerosis and CHDs. The role of HDL in RCT is largely mediated by the HDL bound apoAI molecules. Lipoprotein bound apoAI mediates the following functions: (i) leads to cholesterol and phospholipid efflux from cells; (ii) activates HDL bound enzyme, lecithin-cholesterol acyl transferase (LCAT) which converts the free cholesterol from cells to cholesterol esters and transfers cholesterol esters to HDL core; (iii) maintains the structural integrity of HDL complexes containing phospholipids and cholesterol esters, and

(iv) binds to hepatic cell surface receptors leading to selective transport of cholesterol esters from HDL to hepatic cells (reviewed in (*19-22*)).

Structure of Lipid-free Human ApolipoproteinAI (apoAI) - Human apoAI is a 243 residue polypeptide synthesized by the liver and intestine and secreted in the circulation. Lipid-free apoAI in solution exists as oligomers at concentrations > 0.1mg/mL. The full length crystal structure of lipid-free apoAI (**Figure-4**) has been reported recently (*23*). Human apoAI shares the helix bundle properties of insect apoLp-III and human apoE.

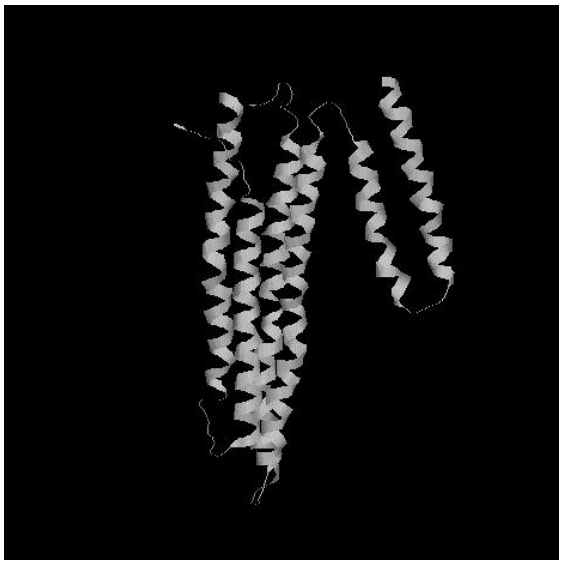

Figure-4: **Structure of human apoAI solved by x-ray crystallography (PDB I.D. 2AO1).** Lipid-free apoAI is made up of 6 amphipathic α-helices, residues 1-188 exist as a compact helical bundle. The C-terminal residues 189-243 exist as a pair of independent helices away from the compact N-terminal helical bundle.

Human ApoAI Lipid-Binding and Significance of Lipid-Bound Conformation-Deletion mutagenesis and Isothermal Titration Calorimetric studies (ITC) of human apoAI suggest the lipid-binding to be initiated by amphipathic α-helices in the C-terminal domain followed by the reorganization of amphipathic α-helices in the N-terminal and central domains (*24*). There are

three different models to explain the final lipid-bound conformation of apoAI in rHDL particles. The first model known as the 'picket-fence' model (**Figure-5a and 5b**) was proposed based on Fourier transform infrared-attenuated total reflection spectroscopy (FTIR-ATR) studies which suggested the α-helices of human apoAI molecules to exist parallel to acyl chains on lipoprotein surface with adjacent apoAI molecules anti-parallel in orientation in terms of helix-sense (*25*). Studies utilizing FRET and molecular modeling support a 'belt model' which suggests two apoAI molecules to exist fully extended in an anti-parallel fashion with the constituent α-helices oriented perpendicular to the acyl chains of phospholipids (**Figure-5c**) (*26, 27*). The 'hairpin model' was proposed based on FRET studies where two apoAI molecules were suggested to exist folded as hairpins (**Figure-5d and 5e**) on reconstituted HDL (rHDL) particles (*28*).

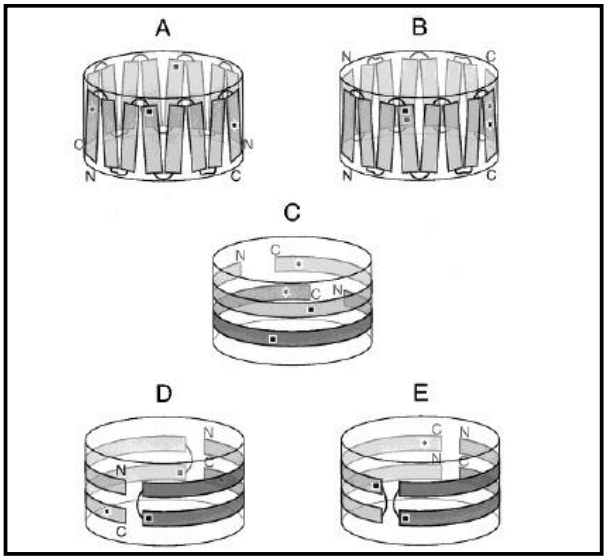

Figure-5: **Models for the orientation of apoAI molecules on reconstituted lipoprotein particles.** N and C designate the N and C terminal of protein. (a) and (b) **Picket-Fence Model**, (c) **Belt Model** ,(d) **Hairpin Model** with two molecules in Head-tail conformation and (e) **Hairpin Model** with two molecules in Head-Head conformation. (**Source**- *Biochemistry* **2001,** *40,* 5065-5074).

Recently two groups reported the structure of lipid-bound apoAI on rHDL investigated by chemical cross-linking using a 12Å homobifunctional cross-linker and mass spectrometry to differentiate between the three proposed models of apoAI organization on rHDL molecules described above (*29-31*). Both the models suggest an anti-parallel orientation of adjacent apoAI molecules in the edge of lipoprotein disks, but there are significant differences in the observed cross-linking data between the two groups.

ApoAI can exist in various states of lipidation in the plasma or in rHDL molecules, which is reflected by the heterogeneity of HLD particle sizes reported in plasma (**Table-1**). Based on the ratio of apoAI to lipids, HDL molecules are classified as small pre-β-migrating HDL or discoidal HDL, and large spherical α-migrating HDL_3 or HDL_2 (*32*). ApoAI is suggested to exist in different conformations based on the lipid content/size of HDL and studies suggest that these multiple conformation aid in regulating the various functions of apoAI mentioned earlier (*33*). It has been shown that the small rHDL particles or pre-β-migrating HDL apoAI molecules in vitro can interact with cells and lead to efficient cholesterol efflux (*34*). Similarly the HDL associated enzyme LCAT is activated by residues 143-165 of lipid-bound apoAI only in pre-β-HDL molecules (*35*), while apoAI associated with cholesterol ester-rich spherical HDL_2 particles or lipid-free apoAI do not activate LCAT (*36*). Immunological studies using monoclonal antibodies raised against specific apoAI epitopes suggest apoAI exists in a different conformation based on the phospholipid and cholesterol content (*37*). All these studies suggest apoAI exists in different conformations in

the lipid-bound state and it is essential to characterize the lipid-bound conformation of apoAI in varying sizes of lipoprotein particles to fully elucidate the mechanism of RCT. This will provide a clear insight as to the actual conformation of apoAI essential for various functions like cholesterol efflux or LCAT activation or receptor binding.

CHAPTER-II

ESSENTIAL ROLE OF THE CONFORMATIONAL FLEXIBILITY OF HELICES 1 AND 5 ON THE LIPID BINDING ACTIVITY OF APOLIPOPHORIN-III

Introduction

Apolipophorin-III (apoLp-III) is an exchangeable apolipoprotein found in the hemolymph of many insect species in a lipid-free state or bound to the major insect lipoprotein, lipophorin (*2, 38*). The structure of apoLp-III from two different insect species has been solved. The structures of *Locusta migratoria* and *Manduca sexta* apoLp-III were determined by x-ray crystallography (*6*) and NMR spectroscopy (*8*), respectively. The structure of apoLp-III is described as an elongated bundle of five amphipathic α-helices, where the nonpolar faces of the helices are oriented toward the protein core. A similar structure, but consisting of a four-helix bundle, is present in the N-terminal domain of human apoE (*39*). *M. sexta* and *L.migratoria* apoLp-III share a large number of physical-chemical properties with the apolipoproteins from humans and other vertebrates (*8, 40, 41*). Among the common features of exchangeable apolipoproteins are their ability to reversibly bind to lipoprotein surfaces, their content and type of amphipathic α-helices(*40*), and their ability to form discoidal lipoprotein particles (*42*).

The association of apolipoproteins with lipids is a complex process that involves several steps including protein conformational changes and the

disruption of the structure of the phospholipid monolayer or bilayer. Because of this complexity, the elucidation of the limiting steps and energy barriers involved in the formation of lipoproteins is also a complex task. Two processes were clearly distinguished in binding of apoLp-III to a planar lipid bilayer (*11*); the first process consisted in an adsorption of apoLp-III to the phospholipid bilayer, whereas the second process involved the insertion of the protein into the lipid bilayer and the formation of lipoprotein complexes (*11*). A recent study with disulfide mutants of apoE has shown that three binding steps involving different conformations of the protein can be distinguished along the pathway that leads to the formation of discoidal lipoproteins of apoE and DMPC (*12*). The initial binding step(s) of the apolipoprotein to the lipid surface may be envisaged as an adsorption process involving small structural changes in the protein. On the other hand, large conformational changes may be needed to achieve the final lipid-bound state, which is thought to involve major interactions between the nonpolar faces of the amphipathic α-helices and the lipid surface (*40-44*). The role of the conformational flexibility is expected to be particularly important for apolipoproteins that have a defined tertiary structure, such as apoA-I, apoE, and apoLp-III. The nonpolar sides of the amphipathic α-helices of these apolipoproteins are mostly buried in the protein core, unavailable for interaction with a lipid surface. A recent spectroscopic study of single Trp mutants of *L. migratoria* apoLp-III in the lipid-free state showed that the helices 1 and 5 are characterized by a greater hydration and mobility than helices 2–4 (*18*). On the basis of the conformational flexibility of helices 1 and 5 and the relevance of this

property to the function of an exchangeable apolipoprotein, we suggested that the separation of the helices 1 and 5 could constitute an important step in the exposure of the hydrophobic core of the protein that is required to achieve the lipid-bound state (*18*). In order to investigate the validity of this model, we have designed a double Cys mutant, which allowed us to tether the helices 1 and 5 of apoLp-III and test the role of their conformational flexibility in the lipid binding properties of the apolipoprotein. The results of this study demonstrate an essential role of the conformational flexibility of the N- and C terminal helices in the lipid binding activity of the apoLp-III.

Experimental Procedures

Site-directed Mutagenesis—Site-directed mutagenesis was carried out using the commercial kit, “QuickChange”, manufactured by Stratagene. A pET-32a plasmid (Novagen, Madison, WI) containing the insert of *L. migratoria* apoLp-III was used for mutagenesis. The polymerase chain reaction containing the plasmid and the primers was performed according to the manufacturer instructions using the *Pfu* DNA polymerase. Competent cells, Epicurian (Stratagene), were transformed with the polymerase chain reaction. The plasmid DNA of the transformed bacteria was sequenced from the S-tag and T7-terminator sites. AD494 expression host cells were transformed with the pET-32aapoIII plasmids containing the correct sequences. Wild type *L. migratoria* apoLp-III contains no Cys residues and two Trp residues at positions 113 and 128. The double Cys mutant was constructed using as template the single Trp mutant W128F. The reason for choosing the single Trp mutant instead of the wild type protein resides in the fact that the former is spectroscopically simpler and therefore will be useful for future fluorescence spectroscopic studies of the double Cys mutant. This strategy was possible because the structural and lipid binding properties of the single Trp mutant are indistinguishable from the properties of the wild type protein. The location of the Cys residues was chosen on the basis of the crystal structure of *L. migratoria* apoLp-III (aep1.pdb). The following substitutions were carried out: T18C (helix 1) and A147C (helix 5). The amino acid sequence surrounding the residues Thr18 and Ala147 are IAEAVQQLNHTIVNAAHEL and EAAEKTKEAAANLQNSIQS, respectively. A

helical wheel representation obtained at the Web site of the ExPASy Molecular Biology Server indicates that Ala147 is located near the center of the hydrophilic face of the α-helix 5, whereas Thr18 is located near the interface of the polar and nonpolar faces of helix 1 (data not shown). On the other hand, from the crystal structure of apoLp-III, and using the program Insight-II, it was inferred that replacement of residues Thr18 and Ala147 by Cys would result in a protein containing a solvent-exposed disulfide bond (**Figure-6**).

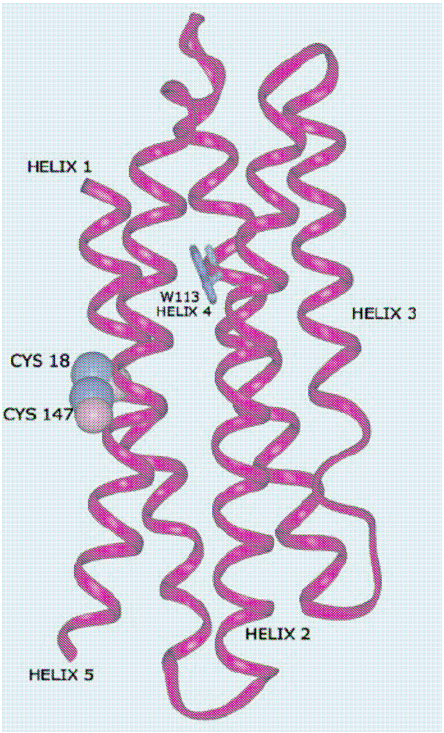

Figure-6: **Tethering of the N-terminal and C-terminal helices of apoLp-III**. Shown is the location of the disulfide bond in the mutantcontaining a Cys residue in helix 1 (*Cys 18*) and another Cys residue in helix 5 (*Cys 147*). Also shown is the single Trp residue at position 113. The location of the residues was represented using the crystallographic coordinates of ApoLp-III (aep.pdb) and the molecular modeling program Insight.

Protein Expression and Purification—Thioredoxin-apoLp-III fusion proteins were overexpressed and isolated from the bacteria as previously reported (*15, 18*). The fusion proteins were purified by standard nickel affinity chromatography. Recombinant locust apoLp-III was cleaved from the rest of the fusion protein with

enterokinase (Novagen, Madison, WI). ApoLp-III does not have any cleavage sites for enterokinase. ApoLp-III was purified from the cleavage reaction by nickel affinity chromatography and ion exchange chromatography in DE52. The purity of the proteins was monitored by SDS-polyacrylamide gel electrophoresis.

Circular Dichroism—CD spectra were acquired in a Jasco-715 CD instrument using a 0.1-cm path length cell over the 190–250-nm range and a 1-cm path length cell in the near-UV (250–315 nm). The CD spectra were acquired at 25 °C every 1 nm with a 2-s averaging time per point and a 1-nm band pass.

Alkylation of the Double Cys Mutant-After its purification, the recombinant double Cys mutant was recovered in a fully oxidized state, disulfide form. The Cys residues were alkylated with iodoacetamide. The reaction was performed in 50 mM potassium phosphate buffer containing 100 mM iodoacetamide and dithiothreitol at pH 6.5. The excess of dithiothreitol and iodoacetamide was removed by dialysis.

Protein Determination-The protein concentration in lipid-free apoLp-III samples was determined by UV absorption spectroscopy in the presence of guanidine HCl using an extinction coefficient of 5700 M^{-1} cm^{-1} for single Trp mutants and 11,400 M^{-1} cm^{-1} for the wild type protein, which contains two Trp residues. UV absorption spectra were recorded with a HP 8453 diode array spectrophotometer.

Kinetics of ApoLp-III-DMPC Interaction-The kinetics of formation of discoidal lipoproteins of apoLp-III/DMPG or apoLp-III/DMPC was monitored by the decrease in absorbance at 325 nm that accompanies the transformation of

the multilamellar liposomes into discoidal lipoprotein particles as described by Pownall *et al (45).* The reactions were performed at 23.4 °C (DMPG) or at 23.9 °C (DMPC), under continuous magnetic stirring, in a Hewlett Packard diode array spectrophotometer equipped with a temperature-controlled cell holder. The reaction was started by the addition of 50 µl of a liposome suspension (2.5 mg of phospholipid/ml). Data acquisition was started within 15 s after the addition of the liposomes. Because the reaction of apoLp-III is much faster with liposomes made of DMPG than DMPC (*46*), the kinetics using liposomes made with DMPG was carried out at a lower (1:86) protein/lipid molar ratio than the reaction with DMPC (1:16).

Results

Structural Properties of the Double Cys Mutant-Using the crystallographic structure of *L. migratoria* apoLp-III (*6*), the residues Thr18 and Ala147 were found suitable to design a disulfide bond tethering the centers of helices 1 and 5. The Cα atoms of these two residues have an optimal distance and orientation for the formation of a disulfide bond without altering the protein structure. The double-Cys mutant W128F/T18C/A147C was constructed, expressed, and purified. The ability of the double Cys mutant to form a disulfide bond was readily assessed by SDS-polyacrylamide gel electrophoresis gel shifts. As expected from other studies of disulfide-containing proteins (*12, 47*), in the oxidized form the double Cys mutant displays a greater electrophoretic mobility than in the reduced state (**Figure-7**). The reduced Cys mutant has the same electrophoretic mobility as apoLp-III molecules containing no Cys residues (wild type protein and W128F mutant). The intensity of the protein bands in Coomassie Blue-stained gels indicates that 100% of the protein is oxidized under nonreducing conditions. The double Cys mutant can be reduced by dithiothreitol in the presence of denaturants or SDS. However, in the native lipid-free state, this mutant spontaneously and rapidly reoxidizes to the disulfide form. Because the reducing agents interfere with the spectroscopic studies of the secondary and tertiary structure of the protein, it was chosen to alkylate the Cys residues with iodoacetamide, which does not modify the protein charge. The protein was readily alkylated by iodoacetamide, and its electrophoretic mobility was identical to that of the wild type protein (**Figure-7**). We will refer to the alkylated protein as

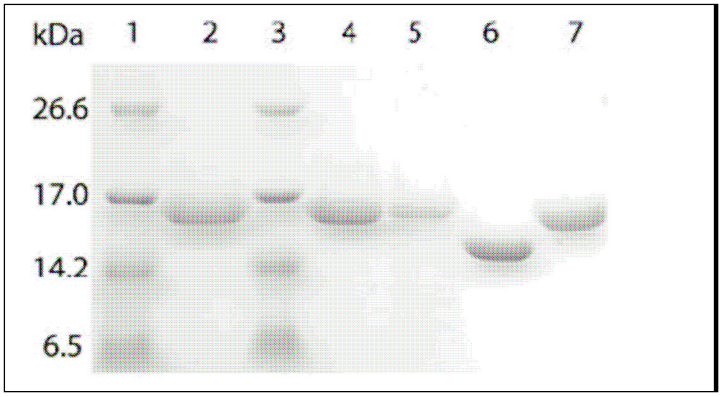

Figure-7: **SDS-polyacrylamide gel electrophoresis of oxidized and reduced forms of disulfide mutant**. *Lane 1*, molecular weight markers; *lane 2*, disulfide mutant reduced state (10 mM dithiothreitol+SDS); *lane 3*, molecular mass markers; *lane 4*, wild type ApoLp-III; *lane 5*, W128F mutant; *lane 6*, disulfide mutant oxidized state; *lane 7*, alkylated disulfide mutant. Electrophoresis was performed in 16% polyacrylamide gels in Tris-Tricine buffer. The protein bands were visualized by Coomassie Blue staining.

the reduced state of the double Cys mutant. A potential perturbing effect of either the mutations *per se* or the state of oxidation of the disulfide bond on the secondary structure of ApoLp-III was assessed by circular dichroism in the far-UV. **Figure-8A** shows the CD spectra of the double Cys mutant in the oxidized and reduced states as well as the spectra of the recombinant wild type apoLp-III and the single Trp mutant W128F, which was used to construct the double Cys mutant. Clearly, there are no significant differences among the far-UV CD spectra of the proteins. These results indicate that the formation of a disulfide bond or the alkylation of the Cys residues had no impact on the structure of apoLp-III. In every case, the CD spectra of the proteins were nearly identical and indicated that the proteins were highly α-helical. An estimate of the α-helical content using the method of Chen and Yang (*48*) indicates that the proteins contain between 56 and 62% of α-helix structure. Potential changes in the packing or tertiary structure of apoLp-III resulting from the mutations or the state

of oxidation of the disulfide bond were investigated by near-UV CD spectroscopy (**Figure-8b**). The CD spectrum of the single Trp mutant containing no Cys residues (W128F) is dominated by the spectroscopic properties of the Trp residue. The intensity of the CD bands observed between 260 and 310 nm indicates strong packing constrains for this Trp residue, which is located in helix 4. The addition of two Cys residues (T18C/A147C) does not change the CD spectrum of the Trp residue of apoLp-III in either the reduced or oxidized state of the disulfide bond. It is interesting to point out the apparent contribution of the disulfide bond in the near UV CD spectrum of the oxidized protein. It can be

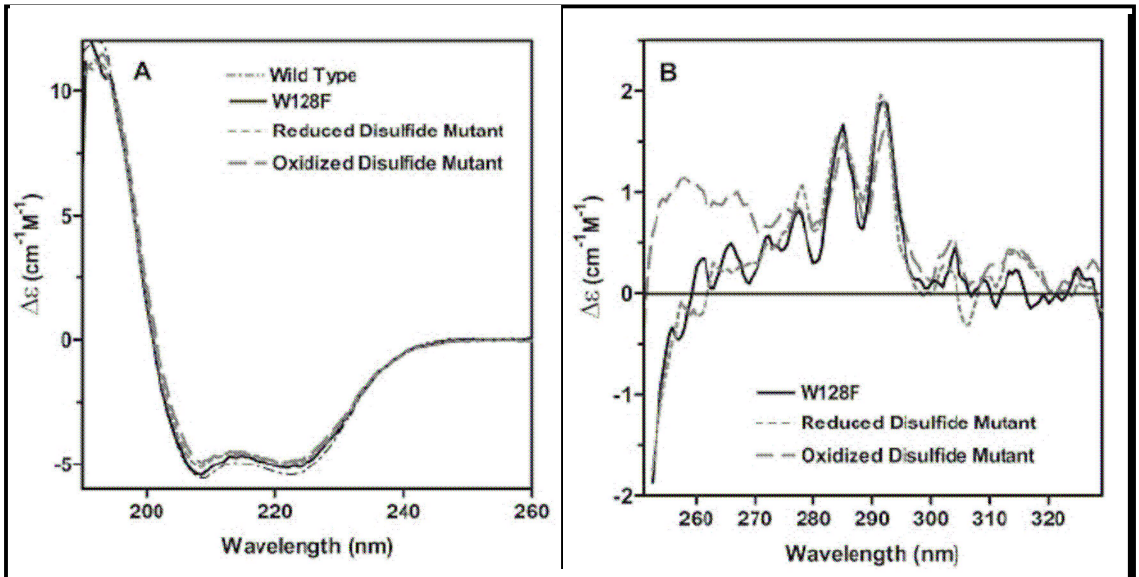

Figure-8: Structural characterization of apoLp-III mutants. *A*, far-UV CD spectra of oxidized and reduced forms of the double Cys mutant, W128F/T18C/ A147C. For comparison, the CD spectra of the wild type protein and the W128F mutant are also shown. All spectra shown were acquired in 50 mM potassium phosphate buffer, pH 6.5, at 25 °C. *B*, near-UV CD spectra of oxidized and reduced forms of the double Cys mutant and the control mutant W128F. The corresponding *symbols* are indicated. The spectrum of the wild type protein is not shown, because it has contributions from an additional Trp residue.

observed in the **Figure-8** that between 250 and 270 nm, the intensity of the CD spectrum is larger when the Cys residues are forming a disulfide bond. This is the region where the CD absorption bands of the disulfide bond are expected(*49*). Overall, the CD studies indicated that the mutants were suitable to study the role of the conformational freedom of helices 1 and 5 on the function of apoLp-III.

Kinetics of Formation of Discoidal Lipoproteins-The ability of apoLp-III to interact with liposomes and form discoidal lipoproteins particles was tested by studying the clearance of turbidity that occurs when exchangeable apolipoproteins interact with liposomes and induce the formation of discoidal lipoprotein particles (*45*). Multilamellar liposomes made of DMPC or DMPG were used in these assays. **Figure-9** shows the decays of turbidity observed with several proteins; the reduced double Cys mutant T18C/QA147C spontaneously reacts with DMPC or DMPG liposomes with a reaction rate similar to that of observed with wild type recombinant apoLp-III or the W128F mutant. In agreement with a recent study on wild type *L. migratoria* apoLp-III (*46*), the reactions were faster with DMPG than DMPC. On the other hand, no differences were observed between the changes in optical density obtained with liposomes alone (blank) or in the presence of the disulfide form of the mutant. This result indicates that when the helices 1 and 5 are tethered by a disulfide bond, apoLp-III is unable to form discoidal lipoprotein particles. A similar result is observed with either DMPC or DMPG liposomes. Moreover, the formation of discoidal

lipoproteins was not apparent even after 24 h of incubation of the liposomes with the disulfide mutant.

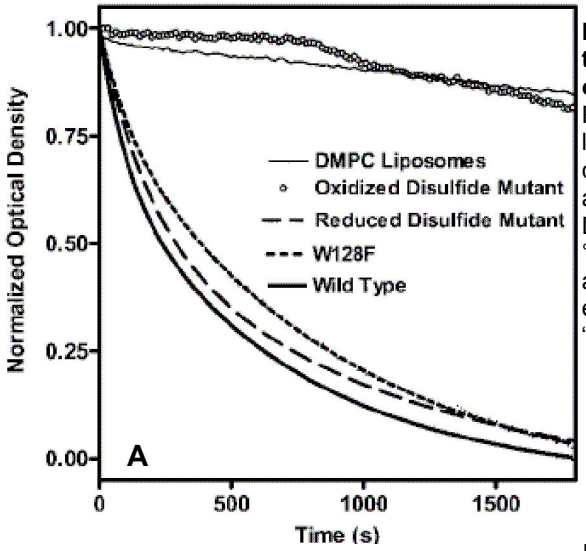

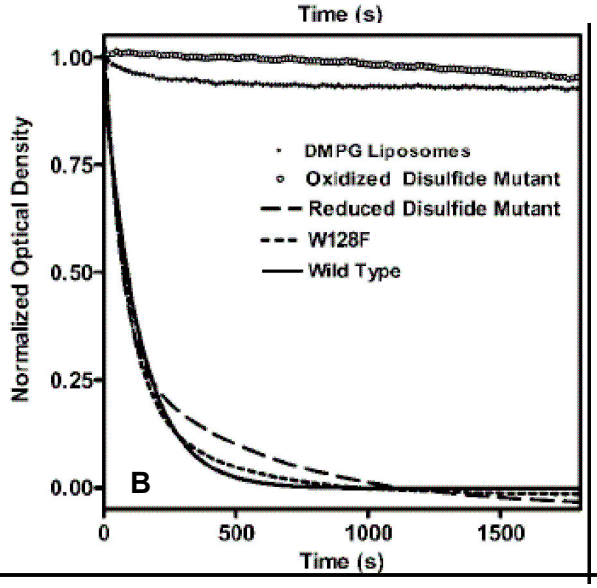

Figure-9: Effect of the disulfide bond tethering helices 1 and 5 on the kinetics of formation of discoidal lipoproteins. Reaction of apoLp-III with multilamellar liposomes of DMPC (A) or DMPG (*B*). The changes in optical density were monitored at 325 nm. Reactions with DMPG and DMPC were carried out at 23.4 and 23.9 °C, respectively. The *symbols* for different apoLp-III samples are indicated. Additional experimental details are given under "Experimental Procedures."

Discussion

Depending on the structure of the lipoprotein, two models are used to describe the interaction of the α-helices of exchangeable apolipoproteins with lipoprotein-lipid surfaces. For spherical lipoproteins, it has been proposed (*39*) that the amphipathic α-helices have an orientation parallel to the phospholipid monolayer surface. In this case, the hydrophobic faces of the helices are embedded in the phospholipid monolayer, whereas the hydrophilic faces remain at the lipid surface and strengthen the lipid-protein interaction by means of ionic interactions with the charged groups of the phospholipid. On the other hand, in discoidal lipoprotein particles, the apolipoprotein is assumed to stabilize the lipoprotein particle by interacting with the acyl chains along the periphery of the lipid bilayer disc (*27, 42, 44, 50, 51*). In any of these two possible final lipid-bound states of the apolipoprotein, a massive interaction of the helices with the lipoprotein lipid surface is thought to take place. Therefore, the achievement of the final lipid-bound state must involve a massive conformational change probably involving the displacement of entire helices to allow the exposure of the protein hydrophobic core. This conformational change is expected to occur at least in some apolipoproteins, such as apoLp-III, apoE, and apoA-I, for which most nonpolar domains of the amphipathic α-helices are buried in the protein core. Thus, it is reasonable to assume that the conformational flexibility of the apolipoprotein may play a major role in the lipid binding process. Two alternative models have been introduced to explain the mechanism of opening of the helix bundle of apoLp-III required for the interaction with the lipid. The first model was

introduced by Breiter *et al.(6)*, who on the basis of the crystal structure of apoLp-III and previous studies suggesting that apoLp-III could adopt two conformations at the water-air interface (*14*) postulated that the five-helix bundle undergoes a lipid-triggered opening at putative hinge domains located between helices 2 and 3 and between helices 4 and 5. This opening would expose a large extent of the hydrophobic interior of the protein allowing the lipid-protein interaction required for the final lipid-bound state. However, a subsequent study with *M. Sexta* apoLp-III showed that cross-linking of the loops connecting helices 1 and 2 and helices 3 and 4 did not prevent the apolipoprotein molecule from interacting with DMPC and forming recombinant lipoprotein particles (*52*). Therefore, we can infer that this mechanism is not taking place or that alternative mechanisms for the exposure of the hydrophobic domains can take place when the loops are tethered. We have recently introduced a second model proposing that one of the early conformational changes of apoLp-III during the lipid-binding process could involve spreading apart helices 1 and 5 (*18*). This model was based on experimental data indicating that helices 2–4 of apoLp-III constituted a well packed domain, whereas helices 1 and 5 were more mobile and hydrated as well as on the assumption that the conformational flexibility constitutes a key property of exchangeable apolipoproteins (*18*). To test the validity of this model, we investigated the effect of decreasing the conformational flexibility of helices 1 and 5 on the lipid binding activity of the apolipoprotein. For this purpose, we constructed a double Cys mutant that in the disulfide state tethered the centers of helices 1 and 5 of apoLp-III. The structure of this mutant as studied by circular

dichroism indicated that the mutations and the formation of the disulfide bond did not introduce a major perturbation in the secondary structure of the protein. Moreover, the internal packing of the protein, as determined by the packing constraints of the single Trp residue, was not altered, indicating that the disulfide mutant in either the alkylated state or the oxidized state was suitable to the study of the functional role of the conformational flexibility of helices 1 and 5. The results obtained in the kinetics of formation of discoidal lipoproteins clearly showed that in the oxidized state the disulfide mutant is unable to promote the formation of discoidal lipoproteins when incubated with either DMPC or DMPG liposomes. These results indicate that the separation of helices 1 and 5 constitutes a key step in the formation of discoidal lipoproteins.

Alternative mechanisms for the exposure of the hydrophobic core of the disulfide-tethered protein are in principle available. For instance, the helical bundle of the disulfide-tethered apoLp-III could still relax and expose its hydrophobic core to the lipid surface by breaking the interactions between any of the other four pairs of neighboring α-helices or by a mechanism similar to that proposed by Breiter *et al. (6)*, in which the interactions between two pairs of helices are simultaneously broken. In this regard, a recent study of disulfide mutants of apoE clearly showed that alternative mechanisms of opening of the helix bundle are available to apoE (*12*). The study with human apoE showed that tethering any of the four contiguous pairs of α-helices with a disulfide bond was not enough to prevent the formation of discoidal lipoproteins. Three disulfide bonds, which effectively prevented opening of the helix bundle, were required to

abolish the ability of apoE to spontaneously interact with DMPC liposomes and form discoidal lipoproteins (*12*). Given the similarities in structure and functional properties shared by the N-terminal domain of human apoE and the full-length apoLp-III (*38, 43*) and the demonstration that alternative lipid-binding mechanisms are available for human apoE (*12*), it was particularly surprising to find that only one disulfide bond was able to abolish the ability of apoLp-III to form discoidal lipoproteins. The inability of the disulfide mutant of apoLp-III to form discoidal lipoproteins clearly indicates that the conformational freedom of helices 1 and 5 is essential to the lipid binding process and cannot be substituted by alternative conformational changes.

The association of apolipoproteins with a lipid surface is a complex process that involves several steps including protein conformational changes as well as changes in the structure of the lipid surface. Because of this complexity, the elucidation of the key steps and energy barriers involved in the apolipoprotein-lipid interaction is a difficult task. Evidence for the existence of at least two binding steps has been reported for apoE (*11*)and for apoLp-III (*12*). The initial binding step of the apolipoprotein to the lipid surface may be envisaged as an adsorption process and could involve a small protein domain. This small domain could be a permanent surface domain or a result of short range conformational fluctuations. Contrarily, to reach the final lipid-bound state, which involves the interaction of large helical regions with the lipid surface, the apolipoprotein must undergo a major conformational change. This conformational change is likely to take place in several steps that gradually increase the extent

of the lipid-protein interaction to achieve the final lipid-bound state. Among these steps, long range concerted movements of entire helices might be needed. The fact that tethering the helices 1 and 5 of apoLp-III renders an inactive apolipoprotein suggests that the movement of helices 1 and/or 5 away from the helix bundle constitutes one of the key and early steps along the complex pathway for the formation of the final apolipoprotein lipid-bound state. Further investigations on the role of helices 1 and 5 in the lipid-protein interaction will be necessary to obtain additional insights into the mechanism of lipid binding. In this regard, the study of the arrangement of the helices in the lipid-bound state may prove to be useful for the understanding of the relevance of helices 1 and 5 in the lipid binding process.

CHAPTER-III

IN VIVO LIPOPROTEIN BINDING ASSAY OF THE INSECT EXCHANGEABLE APOLIPOPROTEIN, APOLIPOPHORIN-III

Introduction

Lipophorin is the only lipoprotein found in insects. It is composed of two structural apolipoproteins similar to human apoB (apoLp-I ~240kDa and apoLp-II ~ 80kDa) and one exchangeable apolipoprotein, apolipophorin-III (apoLp-III, 17kDa). ApoLp-III is an exchangeable apolipoprotein, which is present in the hemolymph of several insects in a lipid-free form, and bound to lipophorin particles of different density (*2*).

Exchangeable apolipoproteins are essential structural and functional protein of circulating lipoproteins (*53*). The most common approach to study the relationship between the structure and the function of exchangeable apolipoproteins resides in the production of mutants of the apolipoprotein molecules and the study of the impact of the mutations in the lipid-binding properties of the molecule. Several lipid-binding assays are used for this purpose. The most commonly used techniques include: 1) the liposomal clearance assay (*45*), which determines the ability of the protein to interact spontaneously with liposomes and lead to the formation of discoidal lipoproteins; 2) leakage of liposome content assay (*54*), which determines the ability of the protein to perturb the packing of a phospholipid bilayer; 3) detergent facilitated

formation of discoidal lipoproteins (*55*), which studies the ability of the protein to form discoidal lipoproteins upon incubation with mixed micelles of phospholipid and cholate; 4) inhibition of phospholipase C dependent lipoprotein aggregation (*56*).

Binding of apoLp-III and exchangeable apolipoproteins with lipids is a complex multistep process (*11, 12*). The use of different assays to study the lipid binding activity apolipoproteins is necessary to elucidate the mechanism of the lipid-protein interaction. However, from a physiological point of view, as well as a tool to investigate the lipid-protein interaction, it is also important to count with a method to study the lipid binding properties of mutant apolipoproteins to native lipoprotein particles. In this study we report an original *in vivo* binding assay for the interaction of locust apoLp-III with *Manduca sexta* lipophorin.

Experimental Procedures

Recombinant Wild Type Locusta Migratoria apoLp-III-Wild type locust apoLp-III was expressed in a pET32a expression vector containing an insert of thioredoxin-wild type apoLp-III fusion protein. The procedure followed for the expression and purification of apoLp-III has been previously reported (*18, 57*).

In vivo binding assays-2 to 3 day old adult (moth) insects from our laboratory colony were selected and injected with 20µg of locust wild type apoLp-III dissolved in 30µL of phosphate buffered saline. Hemolymph was collected 30 min. after the injection of locust apoLp-III and subjected to fractionation by ultracentrifugation in a KBr gradient, at 350,000 x g, at 4°C for 1 hour in a VTi 65.2 rotor (*58*). The gradient was fractionated into four fractions, fraction-1 (LDLp, density <1.05), fraction-2 (HDLp, density 1.06-1.11 g/cm^3), fraction-3 (HDLp, density 1.12-1.16 g/cm^3) and fraction-4 (free protein, density 1.17-1.25 g/cm^3). The fractions were dialyzed against 25mM phosphate buffer, pH6.5 containing 0.002% sodium azide for 2 hours at room temperature and used for SDS PAGE and western blot analysis.

SDS PAGE and Western Blot Analysis-To allow a direct quantitative estimation of the amounts of apoLp-III in the lipid-free and lipidbound fractions, proportional volumes of the KBr density fractions were loaded into a 4-20% Tris-glycine polyacrylamide gel. Standard Coomassie staining was used to visualize *M. sexta* apoLp-I, apoLp-II and apoLp-III bands. The stained gel was scanned horizontally and analyzed by densitometry to determine the relative abundance of apoLp-III and lipophorin in different density fractions. An identical gel was blotted

onto nitrocellulose membranes by semi-dry transfer in a Trans-Blot SD instrument (Bio-Rad, CA) and used to determine the amounts of locust apoLp-III in the lipoprotein fractions and in the lipid-free fractions (unbound). The blotted membrane was probed with a primary rabbit anti-locust apoLp-III antibody and a secondary goat-anti-rabbit IgG with a horseradish peroxidase tag. The bands were visualized by H2O2/lumino based chemiluminiscence assay kit (Chemicon International, CA).

Results and Discussion

Manduca sexta hemolymph contains 1-1.5mg of apoLp-III at a concentration of 20-30mg/ml. Ultracentrifugation of the hemolymph in a KBr density gradient readily separates lipid-free apoLp-III, which accumulates at the bottom of the gradient, from lipophorin-bound apoLp-III. Lipophorin-bound apoLp-III is distributed between high-density lipophorin, HDLp, and low-density lipophorin, LDLp, subspecies. These lipoprotein fractions are found in the top-half of the gradient (**Figure-10a**). HDLp and LDLp are interconverted in circulation by gaining, or losing, lipid molecules and apoLp-III (*5, 59-62*). This study was carried out with resting insects. Under this condition, nearly 40 % of *Manduca sexta* apoLp-III is found in the lipid-free fraction (Figure 10a, and Table-2) and the remaining is distributed between LDLp and HDLp. The presence of LDLp in resting *Manduca sexta* moths is a well-known fact (*62, 63*).

Because apoLp-III molecules from these two insect species share identical functions and structures (*64*), the possibility of studying the *in vivo* lipid binding activity of *Locusta migratoria* apoLp-III using *Manduca Sexta* (moth) insects was investigated. Given the fact that the sequence identity of locust and moth apoLp-III molecules is very low (*2*), antibodies raised against one of these molecules do not cross-react with the other apoLp-III. Therefore, we have made use of antibodies to detect and quantify the distribution of locust apoLp-III between the lipid-free and lipoprotein bound fraction. As shown in Figure-10b, wild-type locust apoLp-III binds to *Manduca sexta* lipoproteins, LDLp and HDLp, and distributes between the lipid-free and lipid-bound fractions in a fashion

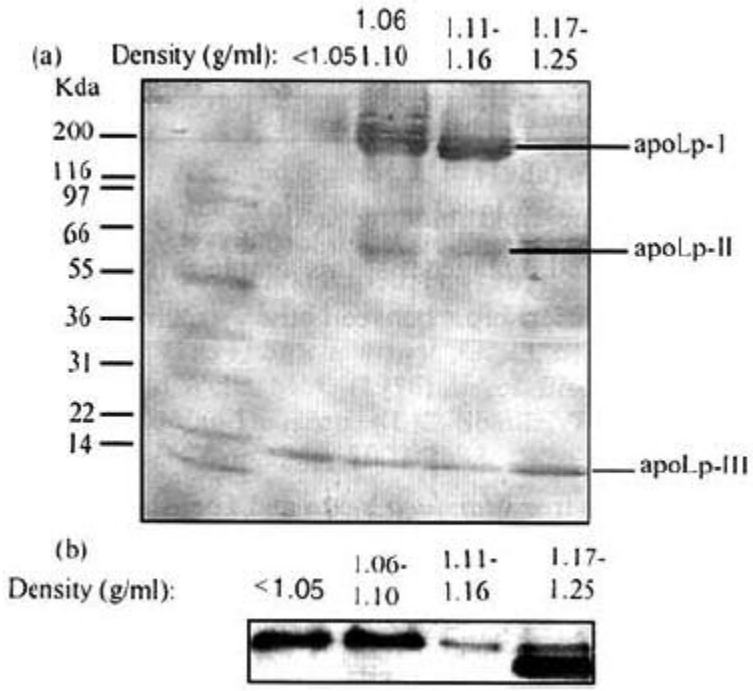

Figure -10: *In vivo* binding of locust apoLp-III to *Manduca sexta* lipophorin. a) Coomassie Blue stained, 4-20% SDS-PAGE of the hemolymph fractions obtained by ultra-centrifugation in a KBr density gradient; b) Western blot with anti-locust apoLp-III IgG.

similar to that of *Manduca sexta* apoLp-III (**Figure-10a**). The amount of *locust* apoLp-III bound to lipophorin was estimated semi-quantitatively by scanning densitometry. In this assay ~ 26% of the *locust* apoLp-III was found bound to LDLp, ~34% bound to HDLp, and the remaining 40% was found in the lipid free fraction. The distribution of *Locusta migratoria* apoLp-III between the density fractions of the hemolymph is nearly identical to the distribution of *Manduca sexta* apoLp-III (**Table-2**) indicating that wild type locust apoLp-III and *Manduca sexta* apoLp-III have similar lipid binding affinities for lipophorin.

Fraction	Density (g/cm^3)	Fraction	Lipophorin %	ApoLp-III (%)	Moles ApoLp-III per Lipoprotein
1	<1.05	LDLp	3.7	29	12
2	1.06-1.11	HDLp	56.9	20	3.0
3	1.12-1.16	HDLp	39.3	13	3.0
4	>1.16	Free protein	--	38	--

Table-2: Distribution of lipophorin and apoLp-III among the KBr density fractions. The relative amounts of lipophorin and apoLp-III in the gradient fractions of *Manduca sexta* hemolymph were estimated by scanning- densitometry of the Coomassie blue stained gel as indicated in Experimental Procedures.

This study indicates that the lipid binding activity of recombinant locust apoLp-III can be assayed *in vivo*. Coupled to site directed mutagenesis, this simple *in vivo* binding technique is expected to be very useful to study the relationship between the structure and function of exchangeable apolipoproteins.

Rationale of the Assay

Referring to the concentration of lipid-free *Manduca sexta* and *Locusta migratoria* apoLp-III as C_A and C_B, respectively, the following two equilibriums must be satisfied in the hemolymph:

$K_A = C_A (n - \nu) / \nu_A$ (1) $K_B = C_B (n - \nu) / n_B$ (equation-1)

Where n is the total number of binding sites in lipophorin and ν is the number of occupied binding sites.

$\nu = \nu_A + \nu_B$, and the terms $(n - \nu)$ in (1) and (1') are identical because both equilibriums occur simultaneously. Thus the ratio of 1/1' is:

$$K_A / K_B = C_A \nu_B / C_B \nu_A \text{ (equation-2)}$$

C and ν can be expressed as function of the total apolipoprotein concentration and the mole fractions of bound and free apolipoprotein as:

$$C_B = C_B^{(total)} (1 - X_B^{(bound)}) \text{ , and } \nu_B = C_B^{(total)} X_B^{(bound)}$$

A similar relationship exists for A, and replacing these relationships in (equation-2):

$$K_A / K_B = (1 - X_A^{(bound)})\, X_B^{(bound)} / (1 - X_B^{(bound)})\, X_A^{(bound)} \quad \text{(equation-3)}$$

This relationship (equation-3) shows that the ratio of the dissociation constants for the host and the test apolipoproteins is only related to the fractions of bound and free proteins. Therefore, determining these fractions we can determine the lipid binding affinity of a test apoLp-III relative to the lipid binding affinity of the host apolipoprotein.

CHAPTER-IV

ROLE OF HELICES AND LOOPS IN THE ABILITY OF APOLIPOPHORIN-III TO INTERACT WITH NATIVE LIPOPROTEINS AND FORM DISCOIDAL LIPOPROTEIN COMPLEXES

Introduction

Apolipophorin-III (apoLp-III) from the hemolymph of the locust (*Locusta migratoria*) is an exchangeable apolipoprotein with a molecular mass of ~17 kDa (*14*). ApoLp-III participates in transporting lipids among the insect tissues (*2, 65*). The X-ray crystal structure of *L. migratoria* apoLp-III in the lipid-free state indicates that the protein has an overall shape of a prolate ellipsoid, composed of a bundle of five amphipathic α-helices (*6*). Similar structures were recently inferred for *Manduca sexta* and *L. migratoria* apoLp-III by NMR spectroscopy (*7, 66*). Both insect apoLp-III molecules share structural and physiochemical properties with the N-terminal four-helix bundle (22 kDa) of the human apolipoprotein E (apoE) (*39*).

Binding of exchangeable apolipoproteins to the lipoprotein lipid surface is a complex process, which is likely to involve several steps and changes in the protein structure as well as changes in the structural organization of the lipid molecules. Binding of human ApoA-I to lipids has been suggested to occur in a multistep process (*67, 68*) involving an initial adsorption followed by penetration of the amphipathic R-helices into the phospholipid bilayer. On the basis of the

lipid-binding activity of disulfide mutants, a similar multistep process has been suggested by Lu et al. (*12*) for human apoE. These studies indicate an initial interaction of apoE with the lipid surface without major helical rearrangements followed by a major rearrangement of constituent R-helices of apoE. Two steps in binding of apoLp-III to a planar bilayer were also distinguished by surface plasmon resonance (*11*). The interaction of apolipoproteins with lipid surfaces is dependent on the properties of both the protein and the lipid surface. The changes in lipid composition of lipoproteins that take place in circulation constitute the driving forces for binding of the apolipoproteins to the lipoprotein, as well as to their dissociation from the lipoprotein lipid surface. On the other hand, the properties of the protein define the rate of the binding process and the affinity of the bound state (*69, 70*). One of the common features of exchangeable apolipoproteins resides in their ability to undergo conformational changes (*71*). The conformational flexibility of apolipoproteins (*70*), and membrane-binding proteins (*72*), may be required for the initial binding steps, such as the adsorption of the protein to the lipid surface, as well as for subsequent structural changes that would lead to a final lipid-bound state.

To investigate the role of the conformational flexibility of different regions of the apoLp-III molecule and its mechanism of interaction with lipid surfaces, disulfide mutants were designed on the basis of the crystal structure of the protein. Two disulfide mutants restricting the conformational flexibility of the neighboring α-helices 1 and 5 (H1-H5) and 3 and 4 (H3-H4) and one disulfide mutant tethering the second and fourth loops (L2-L4) were successfully

constructed and expressed. The ability of these mutants to form discoidal lipoproteins upon interaction with both phospholipid bilayers and preformed discoidal micelles was investigated. Moreover, the lipid-binding activity of the proteins was studied in vivo providing information on the mechanism of interaction of apoLp-III with native spherical insect lipoproteins. The comparison of the lipid-binding properties of these mutants provided information about the role of different regions of the apoLp-III molecule in the insertion of the protein into phospholipid bilayers and spherical monolayers.

Experimental Procedures

Site-Directed Mutagenesis and Protein Expression-Wildtype apoLp-III was cloned in a pET32a expression vector (Novagen, Inc., Madison, WI) and used as template for sitedirected mutagenesis. Mutagenesis was carried out using the QuickChange kit from Qiagen Sciences, MD. The procedures followed for the expression and purification of wild-type and cysteine mutants of apoLp-III are the same as reported earlier (*57, 73*). The proteins were expressed in bacteria as thioredoxin-apoLp-III fusion proteins, cleaved with enterokinase, and purified by affinity chromatography. To facilitate the spectroscopic characterization of the proteins, the disulfide mutants were constructed after obtaining the single Trp mutant W128F, which has structural and lipid-binding properties similar to the wild-type protein (*15*). The location of the residues potentially suitable for the formation of a disulfide bond was selected by visual inspection of the crystal structure (1aep PDB) and replaced by Cys using the molecular modeling program Insight-II. The distances between the S-atoms were measured for different combinations of rotamers of the Cys side chains. Those residues that provided the shortest distance of separation between the sulfur atoms were selected for mutagenesis. The mutant H3-H4, which tethers the centers of α-helices 3 and 4, has the following substitutions: W128F, N81C (helix-3), and Q112C (helix-4). The mutant L2-L4, which tethers the loops connecting helices 2-3 and 3-4, has the following substitutions: W128F/S70C/A127C. The construction and expression of T18C/A147C has been reported earlier (*73*).

Alkylation of Cysteine Mutants-The purified double cysteine mutants were fully oxidized (disulfide state). To study the reduced form of the mutants, it was necessary to alkylate the Cys residues. Alkylation was carried out with iodoacetamide as described previously (*73*).

Circular Dichroism-Far and near UV CD spectra were obtained in a Jasco-715 CD instrument, as described previously (*73*). The concentration of the free apoLp-III mutant and wild-type were determined by UV absorption spectroscopy in the presence of 3 M Gdm-HCl.

Kinetics of the Spontaneous Formation of Discoidal Lipoproteins-The kinetics of formation of discoidal lipoproteins was studied using multilamellar vesicles of DMPC, as described by Pownall et al. (*45*). The reaction was performed at 23.9 °C, in 50 mM potassium phosphate buffer pH 6.5, with continuous magnetic stirring in a Hewlett-Packard 8453 diode array spectrophotometer equipped with a temperature-controlled cell holder at a protein to lipid molar ratio of 1:20. The reaction was started by the addition of 25 *μ*L of 2.5 mg/mL DMPC (MLV), and data acquisition was started within 15 s after the addition of liposomes. Data were acquired continuously over a 30 min time period.

To determine the sizes of lipoprotein disks formed by spontaneous interaction, a concentrated sample of apoLp-III and MLV of DMPC (47.5 *μ*M protein in a final volume of 40 *μ*L) was prepared using a 1:20 protein to lipid molar ratio. ApoLp-III was incubated for 24 h with MLV of DMPC at 23.9 °C, and

then, the reaction mixture was subjected to nondenaturing gradient PAGE in 4-20% gels for 12 h at 120 V.

Preparation of ApoLp-III-DMPC Discoidal Complexes by Detergent Dialysis- Discoidal complexes of apoLp-IIImutants and DMPC were prepared by a cholate dialysis method (*55*) using a protein/DMPC/cholate molar ratio of 1:60:60. Cholate was removed from the mixture by extensive dialysis against 25 mM potassium phosphate buffer, 125 mM NaCl, pH 7.3. After dialysis, the apoLp-III/DMPC complexes were characterized by nondenaturing gradient gel electrophoresis and KBr density gradient ultracentrifugation. The sizes of the lipoprotein particles were calculated from the *R*f values and calibration curve of the high range molecular weight markers (Pharmacia).

Ultracentrifugation-The lipoprotein complexes formed by cholate dialysis were characterized by ultracentrifugation in a KBr density gradient (*58*). The samples (0.1 mL, 100 *μ*g of protein) were mixed with 2.0 mL of KBr solution (0.5g/mL), prepared in buffer 0.15 M NaCl, 0.001% EDTA, pH 7.5, and loaded in OptiSeal polyallomer tubes (Beckman Instruments, Inc. Palo Alto, CA). The samples were over layered with 2.9 mL of saline and centrifuged at 328 000g in a VTi-65.2 vertical rotor. After centrifugation, each tube was fractionated, and the density of the fractions was estimated by refractometry. The protein concentration was estimated from the second derivative spectra of the fractions.

In Vivo Binding of Recombinant L. migratoria apoLp-III to M. sexta Lipophorin. Binding of the disulfide mutants or wild-type locust apoLp-III to native spherical lipoproteins was studied in vivo as recently described (*74*). Adult male

M. sexta insects were injected with 20 *μ*g of locust apoLp-III mutant. Hemolymph was collected 120 min after the injection of the protein and subjected to fractionation by ultracentrifugation in a KBr gradient. The fractions were dialyzed against 25 mM phosphate buffer, pH 6.5, for 2 h at room temperature and used for SDS-PAGE and Western blot analysis. The relative amounts of locust apoLp-III associated with each fraction were determined by Western blotting using a rabbit anti-locust apoLp-III antibody. The blot was developed by chemiluminescence using horseradish peroxidase tagged goat anti rabbit IgG.

Results

The conformational flexibility of different helical and loop regions of apoLp-III was restricted by means of disulfide bonds, and the effect of the disulfide bonds on the ability of apoLp-III to form lipoprotein complexes was investigated in three different lipid-binding systems. In the first group of experiments, the ability of apoLp-III mutants to form lipoprotein complexes upon spontaneous interaction with liposomes of phosphatidylcholine was studied. In a second group of experiments, the ability of apoLp-III mutants to form discoidal lipoproteins upon interaction with discoidal mixed micelles of phosphatidylcholine and Na^+-cholate was investigated. Finally, the ability of apoLp-III mutants to interact with native spherical insect lipoproteins was studied in a novel in vivo lipid-binding assay.

Characterization of the Disulfide Mutants-The location of the Cys residues was selected on the basis of the coordinates reported with the crystal structure of apoLp-III (*6*), taking into account the predicted distances and angles of orientation between the sulfur atoms of the Cys residues. The disulfide bonds were designed to reside on the protein surface to minimize potential perturbations in the internal packing of the protein. Three disulfide mutants of apoLp-III were designed and expressed: the H3-H4 (N81C/Q112C) and H1-H5 (T18C/A147C) mutants have a disulfide bond tethering the centers of helices 3 and 4 and 1 and 5, respectively. The L2-L4 mutant (S70C/A127C) has a disulfide bond linking the second and fourth loops of the five-helix bundle of apoLp-III. The position of the Cys residues in the H3-H4 mutant and L2-L4 mutant

(S70C/A127C) is illustrated in **Figure-11**. The location of the disulfide bond on the H1-H5 mutant has been reported already (*73*).

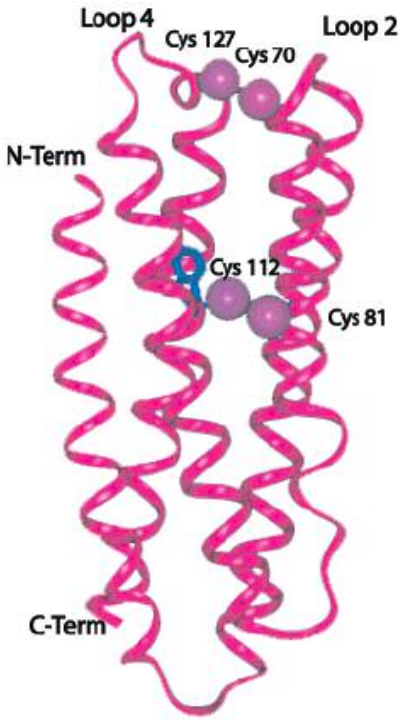

FIGURE-11: Position of the disulfide bonds tethering α-helices 3 and 4 (H3-H4 mutant) and loops 2 and 4 (L2-L4 mutant). The location of the single Trp residue, W113, of these mutants is also shown.

ApoLp-III mutants were expressed and purified to homogeneity. The difference between the electrophoretic mobility of oxidized and reduced disulfide mutants was used to investigate the formation of the disulfide bonds (*12, 47, 73*). The formation of disulfide bonds was complete for all mutants included in this study (See Appendix).

The far UV CD spectra of oxidized and reduced (alkylated) forms of the H3-H4 and L2-L4 mutants (**Figure-12**) showed that the proteins are predominantly α-helical. The wild-type protein and the disulfide mutants H3-H4

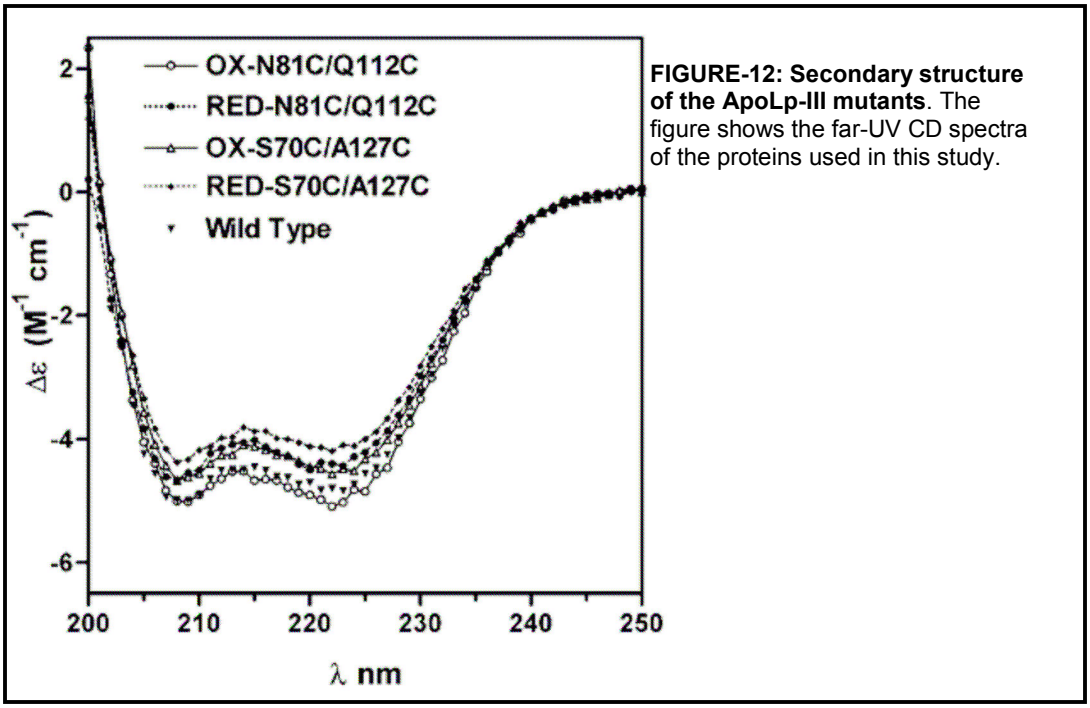

FIGURE-12: Secondary structure of the ApoLp-III mutants. The figure shows the far-UV CD spectra of the proteins used in this study.

and L2-L4 have α-helical contents of 61, 61, and 55%, respectively. Reduction of the disulfide bonds by alkylation decreased the α-helical content of both the H3-H4 and the L2-L4 mutants to 41%. As reported before (*73*), the estimated α-helical content of the oxidized H1-H5 is nearly identical to that of the wild-type protein. The structure of the mutants was also studied by fluorescence spectroscopy. The disulfide mutants used in this study contain a common single Trp residue in helix4 (W113, **Figure 11**). For all mutants, the fluorescence maximum was located at 314-315 nm, which is consistent with the nonpolar environment expected for the single Trp residue (*18, 75*).

Spontaneous Interaction of Disulfide Mutants with Multilamellar Vesicles (MLV) of DMPC-The kinetics of the formation of discoidal lipoproteins upon the spontaneous interaction of apoLp-III with MLV of DMPC was monitored spectrophotometrically. The transformation of the large MLV into small discoidal

lipoproteins is accompanied by a nearly complete clearance of the turbidity of the reaction mixture. **Figure-13A** shows the turbidity decays obtained for the disulfide mutants in both reduced and disulfide states as well as the decay obtained with the wild-type protein. In the reduced state, the mutants H3-H4 and L2-L4 clear the liposomal turbidity completely and at a rate comparable to that of the wild-type protein. However, both H3-H4 and L2-L4 mutants appear to be inactive in the oxidized state. It has been previously shown that the mutant H1-H5 is unable to interact with MLV of DMPC in the disulfide state but associates normally upon reduction (*73*).

Because of the short time span of the turbidimetric assay, a mutant characterized by a very slow rate of formation of discoidal lipoproteins could be seen as an inactive protein. To investigate this possibility, the ability of the mutants to form discoidal complexes was also studied using longer incubation times (24 h) and a higher protein and lipid concentration (45 μM protein) than that used in the turbidity assay (~4 μM). After incubation, an aliquot of the samples was used to determine the turbidity, and the remaining solution was analyzed by nondenaturing PAGE to determine the size of the lipoproteins. No discoidal lipoprotein complexes were detected by electrophoresis for oxidized H1-H5 and H3-H4 mutants (**Figure-13B**), confirming the lack of activity of the mutants H1-H5 and H3-H4 observed in the kinetics. However, after 24 h of incubation, a nearly complete clearance of liposomal turbidity was observed with the disulfide mutant L2-L4, and analysis of the samples by gradient gel electrophoresis confirmed the ability of the L2-L4 mutant to form lipoprotein complexes. The

lipoproteins obtained with this mutant were slightly larger than those obtained with the wild-type protein (**Figure-13B**, lanes 7 and 8).

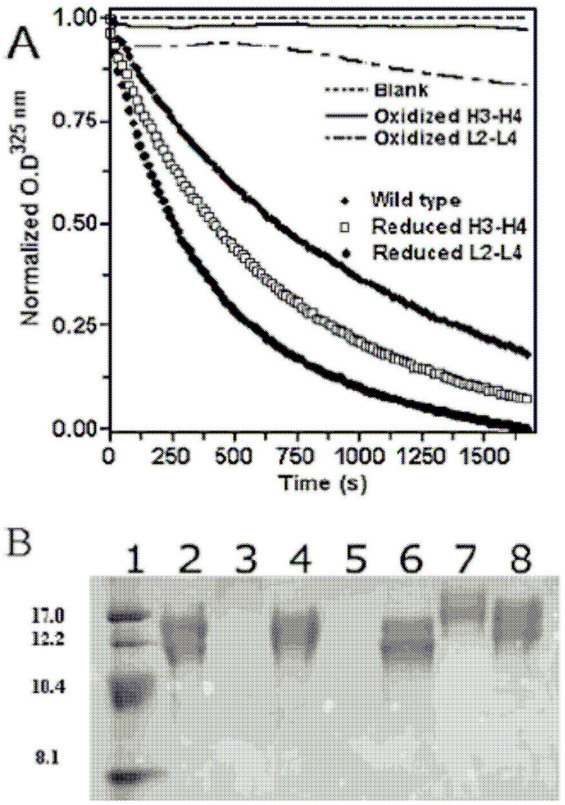

FIGURE-13: Spontaneous interaction of apoLp-III with multilamellar liposomes. (A) The kinetics of formation of discoidal lipoproteins was studied using aprotein to DMPC molar ratio of 1:20. The assay was performed at 23.9 °C for 30 min time period with 4 *i*M apoLp-III; (B) Nondenaturing 4-20% gradient PAGE of lipoprotein complexes obtained upon 24 h incubation of apoLp-III mutants (45μM) with DMPC: lane 1, high range molecular weight markers (Pharmacia); lane 2, wild-type; lane 3, oxidized H1-H5 mutant; lane 4, reduced H1-H5 mutant; lane 5, oxidized H3-H4; lane 6, reduced H3-H4; lane 7, oxidized L2-L4; and lane 8, reduced L2-L4. The numbers on the left side of the figure indicate the apparent diameters, in nanometers, of the markers loaded in lane 1.

Interaction of ApoLp-III Disulfide Mutants with Preformed Discoidal DMPC Micelles-ApoLp-III mutants were allowed to interact with preformed mixed micelles of DMPC and Na+-cholate, and their ability to lead to the formation of discoidal lipoproteins upon removal of the detergent was investigated. The H1-H5 mutant was the only inactive protein in the disulfide state. The disulfide mutants H3-H4 and L2-L4 promoted the formation of lipoprotein particles. The lipoproteins formed were characterized by their size (**Figure-14**) and density (**Figure-15**). The comparison of the sizes of the lipoprotein complexes obtained with the mutants H3-H4 and L2-L4 in both oxidized and reduced states shows

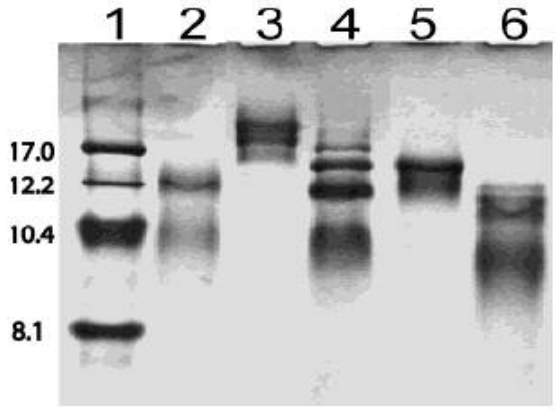

FIGURE-14: Interaction of ApoLp-III disulfide mutants with Cholate/DMPC mixed micelles. Nondenaturing PAGE of the lipoproteins prepared using a 1:60:60 protein/DMPC/cholate molar ratio: lane 1, high range molecular weight markers; lane 2, wild-type; lane 3, oxidized H3-H4; lane 4, reduced H3-H4; lane 5, oxidized L2-L4; and lane 6, reduced L2-L4. The numbers on the left side of the figure indicate the apparent diameters, in nanometers, of the markers loaded in lane 1.

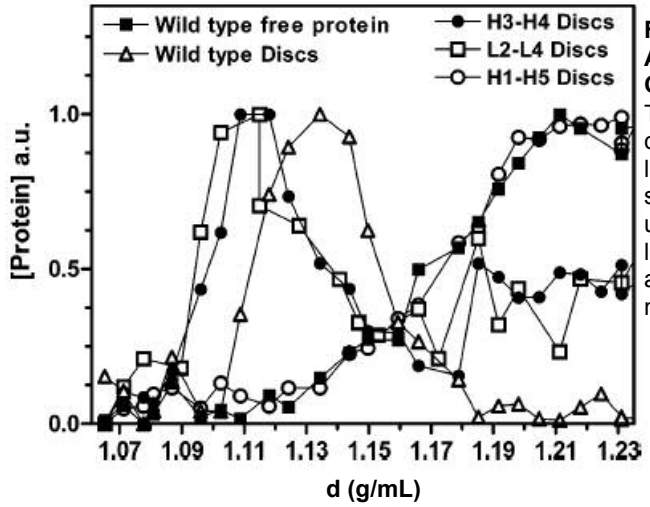

FIGURE-15: Interaction of ApoLp-III disulfide mutants with Cholate/DMPC mixed micelles. The density of the lipoprotein complexes and the presence of lipid-free (unbound) apoLp-III were studied by KBr density gradient ultracentrifugation. The lipoproteins were obtained using an initial protein/DMPC/ cholate molar ratio of 1:60:60.

that in the oxidized state the mutants produce larger lipoprotein particles than the wild-type protein. In the reduced state, these two mutants and the wild-type protein formed similar lipoproteins (**Figure-14**).

The density of the lipoproteins formed and the fraction of unbound apolipoprotein were studied by ultracentrifugation in a KBr density gradient. At a protein to DMPC molar ratio of 1:60, wild-type apoLp-III forms lipoprotein complexes with an average density of 1.135 g/cm^3 (**Figure-15**). The samples prepared with

oxidized H3-H4 and L2-L4 mutants form lipoprotein complexes with average densities of 1.105 g/cm^3. The lower density of the lipoprotein complexes obtained with the disulfide mutants is consistent with the fact that 30% of the protein remains in the lipid-free state accumulating at the bottom of the gradient. On the other hand, ultracentrifugation of the samples prepared with the H1-H5 mutant (oxidized state) indicated that 100% of the apolipoprotein is in the lipid-free state and found in the bottom half of the gradient (**Figure-15**).

On reducing the disulfide bonds, the density of the disks formed by the mutants is restored to the wild-type density of 1.13 g/mL (data not shown).

In Vivo Lipid-Binding Activity of ApoLp-III Disulfide Mutants-The hemolymph of adult *M. sexta* insects contains 1-1.5 mg of apoLp-III, which is found in the lipid-free form and bound to lipophorin particles of different density. Ultracentrifugation of the hemolymph in KBr density gradient readily separates lipid-free apoLp-III, which accumulates at the bottom of the gradient, from lipophorin-bound apoLp-III, which is distributed between HDLp and LDLp subspecies and found in the top-half of the gradient (*59*). ApoLp-III molecules from *M. sexta* and *L. migratoria* insects share identical functions (*64*) and structures (*8*). We have recently shown that wild-type *L. migratoria* apoLp-III injected into the circulation of *M. sexta* insects binds to the insect lipoproteins with an affinity similar to that of the endogenous, native, apoLp-III (*74*).
To study the in vivo lipid-binding activity of the disulfide mutants, we have compared the distribution of apoLp-III mutants between the lipid-free and the lipoprotein-bound fractions of the hemolymph with the distribution of wild-type

locust apoLp-III. **Figure-16** shows the distribution of wild-type *L. migratoria* apoLp-III and the disulfide mutants H1-H5, H3-H4, and L2-L4 among the lipoprotein-bound and lipid-free fractions of the *M. sexta hemolymph.* A simple inspection of Figure-16 shows major differences between the distribution of the wild-type protein, 45% of which is associated to lipoproteins (LDLp + HDLp fractions), and the distributions of the disulfide mutants H1-H5 and H3-H4, for which the fraction of lipoprotein bound apoLp-III represents only ~5%. These results indicate that the disulfide bonds tethering α-helices 1 and 5, or 3 and 4, inactivate apoLp-III. On the other hand, the L2-L4 mutant is distributed among the lipoprotein bound (36%) and lipid-free forms in a fashion similar to the wild-type protein indicating that tethering of the loops 2 and 4 has a minor impact on the lipid-binding activity of apoLp-III.

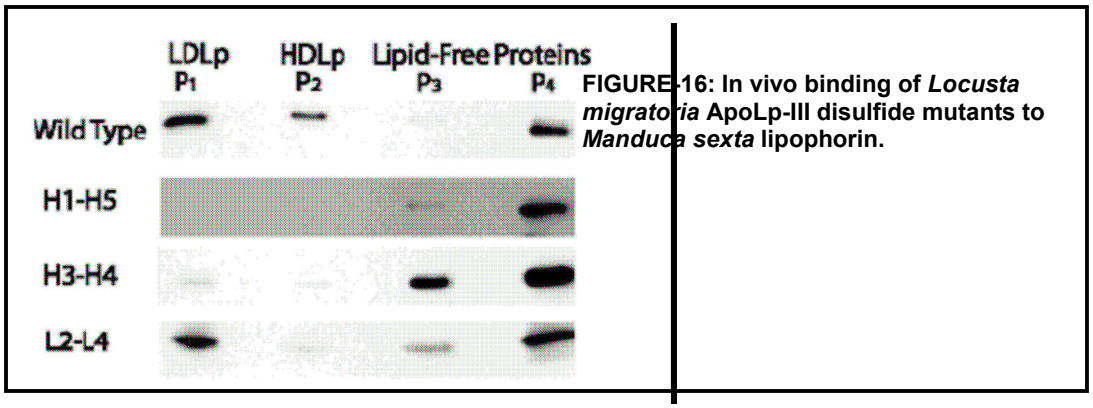

FIGURE-16: In vivo binding of *Locusta migratoria* ApoLp-III disulfide mutants to *Manduca sexta* lipophorin.

The distribution of *L. migratoria* apoLp-III mutants among the density fractions of *M. sexta* hemolymph was determined by Western blotting as indicated in the Experimental Procedures. The hemolymph was separated into four density fractions by ultracentrifugation in a KBr gradient; pool 1(P1): LDLp

(low-density lipophorin, $\delta < 1.06$ g/cm^3); pool 2 (P2): HDLp ($1.06 < \delta < 1.12$ g/cm^3); pool 3 (P3) and pool 4 (P4) contain lipid-free proteins ($\delta > 1.12$ g/cm3).

For the sake of clarity, a summary of the activity of the disulfide mutants of apoLp-III observed in different lipid-binding assays is shown in **Table-3**.

Table-3: Summary of Lipid-Binding Activity of the Disulfide Mutants of Apolipophorin-III

assay\mutant	WT	H1-H5	H3-H4	L2-L4
spontaneous interaction with liposomes	yes	no	no	yes
interaction with discoidal micelles	yes	no	yes	yes
in vivo binding to lipophorin	yes	no	no	yes

Discussion

The association of apolipoproteins with the lipid surface of lipoproteins and membranes may involve several steps. Among the possible steps, we could distinguish adsorption of the protein to the lipoprotein lipid surface, insertion into the phospholipid monolayer, or bilayer, and one or more conformational changes that would be required to achieve the extended protein conformation of the final lipid bound state. The protein conformational changes required in different steps along the binding process are not known. Some of the conformational fluctuations available to the protein in the lipid-free state could be particularly important for the lipid-binding activity of the protein. For instance, concerted conformational fluctuations of one or more α-helices could be necessary for the initial interaction of the protein with the lipid surface or for the insertion of the protein into a phospholipid bilayer or monolayer. Other conformational changes may occur after an initial association of the apolipoprotein with the lipid surface. The role of the conformational flexibility in the lipid-binding activity of apoLp-III was investigated using three disulfide mutants, which introduced well-defined structural restrictions in different regions of the apoLp-III molecule.

Differences between the Lipid-Binding Assays-Because the lipid-protein interaction is in general dependent on the physical and chemical nature of the lipid structure (*76*), the impact of the disulfide bonds on the lipid-binding activity of apoLp-III was studied in three different lipid-binding assays. The assays used imposed different restrictions to the lipid-binding activity of the protein providing additional information on the role of the conformational flexibility as well as on the

mechanisms of interaction. The spontaneous formation of lipoprotein particles upon interaction of the apolipoproteins with liposomes involves multiple steps including, among others, the insertion of the apolipoprotein into the bilayer and the breakdown of the large liposomal structures into small lipoprotein particles. On the other hand, the spontaneous association of apoLp-III with native spherical lipoproteins is limited by the ability of the protein to interact and become inserted into a spherical phospholipid monolayer. Finally, the interaction with discoidal micelles of DMPC overrides the initial steps of the lipid-protein interaction, such as the penetration of the protein or some of its R-helices in the lipid bilayer. In this assay, the protein activity would be limited by the ability of the protein to form a stable lipoprotein complex upon interaction with a lipid structure that is already small, discoidal, and has a preexposed hydrophobic surface around the bilayer disk (*77*). Thus, the interaction of apoLp-III with discoidal micelles of DMPC may not be impaired by the structural restrictions imposed by disulfide bonds to the extent that it impaired the interaction of the protein with a liposomal structure or with native lipoproteins.

Conformational Flexibility of Helices 3 and/or 4 Is Necessary for the Insertion of ApoLp-III into the PhospholipidMonolayer of Spherical Native Lipoproteins- The role of the conformational flexibility of helices 3 and 4 in the lipid-binding activity of apoLp-III was investigated with the mutants H3-H4 and L2-L4. Both mutants effectively prevent the separation of helices 3 from 4 (**Figure-17**). However, the disulfide present in the L2-L4 mutant tethers the N- and C-term residues of helices 3 and 4, respectively; therefore, it is expected to

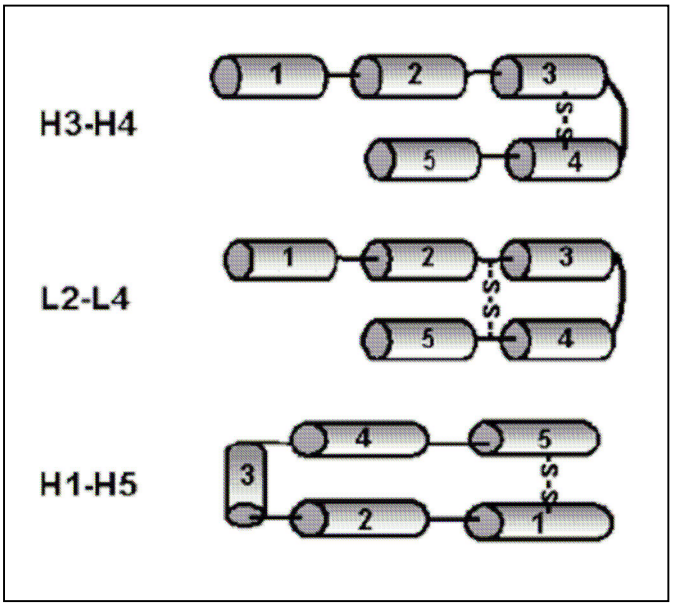

FIGURE-17: Sketched representation of the extended conformations that could be adopted by different disulfide mutants in the lipid-bound state.

reduce the conformational freedom of helices H3 and H4 to a lesser extent than the H3-H4 mutant, which tethers the centers of the helices.

The inability of the oxidized H3-H4 mutant to interact spontaneously with DMPC vesicles, or in vivo, with native spherical lipoproteins suggests that the conformational flexibility of helices 3 and 4 is essential in the disruption of the packing of both phospholipid monolayers and bilayers. Two facts support this interpretation; in first place, the H3-H4 mutant forms discoidal lipoproteins upon incubation with discoidal micelles of DMPC and cholate, indicating that it can interact with disk bilayers when the acyl chains are preexposed. In second place, the fact that the loop mutant interacts spontaneously with MLV of DMPC as well as with native lipoproteins indicates that the greater flexibility of the helices H3 and H4 tethered by the ends, as compared to the flexibility of the helices tethered by their centers, could be responsible of the lipid-binding activity observed in the

loop mutant. Because in a fully extended conformation both mutants could adopt similar structures (**Figure-17**), the activity of the loop mutant could not be explained by a difference in the stability of the lipid-bound state. This is also supported by the fact that H3-H4 and L2-L4 mutants lead to the formation of lipoproteins of similar properties when incubated with discoidal micelles (**Figure-14**). Thus, these results suggest that the conformational flexibility of helices 3 and/ or 4 is needed in the initial binding steps, including the insertion of the protein, or some of its regions, in phospholipid monolayers. For instance, as sketched in **Figure-18B**, unfolding of one of these helices could be required for the insertion of the protein into the phospholipid monolayer of native lipoproteins.

Interaction of Loops 2 and 4 with the Lipid Surface Does Not Mediate Opening of the Helix Bundle of ApoLp-III- The presence of surface exposed nonpolar residues, and the conformational flexibility of the loop regions of apoLp-III, have inspired models of apolipoprotein-lipid interaction in which the loops initiate the interaction with the lipid surface defect, and this interaction would, subsequently, trigger the opening of the helix bundle (*6, 7*). This type of mechanism was recently proposed on the basis of the conformational dynamics of loop 4, inferred from solution NMR studies (*7*). This model of interaction is represented in **Figure-18A**, and it suggests that loop 4 would initiate the interaction of apoLp-III with the lipoprotein surface leading to the separation of loops 2 and 4. The importance of this mechanism was tested in the present study by means of the L2-L4 mutant, which restricts the conformational flexibility of the loops and prevents the opening of the helix bundle through the separation of the

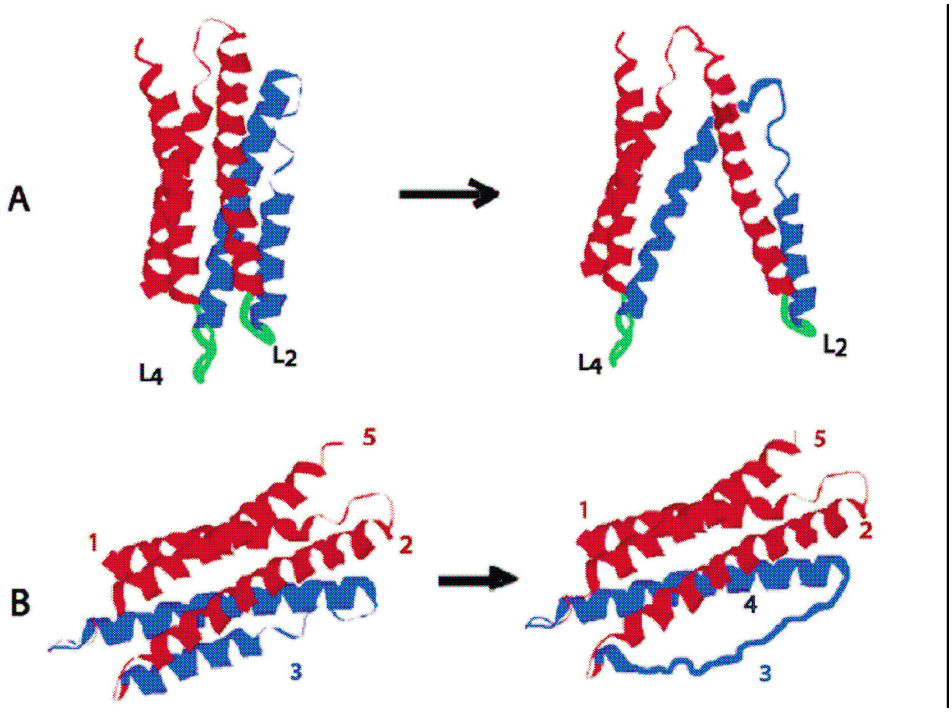

FIGURE-18: Models of interaction of ApoLp-III with lipoprotein lipid surfaces. Two models of the initial apolipoprotein-lipid interaction steps are sketched: (A) recently proposed model of initial apoLp-lipid interaction and opening of the helix bundle (Fan et al. (*6*)). In this model, the initial interaction of the loop 4 with the lipid surface would precede the opening of the helix bundle. (B) Alternative mechanism consistent with the observations made in the present study. In this model, the unfolding of helix 3 is involved in the initial insertion of the protein into the phospholipid structure. Similar models involving helix 4 or helices 3 and 4 simultaneously are also consistent with the results of this study. Helices 1 and 5 could also be involved in the initial steps of the lipid-protein interaction. However, because the disulfide mutant tethering helices 1 and 5 is inactive, our study provided no information on this regard.

loops 2 and 4. As shown in the Results, this disulfide mutant was able to form discoidal lipoproteins upon interaction with either liposomes or discoidal micelles. Moreover, this mutant was able to interact with native spherical lipoproteins in a fashion similar to that observed with the wild-type apoLp-III. The fact that tethering of loops 2 and 4 does not affect the lipid-binding properties of apoLp-III in vivo indicates that the interaction of these loops with the lipoprotein lipid surface is not necessary for either the initial recognition of the lipoprotein lipid surface or for the opening of the helix bundle. It has also been proposed that

interaction of loops 1 and 3 with the lipid surface would trigger an opening of the helix bundle (*6*). This hypothesis was tested in *M. sexta* apoLp-III, which has a similar structure to *L. migratoria* apoLp-III, by means of a disulfide mutant that was predicted to tether loops 1 and 3 (*52*). Interestingly, tethering of loops 1 and 3 did not prevent apoLp-III from interacting spontaneously with liposomes leading to the formation of discoidal lipoproteins. Therefore, it would appear that the interaction of the loops with the lipid surface is not necessary for either the initial recognition of the lipid surface or for the opening of the helix bundle.

Helices 1 and 5 Play a Major Role in the Stability of the Lipid-Bound State- We have recently shown that the conformational flexibility of helices 1 and 5 is required for the spontaneous interaction of apoLp-III with liposomes of phosphatidylcholine (*73*). In the current study, we have investigated further the role of helices 1 and 5 through the study of the interaction of the H1-H5 mutant with mixed discoidal micelles of DMPC and cholate and native spherical lipoproteins in vivo. The fact that this mutant does not associate with native spherical lipoproteins in vivo suggests that helices 1 and/or 5 could play an important role in the insertion of apoLp-III into the phospholipid monolayer of spherical lipoproteins. However, the fact that this mutant cannot form discoidal lipoproteins even upon interaction with discoidal micelles indicates that the conformational freedom of helices 1 and/or 5 is essential to achieve a strong lipidprotein interaction and thus for the formation of stable lipoprotein complexes. Although helices 1and 5 play a major role in stabilizing the lipid-bound state, our

results do not discard the involvement of these helices in the insertion of the protein in phospholipid monolayers and/or bilayers.

Multiple Lipoprotein-Bound Conformations of ApoLp-III-The preferred conformation of apoLp-III in discoidal lipoproteins appears to be one where the polypeptide chain adopts a fully extended conformation around the periphery of the disk bilayer (*16, 78, 79*). Because of the restriction imposed by the disulfide bond, none of the disulfide mutants used in this study could adopt such a conformation (**Figure-7**). Therefore, the ability of the L2-L4 and H3-H4 mutants to form discoidal lipoproteins indicates that other apolipoprotein conformations are compatible with the formation of stable discoidal lipoproteins. Recent studies of human apoA-I in discoidal lipoproteins provided evidence consistent with the presence of multiple apolipoprotein conformations, including variable apolipoprotein arrangements (*28, 80*). Two lipid-bound conformations of apoE were also inferred in a recent study with reconstituted spherical lipoproteins (*81*). The present study provides strong evidence indicating that multiple apolipoprotein conformations, or alternative conformations, are possible not only in discoidal lipoproteins but also in spherical native lipoproteins. This is supported by the fact that the L2-L4 mutant has an in vivo lipid-binding activity similar to that of the wild-type protein.

CHAPTER V

LIPID-BOUND CONFORMATION OF HUMAN APOLIPOPROTEIN AI

INTRODUCTION

An inverse correlation exists between the circulating levels of high density lipoprotein (HDL) in human circulation and coronary heart diseases (CHD) (*82-85*). Approximately 50% w/w of a HDL molecule is protein and apolipoprotein AI (apoAI) is the major protein associated with HDL(*86*). HDL molecules in the circulation are highly heterogeneous (*20, 87*) and can exist as large spherical HDL and small discoidal HDL particles. The small discoidal HDL molecules are efficient in removing cholesterol from peripheral tissues (*22*). HDL bound apoAI mediates cholesterol efflux from peripheral tissues and activation of cholesterol esterification enzyme lecithin-cholesterol acyl transferase (LCAT), two essential steps in the process of reverse cholesterol transport and prevention of CHDs (*19, 21, 36, 68, 88*). To better understand the physiology of lipid-bound apoAI it is essential to elucidate the structure of apoAI molecules in the lipid-bound state. Until recently, attempts to solve the lipid-bound conformation of exchangeable apolipoproteins have been by X-ray diffraction at 8 Å resolution (*89, 90*). The lack of high-resolution X-ray diffraction data of lipid-bound apolipoproteins can be attributed to the difficulties in obtaining diffraction quality lipoprotein crystals. This lack of high resolution structure of lipid-bound apoAI has been a major impediment in apoAI structure-function research. Novel technique utilizing

chemical cross-linking with a fixed arm length cross-linker coupled with mass spectrometry provides distance constraint data which aid in elucidating the low-resolution three-dimensional conformation of proteins (*91-98*). Discoidal HDL particles containing two molecules of apoAI can be easily reconstituted and owing to the physiological significance of these discoidal lipoprotein particles in reverse cholesterol transport (RCT) understanding the conformation of apoAI molecules in discoidal lipoproteins is relevant. Recently the lipid-bound structures of apoAI bound to reconstituted discoidal lipoprotein molecules have been studied utilizing chemical cross-linking and mass spectrometry (*29-31*). Some advance has been made in identifying potential cross-links and the data till date suggest two adjacent apoAI molecules to be organized in an anti-parallel fashion on the periphery of discoidal lipoprotein surface forming a belt.

To further elucidate the organization of two adjacent apoAI molecules, bound to discoidal lipoprotein surface using the chemical cross-linking coupled with mass spectrometry in this study we prepared rHDL molecules with a mixture of wild-type apoAI and ^{15}N labeled recombinant apoAI molecules. The presence of 2 different types of apoAI molecules that could be distinguished by mass spectrometry makes the identification of intramolecular and intermolecular cross-links less ambiguous. To identify potential interactions between adjacent lipid-bound apoAI molecules in this study we have used chemical and enzymatic cleavage methods and tried to identify the resulting peptides by MALDI-TOF mass spectrometry. The drawbacks associated with using the chemical cross-

linking and mass spectrometry strategy to solve the conformation of proteins and possible alternatives are discussed.

Experimental Procedures

Purification of human Apolipoprotein AI from HDL (^{14}N ApoAI)-HDL (d = 1.21 – 1.06 g/mL) was isolated from plasma by sequential KBr density ultracentrifugation as described earlier (*99*). Frozen human plasma was obtained from Oklahoma Blood Institute (Oklahoma City, OK). The plasma was thawed at room temperature and the density (d) of the plasma was adjusted to 1.35g/mL by adding dessicated KBr. 8.0mL of plasma (d= 1.35g/mL) was transferred to 25.0mL Ti-70 ultracentrifuge tube. The plasma was then layered with successive layers of KBr solution prepared in saline (1.1% NaCl and 0.1% Na_2EDTA). First the plasma was layered with 7.0mL of d=1.21 g/mL KBr solution. Next the d=1.21 g/mL layer was overlaid with 6.0 mL d=1.06 g/mL KBr solution. The top of the gradient was layered with 2.0mL saline and the tubes were centrifuged at 55,000 rpm at 5˚C for 4 hours in a Ti-70 rotor. After centrifugation the tubes were fractionated into 3 mL fractions and the density of the fractions determined by standard refractometry. For second centrifugation the fractions with densities between 1.09-1.15 g/mL were pooled and the density adjusted to 1.26g/mL by adding dessicated KBr. 6.0mL of d=1.26 g/mL pool was layered in the bottom of Ti-70 ultracentrifuge tubes and successively layered with 8.5mL d=1.20 g/mL KBr solution, 4.0mL of 1.06 g/mL KBr solution and 2.0 mL of saline. The second centrifugation was performed under similar conditions as the first centrifugation. The tubes were fractionated into 3.0 mL fractions. Aliquots (200 µL) of the fractions from the second centrifugation were dialyzed against 50mM phosphate buffer for SDS-PAGE. Based on the SDS-PAGE fractions containing apoAI and

apolipoprotein AII (apoAII), corresponding to HDL was pooled. The isolated HDL was freeze dried and proteins delipidated by acetone precipitation. Following acetone precipitation the pellet was suspended in 50mM sodium phosphate, 3M guanidine hydrochloride pH 7.5, applied to a pre-equlibrated Sephacryl S-300 gel-filtration column (Amersham Bioscience, Piscataway, NJ) and eluted at a flow-rate of 0.4 mL/min. Eluted sephacryl-S300 fractions corresponding to apoAI as determined by SDS-PAGE were pooled, dialyzed against 10mM ammonium bicarbonate buffer, lyophilized, resuspended in 3M guanidine hydrochloride and stored at -20˚C. Before use the apoAI stock was dialyzed against 50mM sodium phosphate, 150 mM NaCl, pH 7.4 (phosphate buffer).

Expression and purification of recombinant ^{15}N labeled apoAI fusion protein-pET30 vectors containing wild-type apoAI construct with a 6 kDa, 51 residue fusion protein tag (containing 6 His residues) were transfected into BL-21 *E.coli* expression hosts. Transfected cells were grown in M9 media supplemented with ^{15}N labeled ammonium chloride (Cambridge Isotope laboratories, Andover, MA). The expression of apoAI was induced by the addition of IPTG to a final concentration of 1mM. IPTG induced cells were pelleted by centrifugation at 9000g for 10 min. at 4˚C. The pellet was lysed by adding lysozyme and deoxycholate. The lysate was centrifuged at 45,000 rpm for 1 hour in a Ti-75 rotor (Beckmann) to remove cell debris. Following ultracentrifugation the apoAI fusion protein was purified from the supernatant by standard nickel affinity chromatography. The purification was monitored by SDS-PAGE.

Estimating The Peptide Masses of Human ApoAI and ^{15}N labeled Recombinant ApoAI Fusion Protein - Peptide mass fingerprinting of human apoAI (^{14}N apoAI) and ^{15}N labeled apoAI fusion protein (^{15}N apoAI-FP) tryptic peptides was performed to estimate the sequence coverage in the mass spectra and the extent of ^{15}N labeling efficiency of ^{15}N apoAI-FP. 5µg each of purified ^{14}N apoAI and ^{15}N apoAI-FP was separated by SDS-PAGE and visualized by coomassie staining. The bands corresponding to ^{14}N apoAI and ^{15}N apoAI-FP were excised, minced and destained extensively in 50% acetonitrile, 25mM ammonium bicarbonate pH 8.0. The destained gel pieces were dehydrated in a speed vacuum concentrator. The dried gel pieces were rehydrated with 15µL 0.016ng/µL (~ 1:20 w/w trypsin: protein) sequencing grade trypsin (Promega) and incubated at 37˚C for 12 hours. After 12 hours of digestion the peptides were extracted with 3 30µL washes of 50% acetonitrile, 0.1% trifluroacetic acid (TFA) solution. 0.5µL of ^{14}N apoAI or ^{15}N apoAI-FP trypsin peptides was mixed with 0.5µL of 5 mg/mL α-cyano-4-hydroxycinnamic acid (α-CHC) solution in 50% acetonitrile, 0.1% TFA and spotted on MALDI-TOF target plates. The mass spectra were acquired in a Voyager-DE Pro (Applied Biosystems, Foster City, CA) mass spectrometer, in the reflectron mode with acceleration at 20,000 V, delay time of 350 nsec and mass range of 500-3000 m/z. The acquired spectra were externally calibrated using peptide calibration mixture containing des-Arg^1-Bradykinin (m/z = 904.47), Angiotensin I (m/z = 1296.69), Glu1-Fibrinopeptide B (m/z = 1570.68), ACTH clip 1-17 (m/z = 2093.087) and ACTH clip 18-39 (m/z = 2465.20) as external calibrants.

Preparation of 96Å rHDL particles- Reconstituted high density lipoprotein (rHDL) was prepared by cholate dialysis method (*55*), at protein to phospholipid (1-palmitoyl 2-oleyl phosphatidylcholine, POPC) ratio of 1:90 (mol/mol). POPC stock in chloroform was dried under N_2 gas and reconstituted in phosphate buffer. Sodium cholate was added to the preparation at a final POPC to sodium cholate ratio of 1:1.5 (mol/mol) and incubated at 37˚C for 1 hour. The protein was added to the POPC-cholate mixture and incubated at 37˚C for 45 min. After the incubation period sodium cholate was removed by extensive dialysis against 4 liters phosphate buffer over 36 hours at 25˚C with changes to fresh buffer solution every 8 hours. The rHDL was prepared with either ^{14}N apoAI only, ^{15}N apoAI-FP only or a mixture of 1:1 molar ratio of ^{14}N apoAI and ^{15}N apoAI-FP as protein component.

The ^{14}N apoAI, ^{15}N apoAI-FP, ^{14}N apoAI/^{15}N apoAI-FP containing rHDL particles prepared by cholate dialysis were purified by size exclusion chromatography in a Superose6 gel filtration column (Amersham Biosciences, Piscataway, NJ) to isolate rHDL particles of homogeneous size (96Å particles). The homogeneity of the purified rHDL particles was assessed by non-denaturing gradient gel electrophoresis (NGGE).

Cross-linking of apoAI bound to rHDL particles- Dithiobis(succinimidyl propionate) DSP (Pierce) was dissolved in dimethyl sulfoxide to a final concentration of 6.5 mg/ml and added within 5 min. of preparation to the rHDL samples (final apoAI concentration of 0.5 mg/mL or lesser in phosphate buffer). 96Å rHDL particles containing ^{14}N apoAI, ^{15}N apoAI-FP or ^{14}N apoAI/^{15}N apoAI-

FP were cross-linked with DSP at 1:10 protein to DSP molar ratio for 30 min. at 25˚C. The reaction was quenched by adding 1 M Tris-HCl, pH 7.5 to a final concentration of 0.1 M Tris-HCl. After quenching the samples were dialyzed against 4 L 25 mM ammonium bicarbonate pH 8.0 for 8 hours at 4˚C to remove the excess cross-linker. After dialysis the cross-linked apoAI monomer, dimers and higher order cross-linked apoAI molecules were separated by (i) SDS-PAGE or urea SDS-PAGE and (ii) size-exclusion chromatography. Separation in urea SDS-PAGE gel was performed to resolve anomalous mobility of cross-linked apoAI molecules in a SDS-PAGE gel without urea (*31*).

In-gel Trypsin digestion- Coomassie blue stained protein bands corresponding to ^{14}N apoAI or ^{15}N apoAI-FP monomers or dimers and ^{14}N apoAI/^{15}NapoAI-FP heterodimers separated by SDS-PAGE were digested with trypsin as described earlier. The types of cross-linked samples used for in-gel digestion and MALDI-TOF mass spectrometry are listed in **Table-4**.

rHDL prepared with	PMF for sample type
^{14}N ApoAI only	^{14}N apoAI control
	^{14}N apoAI DSP modified monomer
	^{14}N apoAI homodimer
^{15}N ApoAI-FP only	^{15}N apoAI-FP monomer (control)
	^{15}N apoAI-FP DSP modified monomer
	^{15}N apoAI-FP homodimer
1:1 ^{14}N apoAI and ^{15}N apoAI-FP (mol/mol)	^{14}N DSP modified monomer
	^{15}N apoAI-FP DSP modified monomer
	^{14}N apoAI homodimer
	^{14}N apoAI:^{15}N apoAI-FP heterodimer
	^{15}N apoAI-FP homodimer

Table-4: Types of cross-linked samples used for in-gel digestion and PMF. The samples were assigned as monomer or dimer based on their relative mobility (molecular weight estimates) in SDS-PAGE.

MALDI-TOF mass spectrometry of trypsin digests- The peptide masses of in-gel trypsin digested samples (listed in **Table-4**) was determined in a Voyager

DE-Pro MALDI-TOF mass spectrometer. The mass spectra were acquired in the reflectron mode in α-CHC matrix with acceleration of 20,000 volts, delay time of 350 nsec under non-reducing conditions. The acquired mass spectra were first externally calibrated with peptide calibration mixture. The externally calibrated spectra were then internally calibrated with unmodified ^{14}N apoAI or ^{15}N apoAI-FP peaks as internal calibrants to ≤ 50ppm error.

CNBr cleavage of ^{14}N apoAI- Cross-linked ^{14}N apoAI monomers and dimers were purified by gel-filtration chromatography. For gel-flitration the cross-linked ^{14}N apoAI rHDL was freeze dried and phospholipids removed by acetone precipitation. The pellet was resuspended in 50mM sodium phosphate, 150mM sodium chloride and 3M guanidine hydrochloride, pH 7.5 and loaded in a Sephacryl-S300 column equilibrated with the same buffer. The purification was assessed by SDS-PAGE. The fractions corresponding to cross-linked monomer and dimer were pooled and stored at -20˚C until further use.

1mg each of control ^{14}N apoAI, DSP cross-linked ^{14}N apoAI monomer and dimer were cleaved with CNBr as described earlier (*100*). The control, DSP modified monomer and dimers were dialyzed against 5 mM ammonium bicarbonate buffer, pH 8.0 and dried in a vacuum concentrator. The dried samples were reconstituted in 70% TFA and transferred to glass vials. Two crystals of CNBr (Sigma) were added to each vial and the samples were incubated in dark at 37˚C for 24 hours. After the end of incubation the samples were dried in a vacuum concentrator to remove CNBr and TFA. The extent of CNBr cleavage was monitored by 16% tris-tricine SDS-PAGE and MALDI-TOF

mass spectrometry in the linear mode. CNBr cleaved apoAI fragments aggregated in aqueous buffer yielding a turbid solution. To prevent aggregation dried CNBr cleavage fragments were dissolved in 6M guanidine hydrochloride and stored at -20˚C until use. For MALDI-TOF analysis the CNBr fragments in 6M guanidine hydrochloride was desalted by C4 Zip-tip® (Millipore, Billerica, MA) micro-chromatography and spotted on MALDI-TOF plates. The spotted samples were allowed to air-dry and overlaid with 1 µL 10 mg/mL Sinapic acid (Sigma) in 50% acetonitrile, 0.1% TFA. The spectra were acquired in a Voyager DE-Pro MALDI-TOF mass spectrometer in the linear mode with accelerating voltage of 25,000 V and a delay time of 600 nsec. The acquired spectra of ^{14}N apoAI CNBr fragments were calibrated with unmodified ^{14}N human apoAI $(M+H)^{+1}$ and $(M+2H)^{+2}$ ions (m/z 28079.62 and 14039.81 respectively) as external calibrants. To identify the CNBr cleaved peptides the peptides were purified by gel-filtration and reverse phase HPLC. Gel filtration was performed in a home made G-50 superfine resin packed in a 50 cmx0.7 cm column and eluted with 25mM citrate buffer, 3M guanidine-hydrochloride pH 3.8 under non-reducing conditions. The reverse phase HPLC was performed in a C18 or C4 columns (Phenomenox, Torrance, CA) under oxidizing and reducing conditions. The bound CNBr peptides were eluted with a linear gradient (0-100%) of 80% acetonitrile, over 15 min. For HPLC runs under reducing conditions to cleave the cross-linked peptides, dithiothreitol (DTT) was added to a final concentration of 25mM to the samples and elution solvents.

Peptide Mass Fingerprinting of CNBr fragments of DSP cross-linked apoAI dimers- CNBr fragments of lipid-free apoAI or DSP cross-linked apoAI dimers separated in 16% Tris-Tricine gels were identified by trypsin digestion and peptide mass fingerprinting. The isolated gel bands were digested with trypsin and samples analyzed in a MALDI-TOF mass spectrometer as described earlier.

Results

Protein Purification- ^{14}N apoAI and ^{15}N labeled apoAI-FP were purified to >95% homogeneity as observed in coomassie blue stained SDS-PAGE gels (Figure-19).

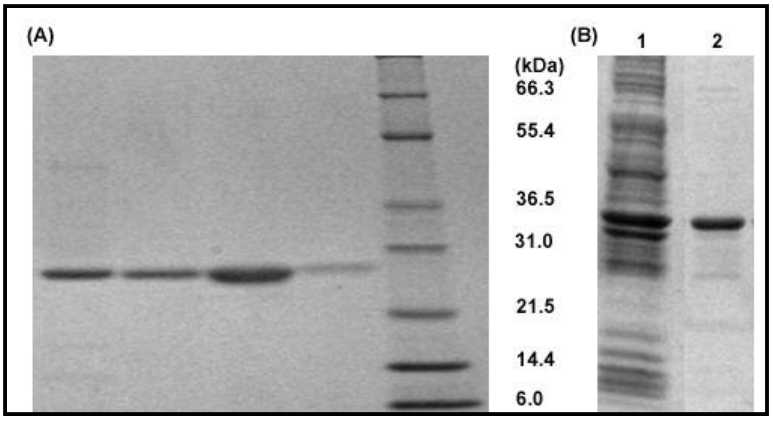

Figure-19: Coomassie blue stained 4-20% SDS-PAGE to monitor the purification of ^{14}N apoAI and ^{15}N labeled recombinant apoAI-FP. A, Shows purified ^{14}N human apoAI (28.0 kDa). B, ^{15}N labeled recombinant apoAI fusion protein (34.0 kDa) purified by Ni $^{2+}$ affinity chromatography. *Lane* 1, lysate and *lane* 2, purified ^{15}NapoAI-FP.

Efficiency of In-gel Trypsin Digestion and ^{15}N Labeling- The mass spectra of ^{14}N apoAI and ^{15}N apoAI-FP was compared against theoretical list of apoAI and ^{15}N apoAI-FP m/z values obtained from online protein digestion software 'MS Digest' (University of California, San Fransisco). Wild-type apoAI has 37 possible trypsin cleavage sites (21 Lys residues and 16 Arg residues) distributed evenly along its sequence. The recombinant apoAI-FP has 42 trypsin cleavage sites (24 Lys residues and 18 Arg residues). The additional 5 cleavage sites are located in the 6kDa fusion-protein tag of the recombinant apoAI. Under the trypsin cleavage conditions used the PMF data covered 87% and 89% ^{14}N apoAI sequence and ^{15}N apoAI-FP respectively (**Figure-20**). ApoAI residues 174-206 (corresponding

(a) Human apoAI sequence (^{14}N apoAI)

```
          10         20         30         40         50         60
DEPPQSPWDR VKDLATVYVD  VLKDSGRDYV SQFEGSALGK QLNLKLLDNW  DSVTSTFSKL

          70         80         90        100        110        120
REQLGPVTQE  FWDNLEKETE GLRQEMSKDL EEVKAKVQPY LDDFQKKWQE EMELYRQKVE

         130        140        150        160        170        180
PLRAELQEGA  RQKLHELQEK  LSPLGEEMRD RARAHVDALR THLAPYSDEL  RQRLAARLEA

         190        200        210        220        230        240
LKENGGARLA  EYHAKATEHL  STLSEKAKPA  LEDLRQGLLP  VLESFKVSFL  SALEEYTKKL

NTQ
```

(b) Recombinant apoAI fusion protein sequence (^{15}N apoAI-FP)

```
          10         20         30         40         50         60
MHHHHHHSSG LVPRGSGMKE  TAAAKFERQH MDSPDLGTDD DDKAMAHFWQ QDEPPQSPWD

          70         80         90        100        110        120
RVKDLATVYV  DVLKDSGRDY  VSQFEGSALG  KQLNLKLLDN WDSVTSTFSK  LREQLGPVTQ

         130        140        150        160        170        180
EFWDNLEKET  EGLRQEMSKD  LEEVKAKVQP YLDDFQKKWQ EEMELYRQKV EPLRAELQEG

         190        200        210        220        230        240
ARQKLHELQE  KLSPLGEEMR  DRARAHVDAL  RTHLAPYSDE  LRQRLAARLE  ALKENGGARL
```

Figure-20: **Sequence coverage in peptide mass fingerprints of (a) ^{14}N apoAI and (b) ^{15}N apoAI-FP.** The underlined sequences were not observed in PMF under the trypsin cleavage conditions used.

to residues 225-257 in apoAI-FP) and residues 14-43 in the fusion-protein sequence were absent in the peptide mass fingerprint data. Pilot in-gel trypsin cleavage experiments were carried out by varying the amount of trypsin and the incubation time but no further improvement in the sequence coverage was observed.

^{15}N apoAI-FP peptide mass fingerprint (**Figure-21**) was compared to a list containing the theoretical m/z of the ^{15}N apoAI-FP tryptic peptides. The theoretical m/z of ^{15}N apoAI-FP tryptic peptides was calculated by adding 1 Da

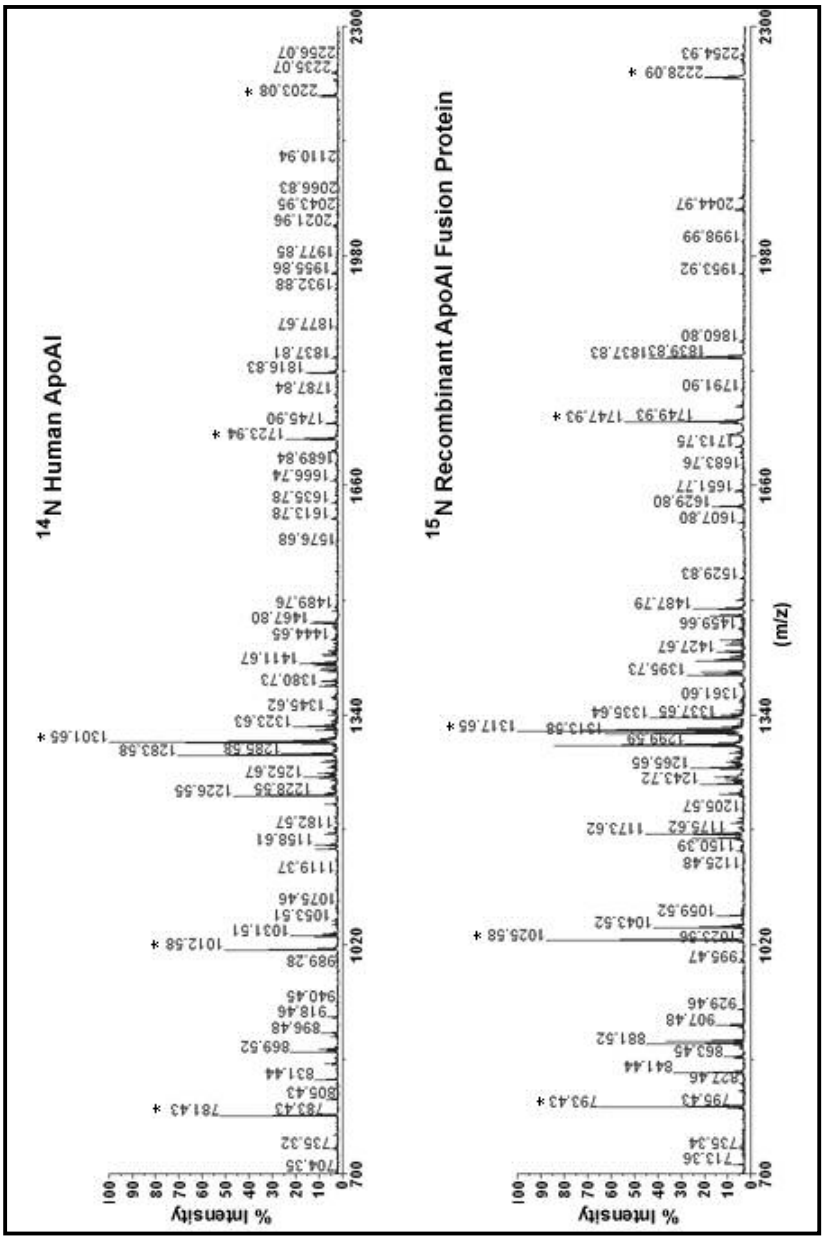

Figure-21: **PMF of ^{14}N apoAI and ^{15}N apoAI-FP to estimate the ^{15}N labeling efficiency by in-gel trypsin digestion and MALDI-TOF mass spectrometry.** ^{15}N apoAI-FP tryptic peptides show an increase in mass (+1 amu/N atom) on ^{15}N labeling as compared to ^{14}N apoAI peptides. For example, in the ^{14}N apoAI PMF spectra 781.43 (m/z) maps to residues 154-160 (sequence: AHVDALR; containing 12 N atoms) this corresponds to m/z 793.43 in ^{15}N apoAI-FP sequence. The mass spectrum of ^{15}N apoAI-FP indicates that the recombinant apoAI-FP was 100% labeled with ^{15}N apoAI. The peaks indicated with an asterix (*) were used as internal calibrants in future MALDI-TOF analyses.

for every nitrogen atom in the corresponding ^{14}N tryptic peptides. Based on this analysis there was 100% ^{15}N labeling of the apoAI-FP.

Cross-linking of rHDL bound apoAI- 96Å rHDL particles containing ^{14}N apoAI, ^{15}N apoAI-FP or 1:1 molar ratio of ^{14}N apoAI: ^{15}N apoAI-FP were purified to homogeneity by gel-filtration chromatography (**Figure-22**). The rHDL particles prepared with ^{14}N apoAI, ^{15}N apoAI-FP or 1:1 molar ratio of ^{14}N apoAI: ^{15}N apoAI-FP did not show any difference in size.

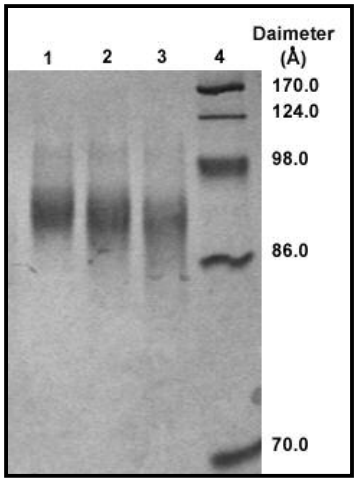

Figure-22: **Coomassie Blue stained 4-20% non-denaturing gradient gel to monitor purification of rHDL particles.** 1:90 apoAI: POPC (mol:mol) rHDL particles purified by gel-filtration. *Lane* 1, rHDL containing ^{14}N apoAI, *lane* 2, rHDL containing ^{15}N apoAI-FP and *lane* 3, rHDL containing 1:1 molar ratio of ^{14}N apoAI : ^{15}N apoAI-FP.

The cross-linked protein molecules were separated by non-reducing SDS-PAGE (**Figure-23**). The results show that cross-linking of rHDL containing ^{14}N apoApoAI, ^{15}N apoAI-FP yield 2 major bands corresponding to dimers and trimers (**Figure 23**, *lanes 4-5*) and minor higher order cross-links. While the DSP cross-linking of rHDL particles containing 1:1 ratio of ^{14}N apoAI: ^{15}N apoAI-FP did have cross-linked dimers and trimers or higher order cross-links (**Figure 23**, *lane 6*) but were smeared and did not separate well in SDS-PAGE gels. The

estimated masses of the cross-linked apoAI molecules in **Figure-23** are tabulated in **Table-5**.

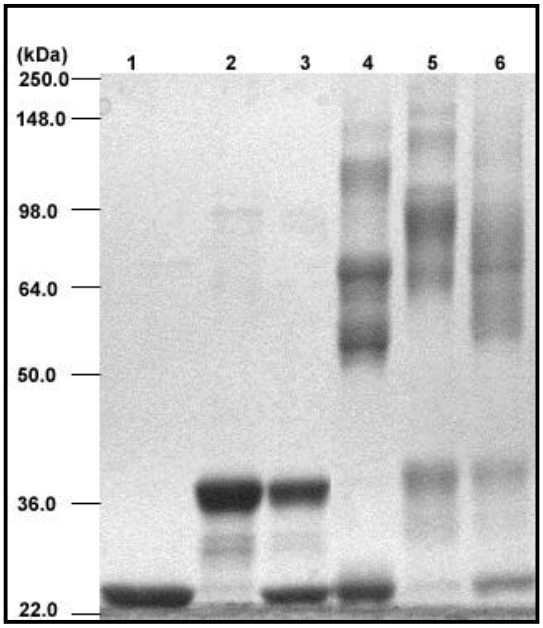

Figure-23: **Coomassie blue stained 4-20% non-reducing SDS-PAGE to separate DSP cross-linked products.** *Lane 1*, Control rHDL containing ^{14}N apoAI only; *Lane 2*, Control rHDL containing ^{15}N apoAI-FP; *Lane 3*, Control rHDL containing 1:1 (mol/mol) ^{14}N apoAI:^{15}N apoAI-FP; *Lane 4*, DSP cross-linked rHDL containing ^{14}N apoAI only; *Lane 5*, DSP cross-linked rHDL containing ^{15}N apoAI-FP; *Lane 6*, DSP cross-linked rHDL containing 1:1 (mol/mol) ^{14}N apoAI:^{15}N apoAI-FP.

	Estimated	Corresponds to possible
Cross-linked ^{14}N ApoAI, Figure-3 *lane 3*	116	^{14}N tetramer
	72	^{14}N trimer
	53	^{14}N dimer
	28	^{14}N monomer
Cross-linked ^{15}N ApoAI-FP, Figure-3, *lane 4*	147	^{15}N tetramer
	90	^{15}N trimer
	69	^{15}N dimer
	37	^{15}N monomer

Table-5: Estimated masses of DSP cross-linked ^{14}N apoAI and ^{15}N apoAI-FP products based on relative mobility values (Figure-23).

To investigate the mobility of cross-linked apoAI molecules in the presence of urea in SDS-PAGE gels cross-linked ^{14}N apoAI molecules were separated in 12% urea SDS-PAGE gels (**Figure-24**). The mobility of 72 kDa band corresponding to ^{14}N apoAI trimer (Figure-6, Panel A, *lane 4-5*) shifts to 53

kDa in the presence of 6M urea (**Figure-24**, Pane B, *lane 2*). This anomalous mobility is attributed to a cross-link between lys 118 and lys 140 in the central region of apoAI molecule (*31*). As reported earlier, this observation suggests the ^{14}N apoAI dimer to exist in 2 different conformations that migrate as 53kDa band corresponding to the theoretical mass of apoAI dimer and a second band which migrates with an apparent molecular weight of 72 kDa in SDS-PAGE gels. Cross-linked rHDL molecules containing ^{15}N apoAI-FP or 1:1 ratio of ^{14}N apoAI: ^{15}N apoAI-FP was not characterized by urea SDS-PAGE.

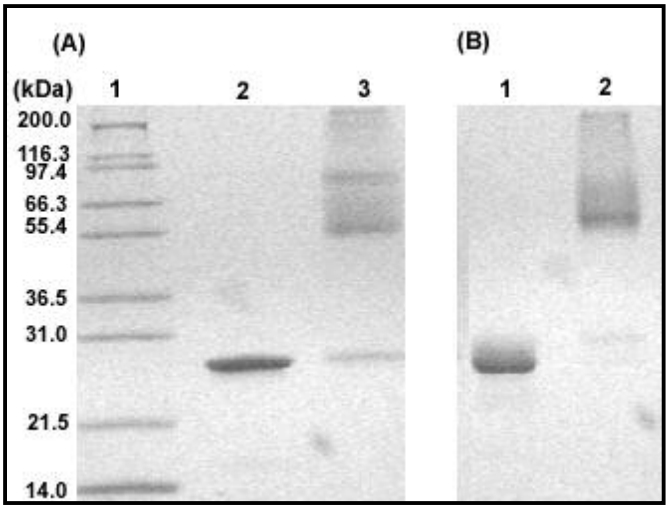

Figure-24: **12% SDS-PAGE to investigate the anomalous mobility of DSP cross-linked ^{14}N apoAI molecules in the presence and absence of 6M urea.** Panel A, DSP cross-linked ^{14}N apoAI molecules separated by 12% SDS-PAGE. *Lane 1*, Mark-12 molecular weight markers; *lane 2*, lipid-free ^{14}N apoAI; *lane 3*, DSP cross-linked ^{14}N apoAI products. Panel B, DSP cross-linked ^{14}N apoAI molecules separated by 12% urea SDS-PAGE. *Lane 1*, lipid-free ^{14}N apoAI; *lane 2*, DSP cross-linked ^{14}N apoAI products.

Estimating The m/z of Trypsin Digested control and cross-linked apoAI Peptides - ^{14}N apoAI and ^{15}N apoAI-FP have total of 37 and 42 possible tryptic peptides respectively. 12 ^{14}N apoAI peptides and ^{15}N apoAI-FP peptides have

m/z < 500 and were not observed in the mass spectra. The mass spectra were acquired in the range of m/z 500-3000.

A list of masses (m/z) from the mass spectra of each sample listed in **Table-4** was generated. The list was analyzed for the presence of unmodified ^{14}N or ^{15}N apoAI peptides, DSP modified hanging ends, intrapeptide, intramolecular and intermolecular. The new peptide masses observed both in monomeric apoAI and in heterodimers or homodimers were treated as potential hanging ends, reduced hanging ends, intramolecular or intrapeptide cross-links. The reduced hanging ends must be absent in the mass spectra of cross-linked apoAI monomers and dimers which was acquired under oxidizing conditions. The structure of DSP, cross-linking reaction, the structures of the various DSP modifications and the associated mass increase are shown in **Figure-25**. DSP modified lysine residues are insensitive to trypsin digestion. In the identification of

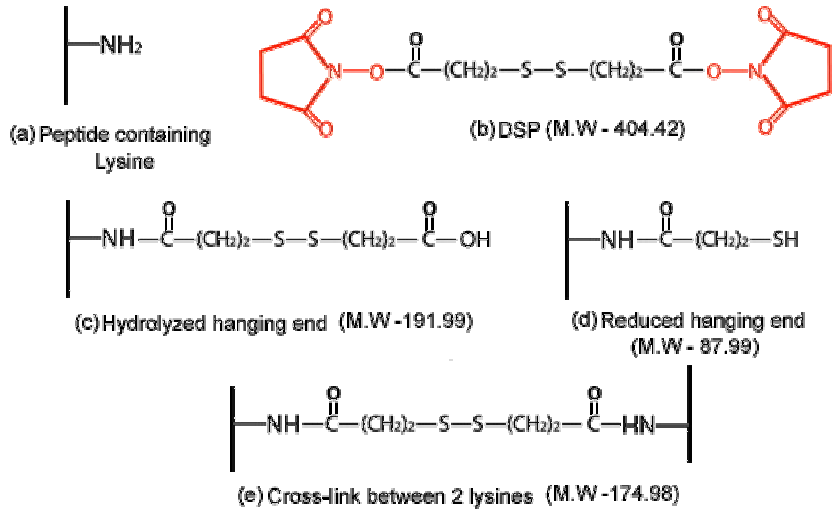

Figure-25: **Structure of DSP, various types of DSP modifications and associated mass increase (Da).**

cross-linked peptides it was assumed that the cleavages at cross-linked lysine residues were skipped. The new peptide masses (m/z) observed exclusively in the ^{14}N apoAI homodimers, ^{15}N apoAI-FP homodimers or ^{14}N apoAI / ^{15}N apoAI-FP heterodimer bands were treated as potential intermolecular cross-links. The hanging ends, intrapeptide, intramolecular and intermolecular cross-links were identified by searching a theoretical list of all possible DSP cross-links of apoAI created in Excel spreadsheet program. The total number (175 m/zs) of new m/z observed in peptide mass fingerprint of various cross-linked apoAI molecules are tabulated in **Table-6** of which 18 m/zs were identified as possible hanging ends or intrapeptide cross-links **Table-7**. The hanging ends and intrapeptide identifications in **Table-7** are the only conclusive identifications, from the in-gel trypsin digestion experiments. Of the remaining 157 no further identifications as intramolecular or intermolecular cross-links could be made.

Sample	# of new m/z observed in the peptide mass fingerprint
^{14}N apoAI DSP modified monomer	32
^{14}N apoAI DSP modified dimer	45
^{15}N apoAI-FP DSP modified monomer	31
^{15}N apoAI-FP DSP modified dimer	32
^{14}N apoAI and ^{15}N apoAI-FP DSP modified heterodimer	35

Table-6: Number of new m/z observed in peptide mass fingerprint of DSP modified apoAI molecules.

1. Identified DSP modified peptides in ^{14}N apoAI						
Observed (m/z)	**Theoretical (m/z)**	**ppm error**	**m/z of unmodified peptide**	**Chemical modifications if any**	**^{14}N apoAI peptide sequence**	**Lysine involved**
(A) Hydrolyzed hanging ends in ^{14}N apoAI-FP						
1204.56	1204.57	8.30	1012.58		(207)A**K**PALEDLR(215)	208
1603.67	1603.66	-6.24	1411.67		(107)**K**WQEEMELYR(116)	107
1619.66	1619.65	-6.17	1427.66	Oxidized methionine	(107)**K**WQEEMELYR(116)	107
1706.84	1706.80	-23.44	1514.81		(227)VSFLSALEEYT**K**K(239)	238
2070.01	2070.03	9.66	1878.03		(11)V**K**DLATVYVDVL**K**DSGR(27)	12/23
2073.95	2073.96	4.82	1881.97		(46)LLDNWDSVTSTFS**K**LR(61)	59
2220.01	2220.03	9.01	2028.04		(189)LAEYHA**K**ATEHLSTLSEK(206)	195
(B) Intrapeptide crosslinks in ^{14}N apoAI						
2052.00	2052.02	9.75	1878.03		(11)V**K**DLATVYVDVL**K**DSGR(27)	12-23
2339.05*	2339.09	17.10	2165.11		(89)DLEEV**K**A**K**VQPYLDDFQK(106)	94-96
2339.05*	2339.12	29.93	2165.14		(132)Q**K**LHELQE**K**LSPLGEEMR(149)	133-140
2383.12	2383.16	16.78	2209.18		(196)ATEHLSTLSE**K**A**K**PALEDLR(215)	206-208
(C) Reduced crosslinks in ^{14}N apoAI						
1605.70	1605.75	31.13	1517.75	Pyroglutamate	(84)QEMS**K**DLEEV**K**AK(96)	88 or 94
2753.36	2753.46	36.32	2665.47		(172)QRLAARLEAL**K**ENGGARLAEYHAK (195)	182
2. Identified DSP modified peptides in ^{15}N apoAI-FP§						
observed	**theoretical**	**ppm error**	**Residue#**	**Chemical modifications**	**^{15}N apoAI-FP peptide sequence**	**Lysine involved**
(A) Hydrolyzed hanging ends in ^{15}N apoAI-FP						
1365.63	1365.62	-7.32	1173.63		(178)LEAL**K**ENGGAR(188)	182
1619.69	1619.66	-18.52	1427.67		(107)**K**WQEEMELYR(116)	107
1635.68	1635.65	-18.34	1443.66	Oxidized methionine	(107)**K**WQEEMELYR(116)	107
2092.01	2092.03	9.56	1900.03		(11)V**K**DLATVYVDVL**K**DSGR(27)	12 or 23
2095.95	2095.96	4.77	1903.97		(46)LLDNWDSVTSTFS**K**LR(61)	59
2244.03	2244.03	0.00	2052		(189)LAEYHA**K**ATEHLSTLSEK(206)	195
(B) Intrapeptide cross-links in ^{15}N apoAI-FP						
2074.02	2074.01	-4.82	1900.03		(11)V**K**DLATVYVDVL**K**DSGR (27)	12-23

* The observed m/z matches to two possible cross-linked intrapeptide links
§ The FP part of apoAI-FP has 51 residues, the fusion protein resiudes 1-51 are numbered from -51 to -1while the apoAI part are numbered form 1-243

Table-7: **Identification of DSP cross-linked peptides**. A, hydrolyzed hanging ends in ^{14}N apoAI; B, Intrapeptide cross-links in ^{14}N apoAI; C, Hydrolyzed hanging ends in ^{15}N apoAI-FP; and D, Intrapeptide cross-links in ^{15}N apoAI-FP.

CNBr Cleavage of apoAI molecules- Pilot CNBr cleavage experiments were performed only with ^{14}N apoAI molecules to optimize the cleavage and separation conditions. Cross-linked ^{14}N apoAI dimers were purified by size exclusion chromatography (**Figure-26**). The cross-linked ^{14}N apoAI dimers were purified to homogeneity as monitored by non-reducing 4-20% SDS-PAGE (**Figure-26** inset). The size of dimers purified by gel-filtration was estimated by MALDI-TOF mass spectrometry. **Figure-27** shows the mass spectra of purified ^{14}N apoAI dimer. The $(M+H)^{1+}$ ion (m/z = 58056.69) and $(M+2H)^{2+}$ ion (m/z = 29027.51) are present. In **Figure-27** there are no peaks at m/z > 58056.69 this confirms the results from urea SDS-PAGE gels (**Figure-24**) that the72k Da band in the cross-linked ^{14}N apoAI dimer to be due to conformational changes leading to differences in migration (**Figure-23**) of apoAI dimers in SDS-PAGE.

The 16% tris-tricine SDS-PAGE (**Figure-28**) shows that under the CNBr cleavage conditions employed the control and DSP modified ^{14}N apoAI molecules to yield major fragments corresponding to complete and partial CNBr cleavages. The only observable difference between the apoAI monomer and dimer in the 16% SDS-PAGE gel is the presence of a ~ 22kDa band in the dimers. This 22kDa band could be a cross-link between 2 N-terminal CNBr fragments (1-86 mass- 9870.95 Da) or 2 C-terminal CNBr fragments (149-243, mass-10725.27 Da) or between N (1-86, mass- 9870.95 Da) and C terminal (149-243, mass-10725.27 Da) CNBr fragments of apoAI molecule.

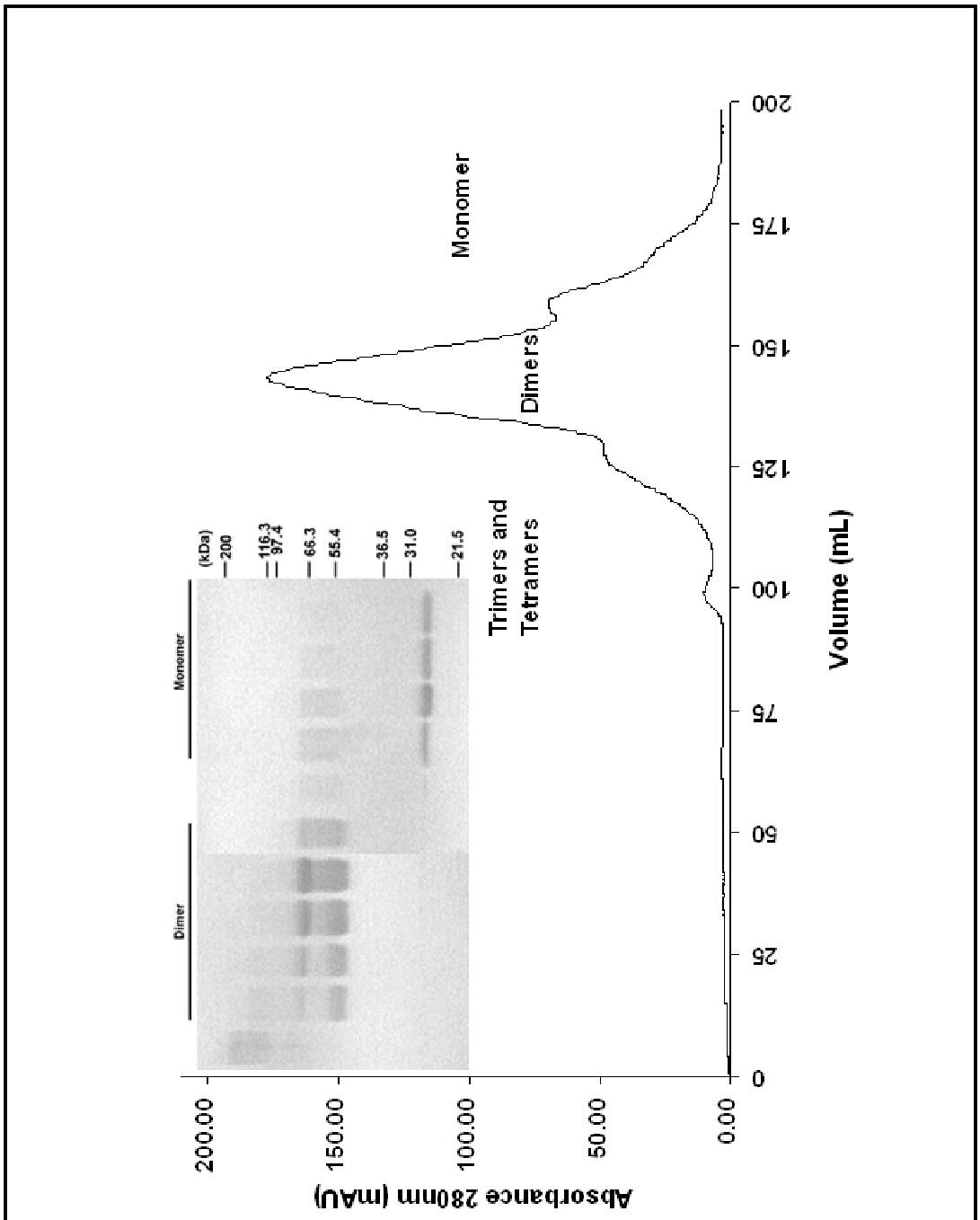

Figure-26: Coomassie blue stained 4-20% SDS-PAGE to monitor the purification of DSP cross-linked ^{14}N apoAI by size-exclusion chromatography in sephacryl S-300 column. Fractions corresponding to dimers and monomers are labeled in the gel.

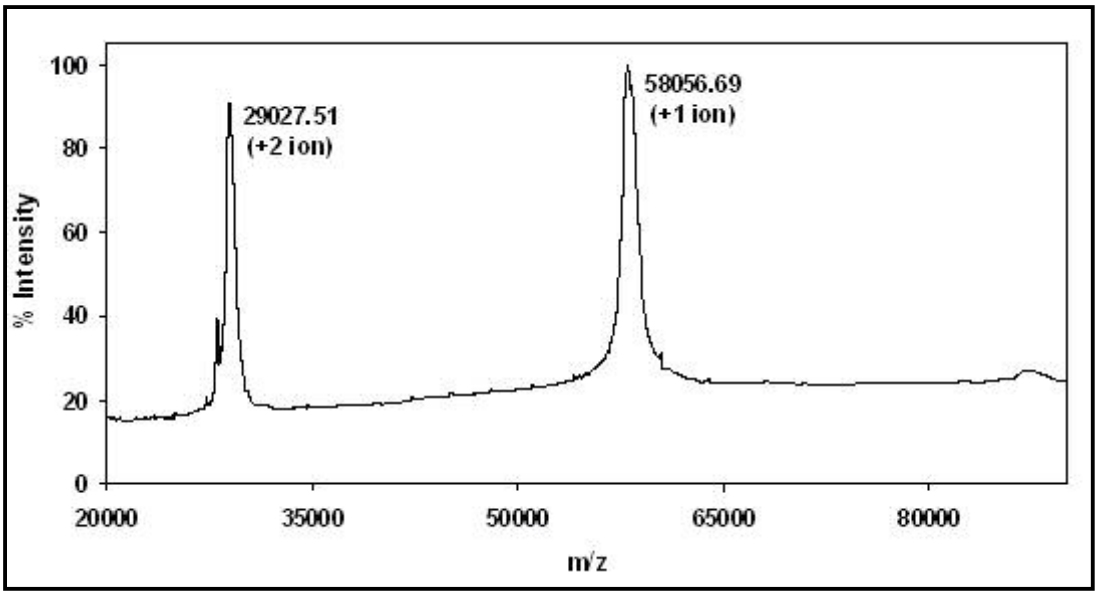

Figure-27: Estimating the size of ^{14}N apoAI dimer by MALDI-TOF mass spectrometry. Purified ^{14}N apoAI dimers were analyzed in the linear mode in a Voyager DE-Pro MALDI-TOF mass spectrometer. The spectra were acquired with sinapic acid matrix at accelerating voltage of 25,000V and delay time of 600 nsec. The acquired spectra were calibrated (200ppm error) with unmodified ^{14}N human apoAI MH+1 ion (m/z 28079.62) as external calibrant.

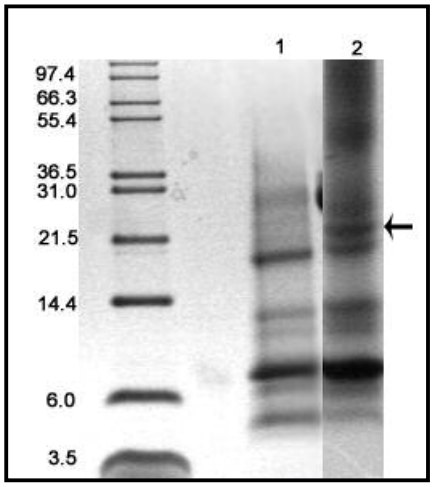

Figure-28: 16% Tris-Tricine SDS-PAGE to characterize the CNBr cleavage of ^{14}N apoAI monomer and dimer. The difference between the CNBr cleavage fragments of apoAI monomer and dimer is a ~ 22kDa band (indicated by an arrow) which is present in the dimer but not in the monomer.

Sizes of CNBr cleaved control or DSP modified ^{14}N apoAI were analyzed by MALDI-TOF mass spectrometer in the linear mode (**Figure-29**). Based on the

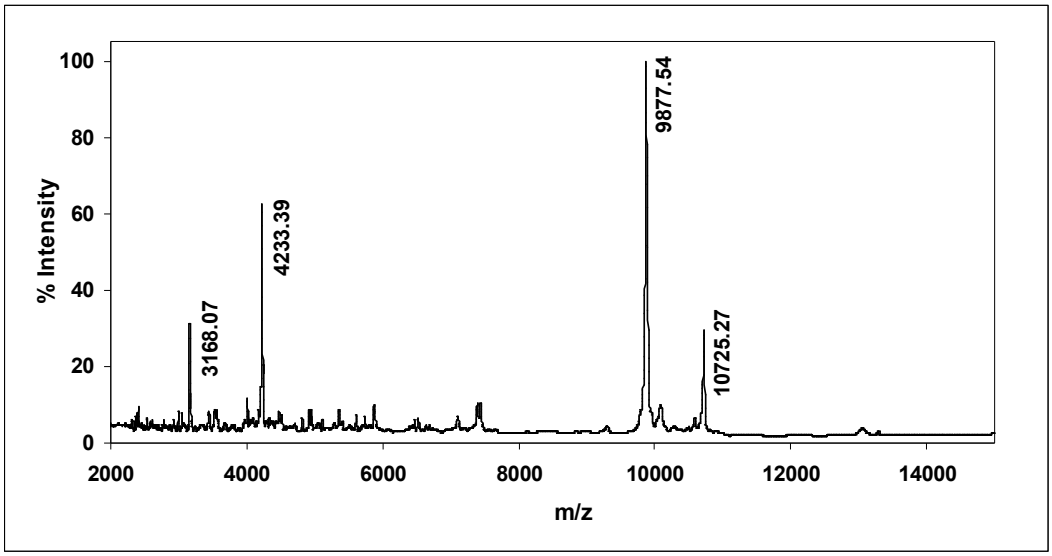

Figure-29: Estimating the masses of CNBr fragments of 14N apoAI by MALDI-TOF mass spectrometry. The four peaks show in the mass spectra corresponds to the complete CNBr cleavage fragments of apoAI. The errors for the estimated masses are with in+/- 7 Da.

mass spectra, only the complete cleavage fragments of apoAI were observed. The CNBr fragments from DSP cross-linked ^{14}N apoAI monomer or dimer did not yield good mass spectra in MALDI-TOF. Due to the lack of mass spectra for the CNBr peptides of cross-linked apoAI dimers the identity of the CNBr peptides in the dimers could not be established and the new 22 kDa peptide in the 16% Tris-Tricine gel could not be mapped to any specific region of apoAI.

The CNBr cleavage fragments of control ^{14}N apoAI molecules were purified by gel-filtration and reverse phase HPLC. The purification by both methods was monitored by 16% tris-tricine SDS-PAGE electrophoresis (**Figure-30 a and b**). Fractions from C4 reverse phase HPLC separation of CNBr fragments of DSP cross-linked ^{14}N apoAI dimers were separated in 16% Tris-Tricine SDS-PAGE (**Figure-30c**). Based on the SDS-PAGE the separation of CNBr fragments of

apoAI monomers or dimers could not be achieved by gel filtration or reverse phase HPLC. To improve the separation of the CNBr peptides in C4 columns the solvent in the organic phase was changed form acetonitrile to more hydrophobic isopropanol (70% isopropanol : 20% acetonitrile in water) but still no good separation could be achieved (data not shown). This could be due the fact that the hydrophobic CNBr peptides of apoAI bind strongly with the C4 or C18 reverse phase matrix and are insensitive to the organic solvent gradient. This will lead to the elution of all the CNBr peptides together at 100% concentration of the organic phase.

To map the CNBr fragments to apoAI sequence the bands from the 16% Tris-Tricine gels (**Figure-30b and c**) were digested with trypsin and the peptide mass fingerprint was acquired in MALDI-TOF mass spectrometer. The tryptic peptides generated from the CNBr fragments of apoAI mapped to all regions of intact apoAI and we were unable to assign the CNBr fragments to the corresponding regions in apoAI sequence. The ambiguity in the peptide mass fingerprinting data can be explained by considering the sizes of apoAI CNBr fragments. The theoretical masses of complete CNBr cleavage fragments of apoAI are 9870.95 Da (1-86), 3164.55 Da (87-112), 4228.81 Da (113-148) and 10725.27 (149-243). The partial cleavage fragments of apoAI will have approximately similar masses and cannot be separated by SDS-PAGE. For example a partial cleavage fragment consisting of apoAI residues 1-148 (17.3 kDa) and 87-243 (18.2 kDa) will have masses very similar and cannot be

separated by SDS-PAGE. So an 18kDa band in SDS-PAGE gel from CNBr cleavage of apoAI will yield the PMF of intact apoAI molecule.

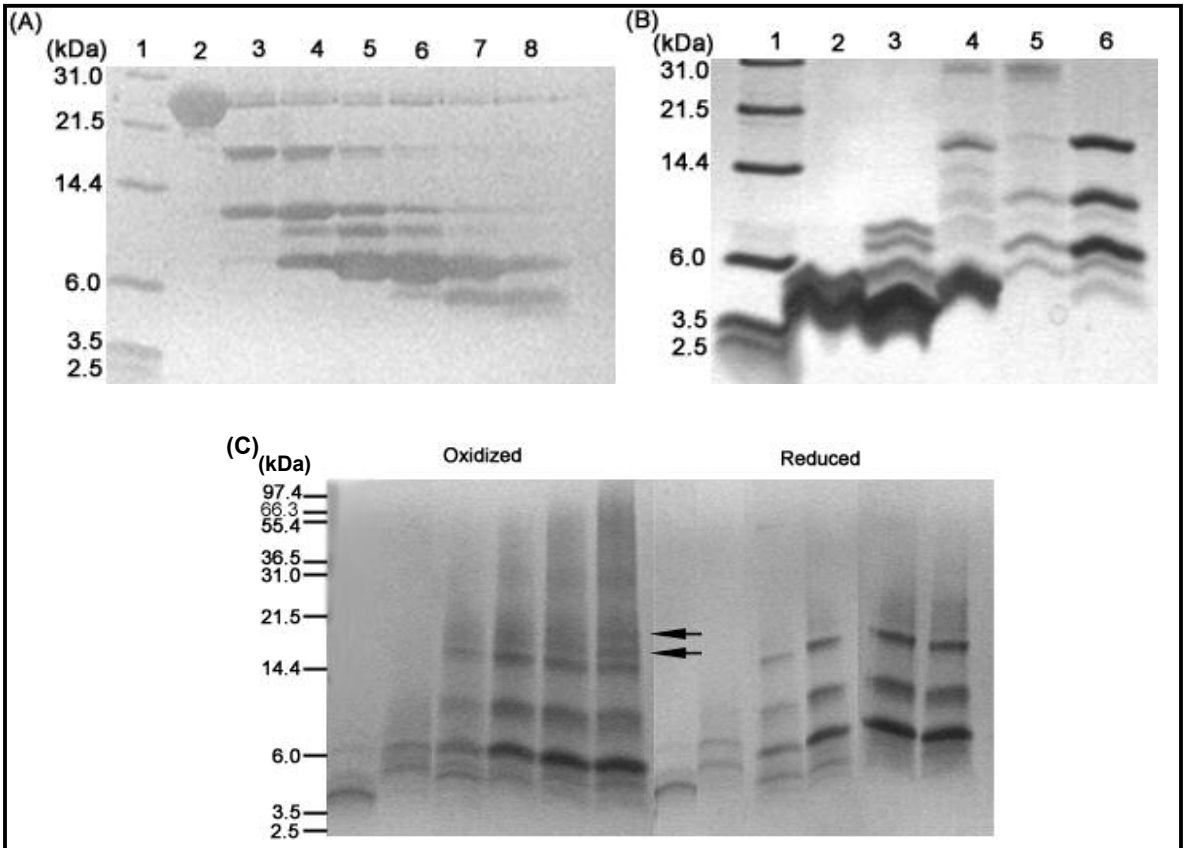

Figure-30: Purification of CNBr peptides of 14N apoAI monomers and cross-linked dimers. (a) Separation of apoAI monomer CNBr peptides by gel-filtration chromatography; (b) Separation of apoAI monomer CNBr peptides reverse phase HPLC in C4 column; and (c) Separation of cross-linked apoAI dimer CNBr peptides reverse phase HPLC in C4 column under reducing conditions.

Discussion

An interesting feature of the cross-linking and MALDI-TOF analysis in this study is that all the identified cross-links were either hanging ends or intrapeptide cross-links only. No cross-links between lysines in two different apoAI tryptic peptides (cross-linked dipeptides) could be identified. The inability to identify intramolecular or intermolecular cross-links could be due to various reasons.

Cross-linking at residues other than lysine- Imidoester chemical cross-linkers have been shown to cross-link at residues other than lysines (*101*). Serine and tyrosine residues are most commonly observed to be cross-linked by imidoester cross-linkers like DSP, which was used for cross-linking in this study. The cross-linking at resiudes other than lysines is a possibility because we were unable to identify more than 90% (157 m/z) of the new m/zs observed. To exclude the possibility of DSP cross-linking at residues other than lysines (at serine and tyrosine residues) the new m/zs from the cross-linking of DSP was compared to a new list containing a list of possible cross-links at lysine, serine and tyrosine residues, but no new identifications could be made.

Inability of cross-linked dipeptides to ionize in MALDI-The tryptic peptides of cross-linked apoAI molecules were ionized in the reflectron mode in MALDI-TOF in the mass range of 500-3000 Da. There is a possibility that the cross-linked peptides are larger than 3000Da and are not observed under the conditions used. To rule out this possibility the peptide mass fingerprint of the cross-linked apoAI molecules was also acquired in the linear mode in the mass range of 4000-10,000 Da. The data acquired in the linear mode did not lead to

the identification any new intra or intermolecular cross-links. This suggests that cross-linked apoaI dipeptides do not ionize efficiently in MALDI. The other observation in this study also supports this possibility, the CNBr cleaved control apoAI molecules did yield good mass spectra but we were able to identify the complete CNBr cleavage fragments from DSP cross-linked ^{14}N apoAI dimer samples in MALDI-TOF.

Decay of cross-linked apoAI molecules-There is a total of 175 new m/zs in cross-linked apoAI samples. But we were able to identify only 18 of the 175 new m/z. In-source fragmentation of cross-linked apoAI molecules could lead to the fragmentation of apoAI peptides leading to the generation of m/zs which are significantly different than the expected m/z. We believe that such in-source decay could be hampering the positive identification of intramolecular and intermolecular links during MALDI. Moreover peptides in MALDI have been reported to spontaneously fragment in source (*102-104*). Spontaneous fragmentation of peptides at Asp-Pro, Asp-X and Glu-X bonds has been observed during MALDI (*105, 106*). ApoAI has 16 Asp and 30 Glu residues. This high abundance of acidic residues in apoAI could possibly lead to spontaneous fragmentation of cross-linked inter and intramolecular molecules during MALDI leading to the generation of unexpected m/z in the mass spectra and complicating the interpretation of data. The inability to identify more than 90% of the new m/zs generated after cross-linking strongly suggests in-source fragmentation of apoAI peptides leading to the generation of peptide fragments

which do not match with the expected theoretical masses of cross-linked apoAI peptides.

In the three recent reports (*29-31*), reconstituted discoidal HDL (96 Å diameter) molecules containing 2 apoAI molecules were cross-linked with lysine reactive homobifunctional cross-linker (12 Å spacer arm) Dithiobis succinamidyl propionate (DSP) or Bis(sulfosuccinimidyl)suberate (BS^3). Cross-linked apoAI dimers were purified and digested with trypsin and the resulting peptides were identified by electrospray ionization mass spectrometry (ESI MS) and MS/MS fragmentation. The intrapeptide, intramolecular and intermolecular cross-links identified by mass spectrometry from the three reports are summarized in **Table-8 a to c.** Table-1 a to c displays very few identifications that are common between the three reports (**Figure-31**). An ideal intermolecular cross-link is not ambiguous if the identified cross-link is between two lysines at the same position or between lysines in 2 peptides corresponding to the same region in adjacent apoAI molecules and the masses corresponding to intermolecular cross-links is present only in the peptide mass finger print (PMF) of cross-linked dimer. Such unique intermolecular cross-links are present in the reported data but there are also other intermolecular cross-links that are between lysines corresponding to different regions of apoAI molecule. In the two reports by Davidson et al, the intermolecular cross-links were assigned by an indirect method, by considering the peak intensities in ESI-MS spectra. If the ratio of any cross-linked peak intensity in dimer to monomer was greater than 1.7 then the peak was identified as an intermolecular cross-link and if the ratio was lesser than 1.7 then the peak

was identified as an intramolecular cross-link. Overall the assignments of intermolecular cross-links in the published reports are few and ambiguous. Moreover, in the three reports the possibility of unexpected cross-linked products due to cross-linking at residues other then lysines and contaminants in the cross-

(a)

Table-8: **Cross-linked apoAI peptides identified in published reports** . Identified (a), intrapeptide; (b), intramolecular; and (c), intermolecular cross-linked apoAI peptides by mass spectrometry in published reports. The report by Davidson et al, 2003 was not supported by MS/MS fragmentation data.

Published Intrapeptide Cross-links			
Davidson, 2003			
ApoAI Peptide	Cross-linked lysines	Observed (Da)	Theoretical (Da)
84-96	K88-K94	1707.75	1707.76
11-27	K12-K23	2051.01	2051.01
132-149	K133-K140	2338.11	2338.11
189-215	K195-(K206 or K208)	3386.56	3386.52
Davidson, 2005			
84-96	K88-K94	1671.84	1671.84
95-107	K96-K106	1716.91	1716.92
11-27	K12-K23	2015.10	2015.11
227-243	K238-K239	2108.11	2108.12
89-106	K94-K96[f]	2302.16	2302.18
132-149	K133-K140[g]	2302.20	2302.20
196-215	K206-K208	2346.25	2346.26
28-59	K40-K45	3728.04	3728.22
Bhat, 2005			
11–27	12–23	2051.01	2051.01
84–96	88–94	1707.75	1707.75
89–106	94–96	2338.09	2338.08
132–149	133–140	2338.11	2338.13

(b)

Published Intramolecular cross-links				
Davidson, 2003				
Peptide-I	**Peptide-II**	Cross-linked lysines	Observed (Da)	Theoretical (Da)
239-243x	**28-45**	K239-K40	2772.35	2772.37
207-215x	**41-59**	K208-K45	3393.69	3393.71
117-123x	**132-149 + H**	K118-(K140 or K133)	3398.62	3398.66
117-123x	**97-116 + H**	K118-(K106 or K107)	3878.75	3878.81
Davidson, 2003				
1-10x	**89-96**	N_T-K94	2294.13	2294.15
107-116x	**117-123**	K107-K118	2417.32	2417.4
84-94x	**95-106**	K88-K96	2923.59	2923.73
Bhat, 2005				
D (1–12) K	**V (11–23) K**	N_T-K12	2861.35	2861.37

(c)

Published Intermolecular cross-links				
Davidson, 2003				
Peptide-I	**Peptide-II**	Lysines	Observed (Da)	Theoretical (Da)
207-215x	**207-215**	K208-K208	2197.12	2197.13
132-140x	**132-140**	K133-K133	2477.24	2477.25
97-107x	**97-107**	K106-K106	2933.4	2933.44
117-123x	**134-149**	K118-K140	2950.47	2950.48
132-140x	**134-149**	K140-K140	3233.59	3233.58
239-243x	**216-238**	K239-K226	3373.72	3373.75
189-206x	**62-83**	K195-K77	4818.28	4818.42
Davidson, 2005				
207-215x	**207-215**	K208-K208	2161.19	2161.21
84-94x	**117-123**	K88-K118	2357.2	2357.22
95-106x	**117-123**	K96-K118	2457.35	2457.37
28-45x	**239-243**	K40-K239	2736.42	2736.44
117-123x	**134-149**	K118-K140	2914.56	2914.67
84-94x	**95-106**	K88-K96	2923.59	2923.73
46-61x	**207-215**	K59-K208	3030.7	3030.8
216-238x	**239-243**	K226-K239	3337.96	3338.11
46-61x	**189-206**	K59-K195	4046.22	4046.38
62-83x	**189-206**	K77-K195	4782.47	4782.57
Bhat, 2005				

11–23	**178–188**	12–182	2792.44	2792.42
239–243	**28–45**	40–239	2772.34	2772.34
117–123	**134–149**	118–140	2950.46	2950.45

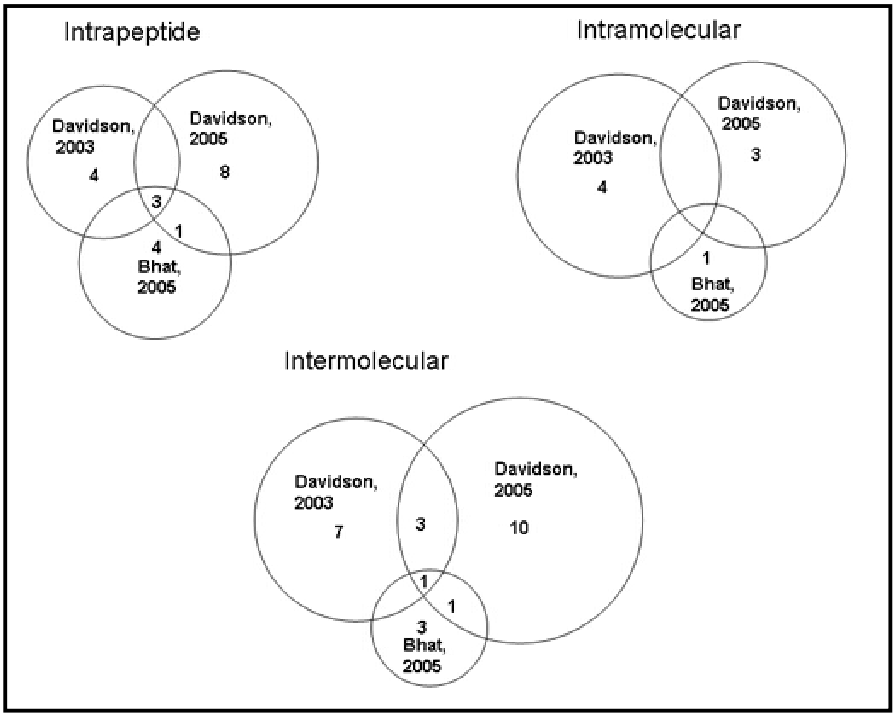

Figure-31: Comparison of the number of intrapeptide, intramolecular and intermolecular cross-links in apoAI trypsin peptides in three different reports. The number of peptides identified in each report is indicated in the non-overlapping parts of the circles. The number of peptides observed in common between the two or three studies is indicated in the overlapping areas of the circles.

linker is not considered. Hence, there is a strong possibility that all the possible cross-links have not been identified.

Future cross-linking studies with apoAI should focus on alternative cleavage protocols to generate large fragments of cross-linked apoAI molecules. Trypsin digestion generates too many peptides of apoAI leading to mass degeneracy and complicating the identification of cross-linked apoAI peptides. The presence of larger fragments of apoAI increases the chances of identifying

the cross-linked domains/regions of apoAI. ApoAI has 4 Met residues and cleavage at CNBr residues has already been tried, the position of the CNBr peptide in apoAI leads to the generation of CNBr peptides that are identical in size and will complicate the separation and identification of the fragments. Cleavage at Trp residues with BNPS-Skatole can be very useful for this purpose. Wild-type apoAI molecule has 4 Trp residues and the fragments of BNPS-Skatole cleavage are of different sizes and will not complicate the identification or separation of the peptides. Currently the possibility of using a mixture of Trp mutants and wild-type apoAI for chemical cross-linking is under way and we believe that this will lead to the identification of potential intermolecular contacts between adjacent apoAI molecules in discoidal lipoprotein molecules. The second factor which could lead to better identification of peptides is to switch from MALDI-TOF mass spectrometry to LC-ES-QTOF mass spectrometery with MS/MS capabilities. MS/MS sequencing of peptides/cross-linked peptides will help in the unambiguous identification of peptides even if mass degeneracy occurs. Unlike MALDI-TOF mass spectrometry, chemical cross-linking of proteins/synthetic peptides and the fragmentation pattern has been well studied by using ES-QTOF mass spectrometers(*91, 101, 107*). This available data will help in the identification of cross-linked apoAI peptides and in the MS/MS sequencing experiments.

Summary

Identification of steps in the lipid-binding associated conformational flexibility of locust apoLp-III- Utilizing disulfide mutants of locust apoLp-III we were able to identify the vital steps during the lipid-binding associated helix-bundle reorganization of apoLp-III. The separation of helices 1 and 5 is an essential step during the lipid-binding process of apoLp-III. The inability helix1-5 tethered disulfide mutant to interact with any kind of lipid-surface suggests the separation of helices 1 and 5 to be an early step during the lipid-binding process of apoLp-III.

ApoLp-III can exist in different conformations in the lipid-bound state- Thethering helices 3 and 4 or loops 2 and 4 imapirs the lipid-binding activity of apoLp-III and leads to the formation of lipoproteins of different sizes as compared to the wild-type apoLp-III. This suggests that apoLp-III can adopt different conformations in the lipid-bound state.

Organization of human apoAI molecules in discoidal lipoprotein particles- The difficulties in utilizing chemical cross-linking, tryspin digestion and peptide mass fingerprinting by MALDI-TOF mass spectrometry is discussed. The data obtained till date suggests the requirement of alternative cleavage protocols to generate larger fragments of cross-linked apoAI and the use of mass spectrometers with MS/MS capabilities to identify the cross-linked peptides of apoAI.

Bibliography

(1) Gotto, A. M., Jr., Pownall, H. J., and Havel, R. J. (1986) Introduction to the plasma lipoproteins. *Methods Enzymol 128*, 3-41.

(2) Soulages, J. L., and Wells, M. A. (1994) Lipophorin: the structure of an insect lipoprotein and its role in lipid transport in insects. *Adv Protein Chem 45*, 371-415.

(3) Redgrave, T. G., Roberts, D. C., and West, C. E. (1975) Separation of plasma lipoproteins by density-gradient ultracentrifugation. *Anal Biochem 65*, 42-9.

(4) Noble, R. P. (1968) Electrophoretic separation of plasma lipoproteins in agarose gel. *J Lipid Res 9*, 693-700.

(5) Ryan, R. O., and van der Horst, D. J. (2000) Lipid transport biochemistry and its role in energy production. *Annu Rev Entomol 45*, 233-60.

(6) Breiter, D. R., Kanost, M. R., Benning, M. M., Wesenberg, G., Law, J. H., Wells, M. A., Rayment, I., and Holden, H. M. (1991) Molecular structure of an apolipoprotein determined at 2.5-A resolution. *Biochemistry 30*, 603-8.

(7) Fan, D., Zheng, Y., Yang, D., and Wang, J. (2003) NMR solution structure and dynamics of an exchangeable apolipoprotein, Locusta migratoria apolipophorin III. *J Biol Chem 278*, 21212-20.

(8) Wang, J., Gagne, S. M., Sykes, B. D., and Ryan, R. O. (1997) Insight into lipid surface recognition and reversible conformational adaptations of an exchangeable apolipoprotein by multidimensional heteronuclear NMR techniques. *J Biol Chem 272*, 17912-20.

(9) Segelke, B. W., Forstner, M., Knapp, M., Trakhanov, S. D., Parkin, S., Newhouse, Y. M., Bellamy, H. D., Weisgraber, K. H., and Rupp, B. (2000) Conformational flexibility in the apolipoprotein E amino-terminal domain structure determined from three new crystal forms: implications for lipid binding. *Protein Sci 9*, 886-97.

(10) Cole, K. D., Fernando-Warnakulasuriya, G. P., Boguski, M. S., Freeman, M., Gordon, J. I., Clark, W. A., Law, J. H., and Wells, M. A. (1987) Primary structure and comparative sequence analysis of an insect apolipoprotein. Apolipophorin-III from Manduca sexta. *J Biol Chem 262*, 11794-800.

(11) Soulages, J. L., Salamon, Z., Wells, M. A., and Tollin, G. (1995) Low concentrations of diacylglycerol promote the binding of apolipophorin III to a phospholipid bilayer: a surface plasmon resonance spectroscopy study. *Proc Natl Acad Sci U S A 92*, 5650-4.

(12) Lu, B., Morrow, J. A., and Weisgraber, K. H. (2000) Conformational reorganization of the four-helix bundle of human apolipoprotein E in binding to phospholipid. *J Biol Chem 275*, 20775-81.

(13) Narayanaswami, V., Szeto, S. S., and Ryan, R. O. (2001) Lipid association-induced N- and C-terminal domain reorganization in human apolipoprotein E3. *J Biol Chem 276*, 37853-60.
(14) Kawooya, J. K., Meredith, S. C., Wells, M. A., Kezdy, F. J., and Law, J. H. (1986) Physical and surface properties of insect apolipophorin III. *J Biol Chem 261*, 13588-91.
(15) Soulages, J. L., and Arrese, E. L. (2000) Fluorescence spectroscopy of single tryptophan mutants of apolipophorin-III in discoidal lipoproteins of dimyristoylphosphatidylcholine. *Biochemistry 39*, 10574-80.
(16) Soulages, J. L., and Arrese, E. L. (2001) Interaction of the alpha-helices of apolipophorin III with the phospholipid acyl chains in discoidal lipoprotein particles: a fluorescence quenching study. *Biochemistry 40*, 14279-90.
(17) Kahalley, J., Stroud, P., Cannon, G., and McCormick, C. L. (1999) Examination of the structure/function relationship in the exchangeable apolipoprotein, apolipophorin-III. *Biopolymers 50*, 486-95.
(18) Soulages, J. L., and Arrese, E. L. (2000) Dynamics and hydration of the alpha-helices of apolipophorin III. *J Biol Chem 275*, 17501-9.
(19) Frank, P. G., and Marcel, Y. L. (2000) Apolipoprotein A-I: structure-function relationships. *J Lipid Res 41*, 853-72.
(20) Asztalos, B. F., and Schaefer, E. J. (2003) High-density lipoprotein subpopulations in pathologic conditions. *Am J Cardiol 91*, 12E-17E.
(21) Segrest, J. P., Li, L., Anantharamaiah, G. M., Harvey, S. C., Liadaki, K. N., and Zannis, V. (2000) Structure and function of apolipoprotein A-I and high-density lipoprotein. *Curr Opin Lipidol 11*, 105-15.
(22) Kontush, A., and Chapman, M. J. (2006) Antiatherogenic small, dense HDL-guardian angel of the arterial wall? *Nat Clin Pract Cardiovasc Med 3*, 144-53.
(23) Ajees, A. A., Anantharamaiah, G. M., Mishra, V. K., Hussain, M. M., and Murthy, H. M. (2006) Crystal structure of human apolipoprotein A-I: Insights into its protective effect against cardiovascular diseases. *Proc Natl Acad Sci U S A*.
(24) Saito, H., Lund-Katz, S., and Phillips, M. C. (2004) Contributions of domain structure and lipid interaction to the functionality of exchangeable human apolipoproteins. *Prog Lipid Res 43*, 350-80.
(25) Wald, J. H., Coormaghtigh, E., De Meutter, J., Ruysschaert, J. M., and Jonas, A. (1990) Investigation of the lipid domains and apolipoprotein orientation in reconstituted high density lipoproteins by fluorescence and IR methods. *J Biol Chem 265*, 20044-50.
(26) Panagotopulos, S. E., Horace, E. M., Maiorano, J. N., and Davidson, W. S. (2001) Apolipoprotein A-I adopts a belt-like orientation in reconstituted high density lipoproteins. *J Biol Chem 276*, 42965-70.

(27) Segrest, J. P., Jones, M. K., Klon, A. E., Sheldahl, C. J., Hellinger, M., De Loof, H., and Harvey, S. C. (1999) A detailed molecular belt model for apolipoprotein A-I in discoidal high density lipoprotein. *J Biol Chem 274*, 31755-8.
(28) Tricerri, M. A., Behling Agree, A. K., Sanchez, S. A., Bronski, J., and Jonas, A. (2001) Arrangement of apolipoprotein A-I in reconstituted high-density lipoprotein disks: an alternative model based on fluorescence resonance energy transfer experiments. *Biochemistry 40*, 5065-74.
(29) Silva, R. A., Hilliard, G. M., Li, L., Segrest, J. P., and Davidson, W. S. (2005) A mass spectrometric determination of the conformation of dimeric apolipoprotein A-I in discoidal high density lipoproteins. *Biochemistry 44*, 8600-7.
(30) Davidson, W. S., and Hilliard, G. M. (2003) The spatial organization of apolipoprotein A-I on the edge of discoidal high density lipoprotein particles: a mass specrometry study. *J Biol Chem 278*, 27199-207.
(31) Bhat, S., Sorci-Thomas, M. G., Alexander, E. T., Samuel, M. P., and Thomas, M. J. (2005) Intermolecular contact between globular N-terminal fold and C-terminal domain of ApoA-I stabilizes its lipid-bound conformation: studies employing chemical cross-linking and mass spectrometry. *J Biol Chem 280*, 33015-25.
(32) Rye, K. A., and Barter, P. J. (2004) Formation and metabolism of prebeta-migrating, lipid-poor apolipoprotein A-I. *Arterioscler Thromb Vasc Biol 24*, 421-8.
(33) Bergeron, J., Frank, P. G., Scales, D., Meng, Q. H., Castro, G., and Marcel, Y. L. (1995) Apolipoprotein A-I conformation in reconstituted discoidal lipoproteins varying in phospholipid and cholesterol content. *J Biol Chem 270*, 27429-38.
(34) Sviridov, D., Miyazaki, O., Theodore, K., Hoang, A., Fukamachi, I., and Nestel, P. (2002) Delineation of the role of pre-beta 1-HDL in cholesterol efflux using isolated pre-beta 1-HDL. *Arterioscler Thromb Vasc Biol 22*, 1482-8.
(35) Dhoest, A., Zhao, Z., De Geest, B., Deridder, E., Sillen, A., Engelborghs, Y., Collen, D., and Holvoet, P. (1997) Role of the Arg123-Tyr166 paired helix of apolipoprotein A-I in lecithin:cholesterol acyltransferase activation. *J Biol Chem 272*, 15967-72.
(36) Nakamura, Y., Kotite, L., Gan, Y., Spencer, T. A., Fielding, C. J., and Fielding, P. E. (2004) Molecular mechanism of reverse cholesterol transport: reaction of pre-beta-migrating high-density lipoprotein with plasma lecithin/cholesterol acyltransferase. *Biochemistry 43*, 14811-20.
(37) Collet, X., Perret, B., Simard, G., Raffai, E., and Marcel, Y. L. (1991) Differential effects of lecithin and cholesterol on the immunoreactivity and conformation of apolipoprotein A-I in high density lipoproteins. *J Biol Chem 266*, 9145-52.
(38) Narayanaswami, V., and Ryan, R. O. (2000) Molecular basis of exchangeable apolipoprotein function. *Biochim Biophys Acta 1483*, 15-36.

(39) Wilson, C., Wardell, M. R., Weisgraber, K. H., Mahley, R. W., and Agard, D. A. (1991) Three-dimensional structure of the LDL receptor-binding domain of human apolipoprotein E. *Science 252*, 1817-22.
(40) Segrest, J. P., Jones, M. K., De Loof, H., Brouillette, C. G., Venkatachalapathi, Y. V., and Anantharamaiah, G. M. (1992) The amphipathic helix in the exchangeable apolipoproteins: a review of secondary structure and function. *J Lipid Res 33*, 141-66.
(41) Smith, A. F., Owen, L. M., Strobel, L. M., Chen, H., Kanost, M. R., Hanneman, E., and Wells, M. A. (1994) Exchangeable apolipoproteins of insects share a common structural motif. *J Lipid Res 35*, 1976-84.
(42) Pownall, H. J., and Massey, J. B. (1986) Spectroscopic studies of lipoproteins. *Methods Enzymol 128*, 515-8.
(43) Weisgraber, K. H. (1994) Apolipoprotein E: structure-function relationships. *Adv Protein Chem 45*, 249-302.
(44) Wientzek, M., Kay, C. M., Oikawa, K., and Ryan, R. O. (1994) Binding of insect apolipophorin III to dimyristoylphosphatidylcholine vesicles. Evidence for a conformational change. *J Biol Chem 269*, 4605-12.
(45) Pownall, H. J., Massey, J. B., Kusserow, S. K., and Gotto, A. M., Jr. (1978) Kinetics of lipid--protein interactions: interaction of apolipoprotein A-I from human plasma high density lipoproteins with phosphatidylcholines. *Biochemistry 17*, 1183-8.
(46) Weers, P. M., Van Der Horst, D. J., and Ryan, R. O. (2000) Interaction of locust apolipophorin III with lipoproteins and phospholipid vesicles: effect of glycosylation. *J Lipid Res 41*, 416-23.
(47) Scheele, G., and Jacoby, R. (1982) Conformational changes associated with proteolytic processing of presecretory proteins allow glutathione-catalyzed formation of native disulfide bonds. *J Biol Chem 257*, 12277-82.
(48) Chen, Y. H., and Yang, J. T. (1971) A new approach to the calculation of secondary structures of globular proteins by optical rotatory dispersion and circular dichroism. *Biochem Biophys Res Commun 44*, 1285-91.
(49) Woody, R. W., and Dunker, A. K. (1996) *Circular Dichroism and the Conformational Analysis of Proteins*, Plenum Press, New York.
(50) De Pauw, M., Vanloo, B., Weisgraber, K., and Rosseneu, M. (1995) Comparison of lipid-binding and lecithin:cholesterol acyltransferase activation of the amino- and carboxyl-terminal domains of human apolipoprotein E3. *Biochemistry 34*, 10953-66.
(51) Raussens, V., Narayanaswami, V., Goormaghtigh, E., Ryan, R. O., and Ruysschaert, J. M. (1995) Alignment of the apolipophorin-III alpha-helices in complex with dimyristoylphosphatidylcholine. A unique spatial orientation. *J Biol Chem 270*, 12542-7.

(52) Narayanaswami, V., Wang, J., Kay, C. M., Scraba, D. G., and Ryan, R. O. (1996) Disulfide bond engineering to monitor conformational opening of apolipophorin III during lipid binding. *J Biol Chem 271*, 26855-62.
(53) Segrest, J. P., Garber, D. W., Brouillette, C. G., Harvey, S. C., and Anantharamaiah, G. M. (1994) The amphipathic alpha helix: a multifunctional structural motif in plasma apolipoproteins. *Adv Protein Chem 45*, 303-69.
(54) Weinstein, J. N., Blumenthal, R., and Klausner, R. D. (1986) Carboxyfluorescein leakage assay for lipoprotein-liposome interaction. *Methods Enzymol 128*, 657-68.
(55) Jonas, A., Kezdy, K. E., and Wald, J. H. (1989) Defined apolipoprotein A-I conformations in reconstituted high density lipoprotein discs. *J Biol Chem 264*, 4818-24.
(56) Liu, H., Scraba, D. G., and Ryan, R. O. (1993) Prevention of phospholipase-C induced aggregation of low density lipoprotein by amphipathic apolipoproteins. *FEBS Lett 316*, 27-33.
(57) Soulages, J. L., Pennington, J., Bendavid, O., and Wells, M. A. (1998) Role of glycosylation in the lipid-binding activity of the exchangeable apolipoprotein, apolipophorin-III. *Biochem Biophys Res Commun 243*, 372-6.
(58) Chung, B. H., Wilkinson, T., Geer, J. C., and Segrest, J. P. (1980) Preparative and quantitative isolation of plasma lipoproteins: rapid, single discontinuous density gradient ultracentrifugation in a vertical rotor. *J Lipid Res 21*, 284-91.
(59) Soulages, J. L., van Antwerpen, R., and Wells, M. A. (1996) Role of diacylglycerol and apolipophorin-III in regulation of physiochemical properties of the lipophorin surface: metabolic implications. *Biochemistry 35*, 5191-8.
(60) Wells, M. A., Ryan, R. O., Kawooya, J. K., and Law, J. H. (1987) The role of apolipophorin III in in vivo lipoprotein interconversions in adult Manduca sexta. *J Biol Chem 262*, 4172-6.
(61) Van der Horst, D. J., Van Marrewijk, W. J., and Diederen, J. H. (2001) Adipokinetic hormones of insect: release, signal transduction, and responses. *Int Rev Cytol 211*, 179-240.
(62) Soulages, J. L., and Wells, M. A. (1994) Effect of diacylglycerol content on some physicochemical properties of the insect lipoprotein, lipophorin. Correlation with the binding of apolipophorin-III. *Biochemistry 33*, 2356-62.
(63) Arrese, E. L., Rojas-Rivas, B. I., and Wells, M. A. (1996) Synthesis of sn-1,2-diacylglycerols by monoacylglycerol acyltransferase from Manduca sexta fat body. *Arch Insect Biochem Physiol 31*, 325-35.
(64) Van der Horst, D. J., Ryan, R. O., Van Heusden, M. C., Schulz, T. K., Van Doorn, J. M., Law, J. H., and Beenakkers, A. M. (1988) An insect lipoprotein hybrid helps to define the role of apolipophorin III. *J Biol Chem 263*, 2027-33.

(65) van der Horst, D. J., van Hoof, D., van Marrewijk, W. J., and Rodenburg, K. W. (2002) Alternative lipid mobilization: the insect shuttle system. *Mol Cell Biochem 239*, 113-9.
(66) Fan, D., Reese, L., Ren, X., Weers, P. M., Ryan, R. O., and Wang, J. (2001) Complete 1H, 15N, and 13C assignments of an exchangeable apolipoprotein, Locusta migratoria apolipophorin III. *J Biomol NMR 19*, 83-4.
(67) Lecompte, M. F., Bras, A. C., Dousset, N., Portas, I., Salvayre, R., and Ayrault-Jarrier, M. (1998) Binding steps of apolipoprotein A-I with phospholipid monolayers: adsorption and penetration. *Biochemistry 37*, 16165-71.
(68) Rogers, D. P., Roberts, L. M., Lebowitz, J., Datta, G., Anantharamaiah, G. M., Engler, J. A., and Brouillette, C. G. (1998) The lipid-free structure of apolipoprotein A-I: effects of amino-terminal deletions. *Biochemistry 37*, 11714-25.
(69) Reijngoud, D. J., and Phillips, M. C. (1982) Mechanism of dissociation of human apolipoprotein A-I from complexes with dimyristoylphosphatidylcholine as studied by guanidine hydrochloride denaturation. *Biochemistry 21*, 2969-76.
(70) Soulages, J. L., and Bendavid, O. J. (1998) The lipid binding activity of the exchangeable apolipoprotein apolipophorin-III correlates with the formation of a partially folded conformation. *Biochemistry 37*, 10203-10.
(71) Brouillette, C. G., Anantharamaiah, G. M., Engler, J. A., and Borhani, D. W. (2001) Structural models of human apolipoprotein A-I: a critical analysis and review. *Biochim Biophys Acta 1531*, 4-46.
(72) Goni, F. M. (2002) Non-permanent proteins in membranes: when proteins come as visitors (Review). *Mol Membr Biol 19*, 237-45.
(73) Soulages, J. L., Arrese, E. L., Chetty, P. S., and Rodriguez, V. (2001) Essential role of the conformational flexibility of helices 1 and 5 on the lipid binding activity of apolipophorin-III. *J Biol Chem 276*, 34162-6.
(74) Chetty, P. S., Arrese, E. L., and Soulages, J. L. (2003) In vivo lipoprotein binding assay of the insect exchangeable apolipoprotein, apolipophorin-III. *Protein Pept Lett 10*, 469-73.
(75) Weers, P. M., Prenner, E. J., Kay, C., and Ryan, R. O. (2000) Lipid binding of the exchangeable apolipoprotein apolipophorin III induces major changes in fluorescence properties of tryptophans 115 and 130. *Biochemistry 39*, 6874-80.
(76) Agasoster, A. V., Halskau, O., Fuglebakk, E., Froystein, N. A., Muga, A., Holmsen, H., and Martinez, A. (2003) The interaction of peripheral proteins and membranes studied with alpha-lactalbumin and phospholipid bilayers of various compositions. *J Biol Chem 278*, 21790-7.
(77) Muller, K. (1981) Structural dimorphism of bile salt/lecithin mixed micelles. A possible regulatory mechanism for cholesterol solubility in bile? X-ray structure analysis. *Biochemistry 20*, 404-14.

(78) Sahoo, D., Weers, P. M., Ryan, R. O., and Narayanaswami, V. (2002) Lipid-triggered conformational switch of apolipophorin III helix bundle to an extended helix organization. *J Mol Biol 321*, 201-14.
(79) Garda, H. A., Arrese, E. L., and Soulages, J. L. (2002) Structure of apolipophorin-III in discoidal lipoproteins. Interhelical distances in the lipid-bound state and conformational change upon binding to lipid. *J Biol Chem 277*, 19773-82.
(80) Li, H. H., Lyles, D. S., Pan, W., Alexander, E., Thomas, M. J., and Sorci-Thomas, M. G. (2002) ApoA-I structure on discs and spheres. Variable helix registry and conformational states. *J Biol Chem 277*, 39093-101.
(81) Saito, H., Dhanasekaran, P., Baldwin, F., Weisgraber, K. H., Lund-Katz, S., and Phillips, M. C. (2001) Lipid binding-induced conformational change in human apolipoprotein E. Evidence for two lipid-bound states on spherical particles. *J Biol Chem 276*, 40949-54.
(82) Boden, W. E. (2000) High-density lipoprotein cholesterol as an independent risk factor in cardiovascular disease: assessing the data from Framingham to the Veterans Affairs High--Density Lipoprotein Intervention Trial. *Am J Cardiol 86*, 19L-22L.
(83) Harper, C. R., and Jacobson, T. A. (1999) New perspectives on the management of low levels of high-density lipoprotein cholesterol. *Arch Intern Med 159*, 1049-57.
(84) Libby, P. (2001) Current concepts of the pathogenesis of the acute coronary syndromes. *Circulation 104*, 365-72.
(85) Navab, M., Ananthramaiah, G. M., Reddy, S. T., Van Lenten, B. J., Ansell, B. J., Hama, S., Hough, G., Bachini, E., Grijalva, V. R., Wagner, A. C., Shaposhnik, Z., and Fogelman, A. M. (2005) The double jeopardy of HDL. *Ann Med 37*, 173-8.
(86) Marcel, Y. L., and Kiss, R. S. (2003) Structure-function relationships of apolipoprotein A-I: a flexible protein with dynamic lipid associations. *Curr Opin Lipidol 14*, 151-7.
(87) Cheung, M. C., Segrest, J. P., Albers, J. J., Cone, J. T., Brouillette, C. G., Chung, B. H., Kashyap, M., Glasscock, M. A., and Anantharamaiah, G. M. (1987) Characterization of high density lipoprotein subspecies: structural studies by single vertical spin ultracentrifugation and immunoaffinity chromatography. *J Lipid Res 28*, 913-29.
(88) Sparks, D. L., Anantharamaiah, G. M., Segrest, J. P., and Phillips, M. C. (1995) Effect of the cholesterol content of reconstituted LpA-I on lecithin:cholesterol acyltransferase activity. *J Biol Chem 270*, 5151-7.
(89) Newhouse, Y., Peters-Libeu, C., and Weisgraber, K. H. (2005) Crystallization and preliminary X-ray diffraction analysis of apolipoprotein E-containing lipoprotein particles. *Acta Crystallograph Sect F Struct Biol Cryst Commun 61*, 981-4.

(90) Peters-Libeu, C. A., Newhouse, Y., Hatters, D. M., and Weisgraber, K. H. (2006) Model of biologically active apolipoprotein E bound to dipalmitoylphosphatidylcholine. *J Biol Chem 281*, 1073-9.
(91) Sinz, A. (2006) Chemical cross-linking and mass spectrometry to map three-dimensional protein structures and protein-protein interactions. *Mass Spectrom Rev*.
(92) Sinz, A. (2003) Chemical cross-linking and mass spectrometry for mapping three-dimensional structures of proteins and protein complexes. *J Mass Spectrom 38*, 1225-37.
(93) Dihazi, G. H., and Sinz, A. (2003) Mapping low-resolution three-dimensional protein structures using chemical cross-linking and Fourier transform ion-cyclotron resonance mass spectrometry. *Rapid Commun Mass Spectrom 17*, 2005-14.
(94) Schulz, D. M., Ihling, C., Clore, G. M., and Sinz, A. (2004) Mapping the topology and determination of a low-resolution three-dimensional structure of the calmodulin-melittin complex by chemical cross-linking and high-resolution FTICRMS: direct demonstration of multiple binding modes. *Biochemistry 43*, 4703-15.
(95) Peterson, J. J., Young, M. M., and Takemoto, L. J. (2004) Probing alpha-crystallin structure using chemical cross-linkers and mass spectrometry. *Mol Vis 10*, 857-66.
(96) Kalkhof, S., Ihling, C., Mechtler, K., and Sinz, A. (2005) Chemical cross-linking and high-performance fourier transform ion cyclotron resonance mass spectrometry for protein interaction analysis: application to a calmodulin/target peptide complex. *Anal Chem 77*, 495-503.
(97) Novak, P., Young, M. M., Schoeniger, J. S., and Kruppa, G. H. (2003) A top-down approach to protein structure studies using chemical cross-linking and Fourier transform mass spectrometry. *Eur J Mass Spectrom (Chichester, Eng) 9*, 623-31.
(98) Back, J. W., de Jong, L., Muijsers, A. O., and de Koster, C. G. (2003) Chemical cross-linking and mass spectrometry for protein structural modeling. *J Mol Biol 331*, 303-13.
(99) Schumaker, V. N., and Puppione, D. L. (1986) Sequential flotation ultracentrifugation. *Methods Enzymol 128*, 155-70.
(100) Morrison, J. R., Fidge, N. H., and Grego, B. (1990) Studies on the formation, separation, and characterization of cyanogen bromide fragments of human AI apolipoprotein. *Anal Biochem 186*, 145-52.
(101) Swaim, C. L., Smith, J. B., and Smith, D. L. (2004) Unexpected products from the reaction of the synthetic cross-linker 3,3′-dithiobis(sulfosuccinimidyl propionate), DTSSP with peptides. *Journal of the American Society for Mass Spectrometry 15*, 736-749.

(102) Spengler, B., Kirsch, D., Kaufmann, R., and Jaeger, E. (1992) Peptide sequencing by matrix-assisted laser-desorption mass spectrometry. *Rapid Commun Mass Spectrom 6*, 105-8.
(103) Brown, R. S., and Lennon, J. J. (1995) Sequence-specific fragmentation of matrix-assisted laser-desorbed protein/peptide ions. *Anal Chem 67*, 3990-9.
(104) Brown, R. S., Feng, J., and Reiber, D. C. (1997) Further studies of in-source fragmentation of peptides in matrix-assisted laser desorption-ionization. *International Journal of Mass Spectrometry and Ion Processes 169-170*, 1-18.
(105) Yu, W., Vath, J. E., Huberty, M. C., and Martin, S. A. (1993) Identification of the facile gas-phase cleavage of the Asp-Pro and Asp-Xxx peptide bonds in matrix-assisted laser desorption time-of-flight mass spectrometry. *Anal Chem 65*, 3015-23.
(106) Wattenberg, A., Organ, A. J., Schneider, K., Tyldesley, R., Bordoli, R., and Bateman, R. H. (2002) Sequence dependent fragmentation of peptides generated by MALDI quadrupole time-of-flight (MALDI Q-TOF) mass spectrometry and its implications for protein identification. *J Am Soc Mass Spectrom 13*, 772-83.
(107) Gaucher, S. P., Hadi, M. Z., and Young, M. M. (2006) Influence of crosslinker identity and position on gas-phase dissociation of lys-lys crosslinked peptides. *J Am Soc Mass Spectrom 17*, 395-405.

Appendix- I

Evidence For The Formation Of Disulfide Bond in ApoLp-III Disulfide Mutants

Gel-shift assay-The formation of disulfide bonds in apoLp-III disulfide mutants used in the studies in Chapter-IV was monitored by mobility shift assay in SDS-PAGE and increased stability as monitored by thermal and chemical denaturation studies. **Figure-32** shows the mobility shift observed for the H3-H4 mutant and L2-L4 disulfide mutants. The presence of a disulfide bond leads to a faster mobility of the disulfide mutants as compared to the wild-type apoLp-III molecule in SDS-PAGE gel.

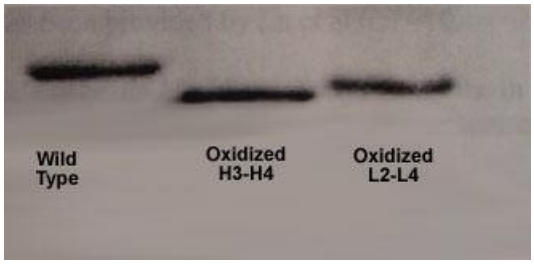

Figure-32: Gel-shift assay to monitor the formation of disulfide bonds in apoLp-III disulfide mutants.

Denaturation Studies- In the thermal (**Figure-33**) unfolding studies apoLp-III disulfide mutants showed increased stability (increased transition temperature) as compared to the wild-type apoLp-III molecule. The thermal unfolding was monitored as a decrease in molar ellipticity at 222nm in CD spectroscopy. The mid-point of transition from thermal unfolding assays is tabulated in **Table-9**. The

increased stability of the oxidized disulfide mutants suggests the formation of a disulfide bond.

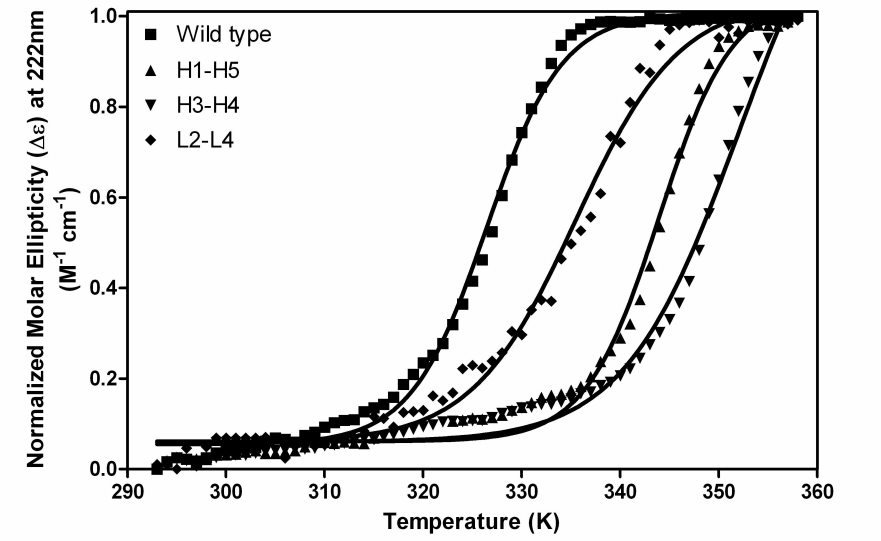

Figure-33: Thermal unfolding of apoLp-III wild-type and oxidized disulfide mutants monitored by CD spectroscopy.

Table-9: Estimated transition temperatures for apoLp-III wild-type and disulfide mutants from the thermal unfolding plots in Figure-33.

	Tm (˚C)
Wild-type	53.25
H1-H5	70.75
H3-H4	78.85
L2-L4	62.35

Appendix-II

Insect Exchangeable Apolipoprotein-III Forms Discoidal Lipoproteins of Discrete Sizes on Reconstitution with Phospholipid/Detergent Mixed Micelles.

Exchangeable apolipoproteins are reconstituted with phospholipids by spontaneous interaction or by cholate dialysis to yield discoidal lipoprotein complexes of discrete size(s). The size or sizes of the discoidal lipoprotein complexes formed depend on the initial protein to lipid-ratio and the conformation of apoLp-III in the final lipid-bound state. At a 1:60 ratio of apoLp-III to phospholipids wild-type apoLp-III forms two discrete sizes of discoidal lipoproteins with 12.2 nm and 10.4 nm Stoke's diameter while the oxidized H1-H4 mutant forms discoidal lipoproteins of 17 nm diameter (see native gradient gel electrophoresis data **Figure-15, Chapter-IV**). Here an attempt is made to explain the formation of discrete lipoprotein sizes in the apoLp-III/phospholipid reconstitution experiments.

Assuming the 12.2 nm, 10.4 nm discoidal lipoproteins complexes of wild-type apoLp-III and the 17nm discoidal lipoprotein complexex of oxidized H3-H4 mutant as perfect cylinders as shown in **Figure**-**34**) the lateral surface area of the phospholipid bilayer or the surface area of the phospholipid acyl chains available for interaction with exchangeable apolipoproteins was calculated by using the **equation-4**.

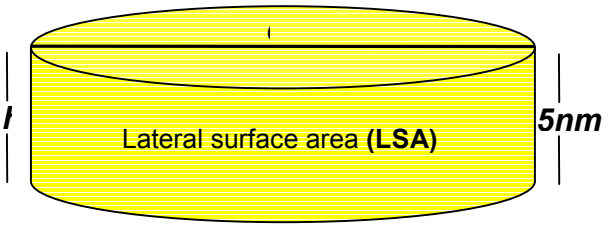

Figure-34: The dimensions of a discoidal lipoprotein molecule used to calculate the lateral surface area of phospholipid acyl chains. ***d***,diameter and ***h***, thickness of DMPC (phospholipid) bilayer. The thickness of a DMPC bilayer is 5nm.

Lateral Surface area = Circumference x thickness (h) of the DMPC bilayer

= (π x d) x h (**equation-4**)

Using the equation for the volume of a cylinder and **equation-4** the volume and lateral surface area of the phospholipids for the 12.2 nm, 10.4 nm and 17 nm disks were estimated (**Table-10)**.

Particle Diameter (nm)	Particle Volume (nm^3)	Lateral Surface area (nm^2)	Lateral Surface area ($Å^2$)
6.1	**584.197**	**191.54**	**19154**
5.2	**424.528**	**163.28**	**16328**
8.5	**1134.325**	**266.9**	**26690**

Table-10: Estimated lateral surface area of phospholipid disks.

The surface area occupied by apoLp-III molecules in the air-water interface is used as an approximation of the surface area in the lipid-bound state. At the air-water interface apoLp-III molecules were estimated to occupy a surface area of 3000$Å^2$/molecule of apoLp-III. Using this value and the estimated lateral surface area of the disks in **Table-10** there are 5 and 6 apoLp-III molecules in

12.2 and 10.4 nm diameter discoidal lipoprotein particles respectively. The difference in the lateral surface area between the 12.2 nm and 10.4 nm diameter particles is ~ 3000Å^2. This suggests that the binding of apoLp-III to the discoidal lipoprotein particles requires sufficent lateral surface area to accommodate an extended apoLp-III molecule. Considering the possibility of 6 apoLp-III molecules in the smaller 10.4 nm particle then there will be an excess of extended apoLp-III molecule(s) not bound to the lipoprotein surface. In the case of 5 molecules bound to the large 12.2 nm particle the apoLp-III molecule cannot occupy the entire lateral surface area and the hydrophobic acyl chains will be exposed to aqueous buffer. Based on the stochiometry and lipid-bound conformation the apoLp-III molecule forms lipoproteins of discrete sizes so as to accommodate optimal number of apoLp-III molecules on the lateral surface area of exposed acyl chains.

Still, this does not explain the large size of the discoidal lipoprotein complex formed by oxidized H3-H4 mutant. In **Table-10** the volume of 17 nm diameter H3-H4 mutant disks to be double that of the 10.4 nm wild-type lipoprotein particles but the lateral surface area of the 17 nm complex just increases by ~1.3 fold. This suggests that with increase in the phospholipid content and eventually the volume of the cylindrical phospholipid bilayer, there is a comparably lesser change in the lateral surface area available for apoLp-III binding and requires the binding of lesser number of apoLp-III particles per unit area of exposed acyl chains.This is consistent with the observed data in **Chapter-4** where ~50% of oxidized H3-H4 mutants did not bind to

cholate/phospholipid mixed micelles and form discoidal lipoproteins. The tethering of helices 3 and 4 in the H3-H4 mutant could prevent the mutant from adopting a fully extended conformation like the wild-type apoLp-III hence the surface area occupied by the H3-H4 in the discoidal lipoproteins will be lesser as compared to the wild-type. The large size of the lipoprotein complexes formed suggest that at 1:60 protein: phospholipid ratio used for making lipoproteins the H3-H4 mutant binds to the same number of phospholipids as compared to the wild-type apoLp-III by forming large lipoprotein complexes.

VITA

Palaniappan (Chetty) Sevugan Chetty

246 Noble Research Center

Department of Biochemistry

Stillwater, OK-74078.

Phone: 405-744-9332

Email:Palaniappan.sevugan.chetty@okstate.edu

CURRENT POSITION:
Doctoral Candidate, Department of Biochemistry and Molecular Biology, Oklahoma State University, Stillwater, OK, 74074. Oct 2000- Present (Tentative Graduation Date- April 2006).
Thesis Advisor: Jose L. Soulages

CURRENT RESEARCH:
Elucidating the structure-function relationship of insect apolipophorin-III and human apolipoprotein AI utilizing chemical cross-linking and mass-spectrometry. The ultimate goal of my research is to elucidate the lipid-bound conformation of insect and human exchangeable apolipoproteins.

EDUCATIONAL QUALIFICATION:

COMPLETED THE REQUIREMENTS FOR THE PHD DEGREE AT OKLAHOMA STATE UNIVERSITY IN MAY, 2006.

Master of Science, Medical Biochemistry, Maharaj Sayaji Rao University, Baroda, Gujarat, India. June 1996- January 1999
Masters Thesis: **Measuring Oxidative Stress during Myocardial Infarction.** Study involved monitoring the serum levels of calcium, magnesium, zinc, copper and malondialdehyde in patients of acute myocardial infarction.

Bachelor of Science, Botany, Loyola College, University of Madras, Chennai, Tamil Nadu, India. April 1993- April 1996
Bachelor's Thesis: **Impact of Acid Fast Dyes on Fresh Water Fishes.** Study investigated the effect of tannery effluents on the life-cycle of fresh water fishes.

PROFESSIONAL EXPERIENCE:
Mass Spectrometry Research Assistant, Protein-DNA Core Facility, Department of Biochemistry and Molecular Biology, Oklahoma State University, Stillwater, OK. July 2003 – Jan 2004.
Job Responsibilities
Establishing a Standard Operating Procedure for MALDI-TOF analysis
Processing client samples for MALDI-TOF Mass Spectrometry
Aquiring data in a Voyager-DE Pro MALDI-TOF Mass Spectrometer
Analyzing Mass spectrometry data of biomolecules and preparing reports for clients

Trainee Clinical Lab Assistant, S.V.P Hospital, Chennai, Tamilnadu, India. Jan 1999-Jan 2000
Job Responsibilities
Receiving/ collecting samples from patients
Performing routine clinical tests on human body fluids
Creating reports of clinical tests for medical doctors

RESEARCH SKILLS
Protein expression and purification
LC and RP-HPLC for separation of proteins and peptides
Chemical Cross-linking of proteins, enzymatic and chemical cleavage of proteins
MALDI-TOF mass spectrometry for peptide mass fingerprinting

SERVICE, ACCOMPLISHMENTS & AWARDS
Vice-President, Biochemistry and Molecular Biology Graduate Student Association, Oklahoma State University (spring 2002-spring 2003)
Student Faculty Representative, Biochemistry and Molecular Biology Graduate Student Association Fall 2005-Present
Web master for Biochemistry and Molecular Biology Graduate Student Association at Oklahoma State University (Spring 2002 to Present)
$ 500.00 award for (Second Place) best poster presentation in the Fall 2005 Biochemistry and Molecular Biology Graduate Student Association Annual Research Symposium